Max-Planck-Institut für Polymerforschung
Max Planck Institute for Polymer Research

JOHANNES GUTENBERG UNIVERSITÄT MAINZ

Blood interactions
of
poly(phosphonate)s

Diplomarbeit zur Erlangung des Grades eines Diplomchemikers am

Institut für Organische Chemie des Fachbereichs Chemie und Pharmazie

der Johannes Gutenberg Universität Mainz

vorgelegt von

Go Kobayashi

geboren in Wiesbaden

am 10.04.1988

Mainz, 2015

Erklärung:

Diese Arbeit wurde in einem Zeitraum von April 2015 bis Dezember 2015 unter der Leitung von Dr. Frederik Wurm im Arbeitskreis von Prof. Dr. Katharina Landfester am Max Plack Institut für Polymerforschung in Mainz durchgeführt.

Hiermit bestätige ich, dass die vorliegende Arbeit selbstständig und ohne fremde Hilfe verfasst wurde. Alle Quellen und Hilfsmittel sind vollständig angegebenen.

_____

Go Kobayashi

Danksagung:

Hiermit möchte ich allen Personen danken, die mich unterstützt haben. Ohne sie wäre der Abschluss nicht möglich gewesen.

Als erstes möchte ich mich bei **Prof. Dr. Katharina Landfester** und **Dr. Frederik Wurm** bedanken, die mich herzlich empfangen und mir ein sowohl spannendes, als auch ein forderndes Thema gegeben haben.

Ein großer Dank gilt auch an **Thomas Wolf**, der mir den Einstieg in das Thema vereinfacht hat und mir immer, auch während des Studiums zu Rate stand. Ohne ihn wäre ein erfolgreiches Abschließen dieser Arbeit nicht möglich gewesen.

Hiermit möchte ich **Dr. Manfred Wagner** und **Dr. Robert Graf** für die NMR Messungen danken. Ohne ihr Wissen und Unterstützung wäre eine erfolgreiche Arbeit nicht möglich gewesen.

Für die Einführung und Hilfe bei SDS PAGE und Protein Assay möchte ich mich bei **Dr. Susanne Schöttler** und **Dipl. Chem. Johanna Simon** bedanken. Ohne Ihre Unterstützung wäre der Einstieg in die biologischen Messmethoden wesentlich schwerer und komplizierter gewesen.

Für die Oberflächenmessungen bedanke ich mich bei **Dr. Noemi Encinas Garcia**.

Ich bedanke mich bei **Christine Rosenauer** und **Ute Heinz** für die GPC Messungen.

Ich möchte mich noch hiermit an allen Mitgliedern des Arbeitskreises Landfester für das angenehme Klima im Arbeitskreis bedanken. Explizit möchte ich mich an bei **Angelika Manhart**, **M. Sc. Keti Piradashvili** für die angenehme Atmosphäre im Büro und Labor bedanken.

Und zuletzt möchte ich mich bei **meiner Familie** bedanken, die mich jederzeit unterstützt haben. Ohne Ihre Unterstützung wäre ein erfolgreicher Abschluss nicht möglich gewesen.

Table of Contents

1 ABSTRACT

Poly(ethylene ethyl phoshonat) (P(EtPPn)) wurde per anionische ringöffnende Polymerisation synthetisiert, welches dann mit Triethoxy (3-isocyanatopropyl)-silane in einer Eintopf Reaktion funktionalisiert wurde. Die Polymere wurden allgemein durch NMR Spektroskopie und MALDI TOF Messungen charakterisiert.

Die funktionalisierten Polymere können für verschiedene Forschungsgebieten angewendet werden. Wie zum Beispiel können diese für Partikelfunktionalisierungen verwendet werden, welche dann wiederrum für Oberflächen Untersuchungen verwendet werden können.

Silan funktionalisierte Polymere, die die mikroskopischen Silica Gel Partikel funktionalisiert haben, können durch Feststoff NMR ausgewertet werden.

Wiederum wurden Phosphor funktionalisierte Partikel mit menschlichen Heparin Plasma inkubiert. Zum Vergleich wurden PEGylierte (Polyethylenglykol) und das nicht funktionalisierte Partikel (SiO$_2$) verwendet. Nach der Inkubation wurden die Partikel mit MilliQ Wasser (MilliPore$^®$) mit einer Leifähigkeit <18.2 MΩ cm gewaschen und mit einer 7M Harnstoff/ 3M Thioharnstoff Mischungen eluiert. Für die Bestimmung der Protein Konzentration und Natriumdodecylsulfat-Polyacrylamidgelelektrophorese (SDS PAGE) wurden alle Fraktionen verwendet.

Poly(ethylene ethyl phoshonate) (P(EtPPn)) was synthesized via anionic ring-opening polymerization (AROP) and in a one-step reaction functionalized with triethoxy (3-isocyanatopropyl)-silane. The polymers were thoroughly characterized via NMR spectroscopy and MALDI TOF MS.

With the functionalized polymers there are several possibilities for research. It can be used for functionalization of particles, which can be used for surface measurements.

Characterization of functionalized microscopic silica gel particle can be observed by solid state NMR (SS NMR).

On the other hand phosphonylated particles were incubated with human heparin plasma. PEGylated (Polytethyleneglycol) and unmodified particles can be used as references. After incubation the particles were washed with MilliQ water (MilliPore®) with a conductivity <18.2 MΩ cm and eluted with a 7M urea/ 3M thiourea mixture. Every fraction was used for calculation of the protein concentration and Sodium Dodecyl Sulfate Polyacrylamide Gel Electrophoresis (SDS PAGE) every fraction was used.

2 MOTIVATION

Aim of this work was use specific interactions of proteins with polymers for the isolation specific of proteins from a complex protein mixture, such as human plasma. Therefore, of silica particles were functionalized with different polymers, which reduce unspecific protein adsorption but show a specific protein adsorption pattern. It is known that functionalization of several Nanoparticles (NPs) changes the adsorption behavior of proteins.[1-5] The goal of this work was to use the findings of previous protein-polymer interactions on nanocarriers to functionalize silica gel or micro particles with "stealth polymers", that should allow to isolate specific proteins after blood contact. PEG and Polyphoshpoesters, specifically poly(ethylene ethyl phosphonate), P(EtPPn) was investigated due to recent results obtained in our group regarding the protein adsorption behavior. These polymers shall show specific protein interactions have been silane-functionalized to enable their attachment to silica surfaces. After incubation with human plasma the amount of adsorbed protein as well as the protein composition was determined. It was the aim to collect the protein corona from PEGylated as well as PPEylated surfaces. This "stealth mixture" may be then used for the loading of other nanocarriers.

In addition a new PPE monomer has been designed which should allow an increase in the polymers hydrophilicity and thus the change in the adsorbed protein pattern.

3 POLYMERS IN BIOMEDICAL APPLICATION

3.1 POLY(ETHYLENEGLYCOL) (PEG)

Over the past 30 years poly(ethylene glycol) (PEG) (Figure 3-1) has been wildly used in the field of biomedical applications like polymer based drug delivery.[6] It is by now generally accepted "gold standard" in this field of research.[6,7] Advantages of PEG in medical chemistry are its high water solubility, non-toxicity, excellent biocompatibility and long term stability. These are all aspects to be considered when designing a material to be used in biomedical application.[7] However, PEG lacks in regards of two other important factor: chemical diversity and excretion of the compound.[7] The first arises from the fact that PEG only provides only two functional groups in the backbone which limits functionalization.[8] Problems with excretion occur due to the otherwise beneficial long term stability of the polyether backbone in aqueous medium. PEG with molecular weight above the upper exclusion limit is known to accumulate in the kidney.[9-11] But in general the stability of polymeric materials depends on several factors, like water content, pH, temperature, UV light, presence of enzymes, oxygen or oxidants.[12,13]
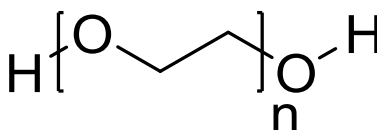

Figure 3-1: Structure of PEG.

Recent studies showed that PEG can decompose under biological oxidative stress to form toxic byproducts.[10,12] Byproducts of the oxidative degradation of PEG were found out by Ulbricht et. al.. They proposed a potential mechanism with formaldehyde being released from the PEG backbone.[12]

Bruns et. al. showed already in 1987, that the PEG has an effect on the mammalian metabolism. They reported that PEG involved in sequential oxidations by alcohol dehydrogenase (ADH) and aldehyde dehydrogenase (ALDH).[14] The metabolites of PEG which are found in the serum and urine of PEG-treated rabbits and burn patients were diacid and hydroxy acid. They indicated that PEG was oxidized *in vivo*.[14]

And the acids were the reason for metabolic acidosis, renal failure.[15,16]

The most prominent byproduct during the synthesis of PEG is cyclic dimer of ethylene oxide, 1,4-dioxane, but they can removed under reduces pressure.[7] However the International

Agency for Research on Cancer (IARC) categorized 1,4-dioxane as a group 2b compound (therefore being possibly carcinogenic in human with sufficient evidence from animal experiments). For pharmaceutical applications the European Pharmacopoeia (Ph.Eur.) limits the 1,4-dioxane content to 10 ppm.[7]
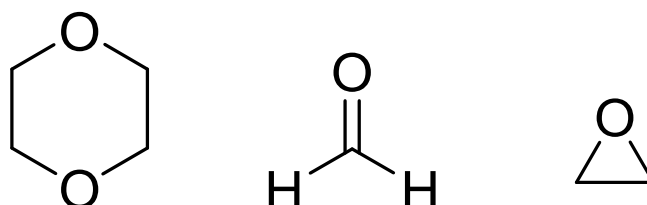

Figure 3-2: Byproducts: 1,4-dioxane (left), formaldehyde (middle) and ethylene oxide (right).

The other byproducts, which are classified by the IARC as a group 1 material (carcinogenic in humans) are formaldehyde and ethylene oxide. Ph. Eur. limits the content of ethylene oxide to 1 ppm and the amount of formaldehyde to 30 ppm in PEG for pharmaceutical applications.[7]

But the degradation of PEG with a molar mass below 400 Da is definitely toxic for humans.[7] With increasing molar mass the oxidative degradation significantly decreases, which is actually the major breakthrough for PEG in biomedicine today.[14]A example in everyday life there is PEG incompatibility in beauty creams and crystallization of PEG on hairs.

To find alternatives to PEG several other potentially biocompatible polymers like poly(hydroxyethyl-l-asparagine) (PHEA), poly-(hydroxyethyl-l-glutamine) (PHEG), poly(2-oxazoline) and poly(glutamic acid) (PGA) are being investigated.[17-19] In this work we focus on the class of poly(phosphoester)s (PPEs), which will be introduced in the next chapter (chapt.).

3.2 POLY(PHOSPHOESTER)S (PPE)

In nature, phosphorus-based polymers are a predominant class of materials, which appear for example in DNA (Deoxyribo Nucleic Acid)/RNA (Ribo Nucleic Acid) and ATP (Adenosine TriPhosphate) (Figure 3-3).
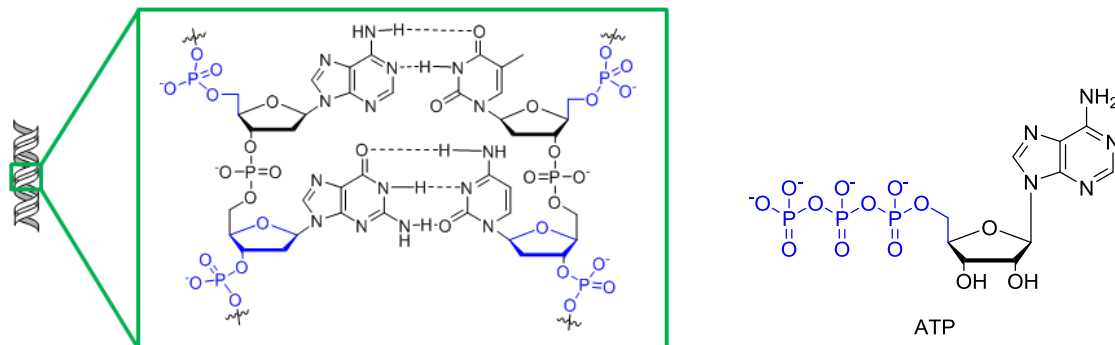

Figure 3-3: Structure of DNA (left), ATP (right).

There they play a crucial role either in energy storing or in the formation of a stable but on demand degradable backbone for data storage. Polyphosphoesters pose the advantage over traditionally used carboxylic acid esters as they have the capability to form triesters. Therefore PPEs may possess functional or solubilizing groups along in the polymer backbone (Figure 3-4). The breakthrough of the synthetic PPEs goes back to the 1970's, when Penczek *et al.* published their pioneering work regarding synthesis and characterization of PPEs by polycondensation, polyaddition, and ring-opening polymerization (ROP).[20-25] They managed to synthesize poly(phosphate)s and poly(alkylene H-phosphonate)s in 1983 (Figure 3-4).[26] Penczek *et al.* synthesized PPE's 1977 via cationic polymerization at 100°C and 1993 the synthesis goes via polycondensation.[20,21]
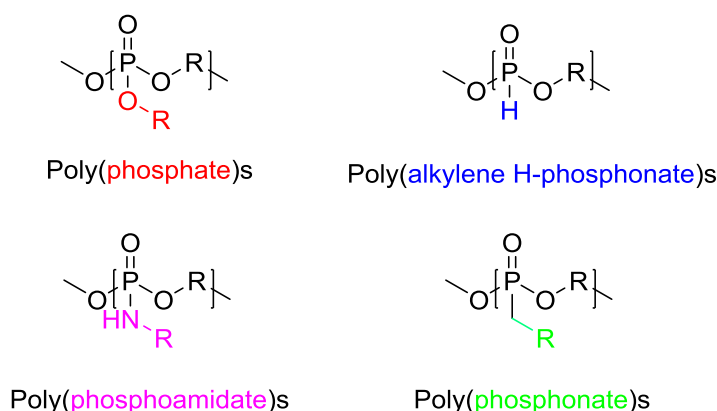

Poly(phosphate)s   Poly(alkylene H-phosphonate)s

Poly(phosphoamidate)s   Poly(phosphonate)s

Figure 3-4: Different types of PPEs.

Iwasaki and co-workers first reported that the organobases, 1,8-diazabicyclo[5.4.0]undec-7-ene (DBU) and 1,5,7-triazabicyclo[4.4.0]dec-5-ene (TBD), also known as "superbases", can be used for the ring opening polymerization (ROP) of PPEs.[27]

2001 Wang, Mao, and Leong studied the degradation of a polyphosphate hydrolysis with pendant amino groups.[28] Then 2013 Wooley and co-workers studied the pH dependency of the hydrolysis of a polyphosphoamidate by ^{31}P NMR spectroscopy.[29] In the same year Wooley and coworkers published an in-depth study of the cytotoxicity, immune toxicity, and bio fouling properties.[30]

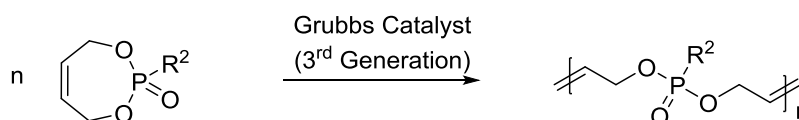Our research group focused their research on the synthesis of PPEs through different methods. Anionic ring opening polymerization (AROP), acyclic diene metathesis polymerization (ADMETP), Ring-opening metathesis polymerization (ROMP) proved to be suitable methods to obtain PPEs with a variety of different properties (Figure 3-5).[31-33]
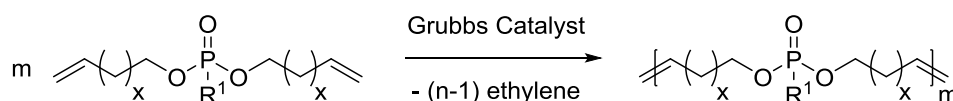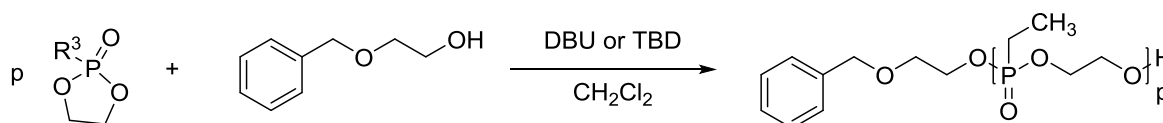

Figure 3-5: Different reaction routes for the synthesis of polyphosphoesters.

3.3 Anionic Ring-Opening Polymerization (AROP)[34],[35]

The anionic ring opening polymerization (AROP) belongs to the chain growth polymerizations. As the name implies a cyclic monomer is ring-opened by nucleophilic attack of an anionic initiator. Several cyclic monomers, like cyclic ethers, lactones or other heterocyclic compounds (thiirane, thietane, dioxaphospholanes) have successfully been polymerized with this type of reaction.[35-37] Figure 3-6 shows a scheme of an AROP.

X= O,S; Y= Li, Na, K, Cs, R_4N^+
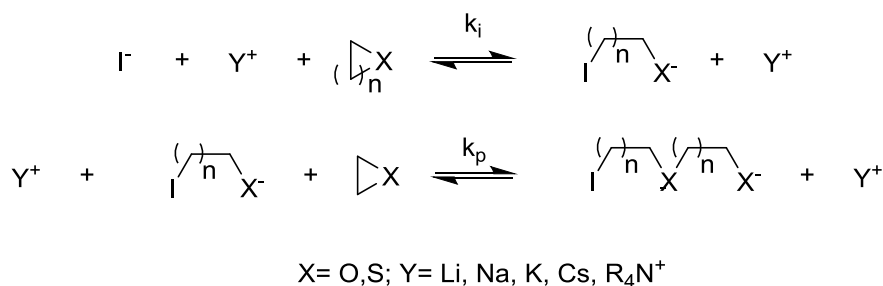
Figure 3-6: General procedure of an AROP of cyclic monomer.

The polymerization begins with the nucleophilic attack of the initiator to the monomer. After initiation the chain grows by subsequent attack on the next cyclic monomer. This propagation continues till the termination is conducted. However, it is possible that unwanted termination takes place in the presence of electrophilic impurities such as water, CO_2.

In the case of AROP Of cyclic phosphates organobases were used for complexation with the initiator for the AROP (cf. chapter 3.1.2). In Figure 3-7 the activation of the initiator (an alcohol) by the organobase (left: DBU) or the activation of both initiator and monomer (TBD) and the attack to the monomer is shown.

Figure 3-7: Activation of 2-(benzyloxy)ethanol with DBU (left)and TBD (right) and attack of activated initiator on the cyclic monomer.

The efficiency of polymerization of a cyclic monomer depends on thermodynamic and kinetic factors.[36,38] Most important thermodynamic factor is the relative stabilities of the cyclic monomer and linear polymer structure.[36,38]

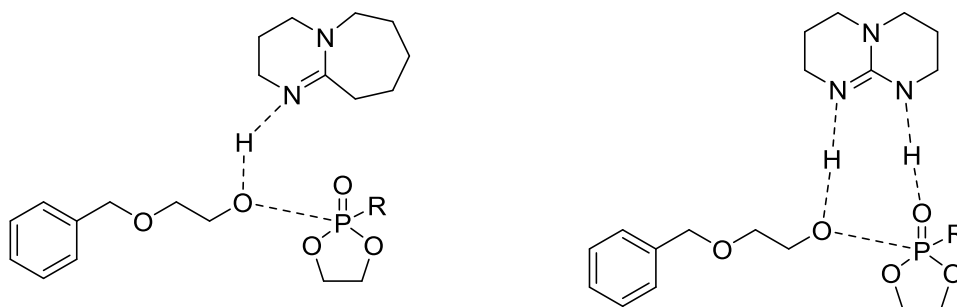It was found out that the polymerization for cycloalkane is favored thermodynamically for all except the 6-membered ring, because the thermodynamic stability of the 6 membered is very stable. The order of the thermodynamic stability of the rings is 3; 4 < 5; 7~13 < 6, 14 (Table 3-1).[36]

Table 3-1: Thermodynamics of Polymerization of
Cycloalkanes at 298 K.

$(CH_2)_n$ ring	ΔH/ kJ mol^{-1}	ΔS/ J mol^{-1} K^{-1}	ΔG/ kJ mol^{-1}
3.00	-113.00	-69.10	-92.50
4.00	-105.10	-55.30	-90.00
5.00	-21.20	-42.70	-9.20
6.00	2.90	-10.50	5.90
7.00	-21.80	-15.90	-16.30
8.00	34.80	-3.30	-34.30

The Gibbs free energy ΔG of the 6 rings is positive so the polymerization is not favored at this condition. But the ring can open by increasing the temperature, where ΔG gets more negative, which is given by the Gibbs–Helmholtz equation ($\Delta G = \Delta H - T \Delta S$). The presence of substituents, Double bonds, heteroatoms, different hybridization of ring atoms decreases thermodynamic feasibility for polymerization.

Because the interactions between substituents are more hard in the linear polymer than in the cyclic monomer.[36]

It is possible that AROP has the process of a living polymerization.[36] A living polymerization is a polymerization where the initiations rate is higher than the propagation rate and there is no termination/ transfer reaction takes place.[39] The lifetime of the growing and active chain is immortal and the reaction ends when the conversion of the monomer is 100 %. A typical graph of polymerization is plotting the degree of polymerization against the conversion, which is shown in Figure 3-8.[40] If it is a living polymerization the graph proceeds linearly.
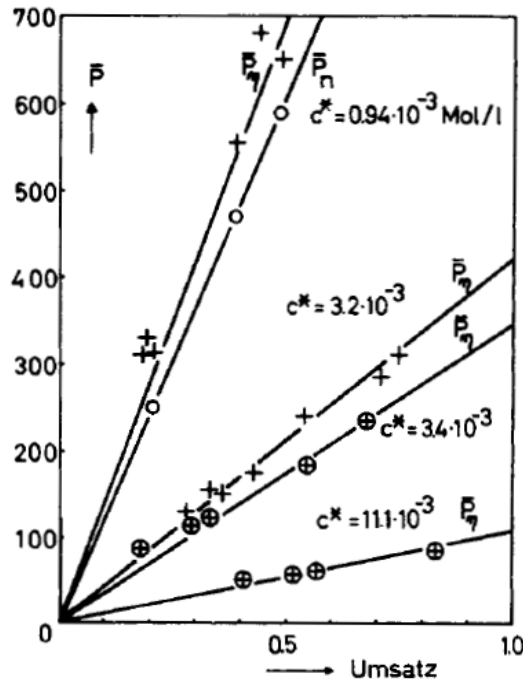
Figure 3-8: Degree of polymerization against conversion of living polymerization.

It is possible that the termination reaction has a transfer reaction character.[35] Because the active center (alcoholate) is not only a nucleophile, at the same time it is a base, too. The reactive chain end can abstract a proton from the monomer or the growing polymer chain (or the solvent). This is the reason why the growing chain can terminate but at the same time it generates a new active center. But to avoid this effect complexing agents, like crown ethers (for epoxides) are used as counter ion. In this case the dissociation and the formation of free ions are favored.[34,35] One application in the industrial process of the AROP is the production of Nylon 6, PEG and Perlon.

3.4 PROTEIN ADSORPTION

In this work, the interaction of silica gel particles with human plasma is studied. Especially, in nanomedicine there has recently been a lot of effort made to understand the impact of protein adsorption on the surface of nanomaterials, as this process highly influences the nanoparticles' behavior in a biological environment.

As soon as a nanoparticle comes in contact with a biological system (e.g. blood) the surface of the material will be covered by proteins, forming what is known as the protein corona.[2,3,41]

The protein corona of nanoparticles critically influences biological parameters including cytotoxicity, body distribution or endocytosis into specific cells.[41-43]
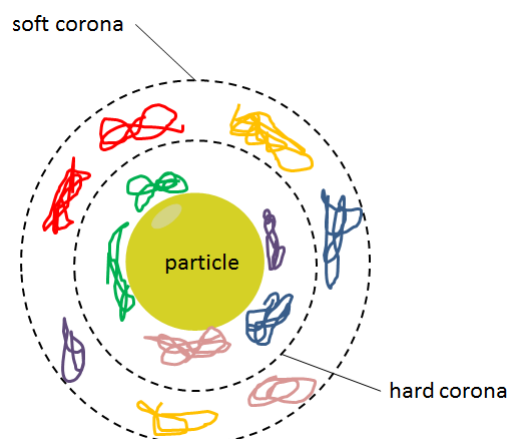
Figure 3-9: Schematic of protein corona formation on a particle surface.

Figure 3-9 shows schematically the formation of the protein corona on the surface of a nanoparticle. The protein corona believed to be divided in two different layers. The inner layer is dominated by proteins which are closely bound and highly interact with the surface of a nanoparticle. This layer is called the "hard corona". The outer layer is characterized by proteins which have a lower affinity to the nanomaterial and are loosely bound. This part is referred as "soft corona".

The interaction of proteins and various nanoparticles e.g. polymeric nanoparticles or silica nanoparticles is extensively being studied.[4,5] There were distinct proteins identified which specially bound to their surface.[44,45]

In addition, the influence of different surface functionalization of nanoparticles and its impact on protein adsorption was analyzed.[46]

Especially, polyethylene glycol (PEG) functionalized nanoparticles were investigated as PEG was found to significantly decrease protein adsorption.[41,47]

This work studied the interaction of non-functionalized or functionalized silica gel particles with human plasma. Those silica gel particles were functionalized with either PPEs or PEG.

3.5 Solid State Nuclear Magnetic Resonance Spectroscopy (SS-NMR- Spectroscopy)[48]

For characterization of the functionalized silica (chap.4.2) we used the SS-NMR. In this chapter a short introduction about the measurement and some techniques are given.

SSNMR is used for solid state samples and samples, which are hard to dissolve in deuterated solvents. In general, the theory for this method is the same as for liquid NMR. However, several techniques have to be applied in SS NMR to get sharp peaks. These techniques explained in the following.

In Figure 3-10 the ^{13}C-NMR measurement of a glycine in water and the glycine (solid) is shown.[48]
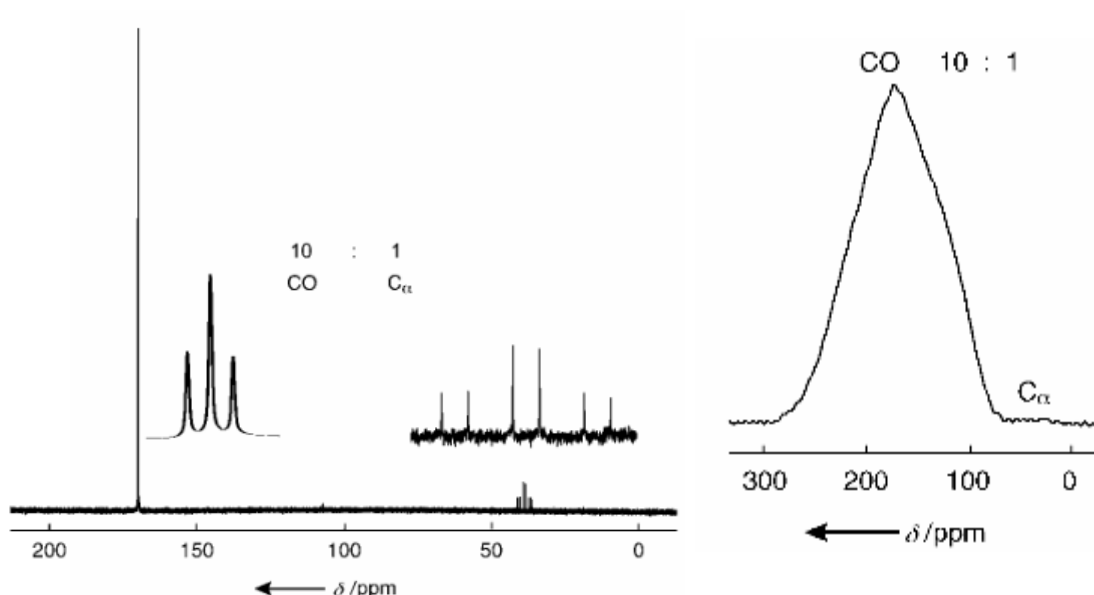
Figure 3-10: ^{13}C NMR of glycine in water (left) and glycine as solid (right).

In the spectra of dissolved glycine (Figure 3.10) there are two intensive and well resolved peaks. But the spectra of the solid state (Figure 3.10) show only very broad peak, which is hard to interpret.[48] In solid state NMR broad peaks are due to several orientation dependent local interactions, such as hetero-nuclear and homo-nuclear dipolar couplings, and chemical-shift anisotropy.[48]

To avoid these broad peaks and enhance the signal, several techniques were developed. In the next two chapters an introduction of the two techniques will be given, which were used for our measurement. These are cross polarization (CP) and the magic angle spinning (MAS).[48,49]

3.5.1 Magic angle spinning (MAS)[48]

We mentioned that the line broadening in the solid state can be the result of several orientation dependent local interactions. All of these orientation dependent interactions have second rank tensorial properties so that orientation dependent contributions vanish at the magic angle (θ_m= 54.74°). In other words dipole dipole interactions between the magnetic moments of the nuclei as well as anisotropic contributions the electronic shielding are zero when the connecting vector between the two magnetic moments or the chemical shift anisotropy tensor is oriented at the magic angle (θ_m= 54.74°) with respect to the outer magnetic field.[48] Making use of the fact, that fast spinning averages all tensorial interactions to effective axial tensorial

Figure 3-11: Solid state[13]NMR of glycine at several spinning speed.

interactions aligned along the spinning axis, fast sample spinning at the magic angle relative to the direction of the magnetic field averages all dipolar couplings between the nuclear spins to zero and the chemical shift anisotropy, resulting from the un-isotropic distribution of electron density around a nuclear spin is averaged to the isotropic value observed on solution NMR spectroscopy. That means that the broadening of anisotropic interactions is removed and spectral resolution is recovered in SSNMR.[50] In solution the isotropic molecular motion is sufficiently fast to average out most of spectral contributions from orientation dependent NMR.

In Figure 3-11 there is a solid state ^{13}C NMR spectrum of glycine at different MAS spinning speeds.[48] We can recognize that at higher spinning speeds the peaks become much finer. That means the chemical shift anisotropy is eliminated with the increase of the spinning.

3.5.2 Cross polarization (CP)[48,49]

To improve the signal-to-noise ratio of rare nuclei (^{13}C, ^{15}N) the cross polarization (CP) is used. This technique is the most important signal enhancement in solid-state NMR.[51] In this method the polarization of an abundant and highly polarized nucleus (mostly ^{1}H) is transferred with lower polarization.

Under Hartmann Hahn conditions first polarization is transferred from the abundant nuclei with the spin *I* (typically ^{1}H), to the rare nucleus with the spin *S* (typically ^{13}C) (Figure 3-
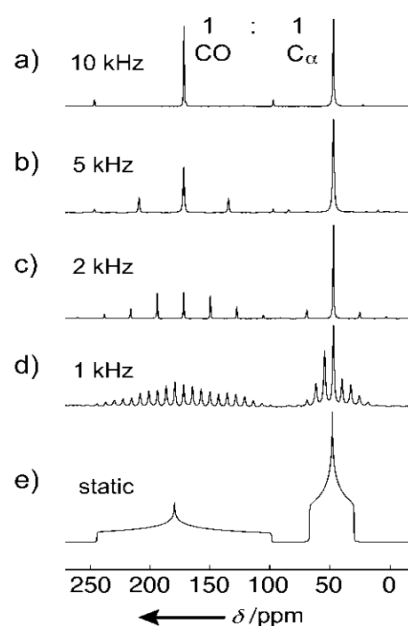
12).[48] Then the signal from spins S is then observed. Normally the spin-lattice relaxation of spin I is faster, so that the CP experiment can be repeated more rapidly, and the signal is accumulated faster.[51]

After the polarization transfer, the proton spins are decoupled from the carbon spins, so that line broadening of the carbon signals due to heteronuclear couplings is suppressed and high resolution carbon signals can be observed when the CP experiment is combined with magic angle spinning (MAS), often referred as CP-MAS.[49,52]
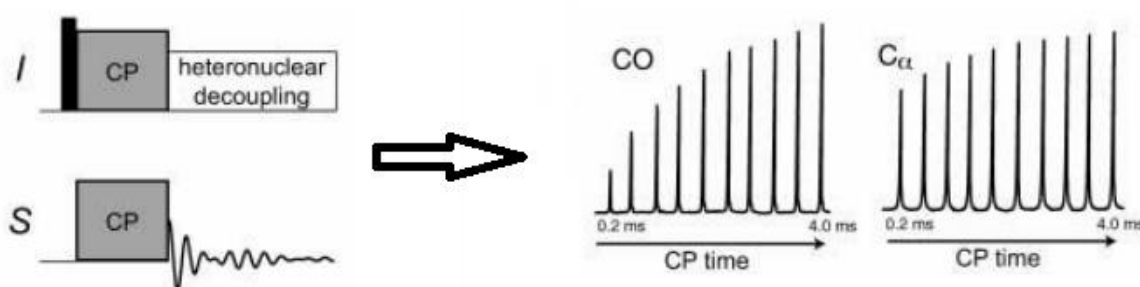

Figure 3-12: Scheme to explain the Hartmann Hahn cross polarization.

3.6 SODIUM DODECYL SULFATE POLYACRYLAMIDE GEL ELECTROPHORESIS (SDS PAGE)[53]

With the SDS PAGE the proteins and protein mixtures can be separated and/or analyzed on a polyacrylamide gel. With this method charged proteins can separated over an electric field. The mobility of the proteins depends on several factors like size, i.e. the molecular weight shape, and strength of the applied electric field.

The electrophoresis gel matrix is commonly made by a copolymer of acrylamide and *N, N'*-methylenebisacrylamide as a crosslinker.

The effect of SDS anions is that they can adhere to hydrophobic region of the proteins and can destroy the native structure of the proteins (polypeptides), whereby the charge the proteins is covered by the SDS, which gives them an anionic character. The result is that the negative charge is proportional to the molecular weight of the protein. SDS PAGE is shown in chap. 4.3.

4 RESULTS

4.1 SILYLETHER FUNCTIONALIZATION OF DIFFERENT POLYMERS

4.1.1 SYNTHESIS OF 2-(BENZYLOXY)-ETHANOL INITIATED POLY(ETHYLENE ETHYL PHOSPHONATE)-ω-)(3-(TRIETHOXYSILYL)PROPYL)CARBAMATE

As described in chapter 5-2, the polymer was synthesized according to literature protocol.[6] To enable efficient coupling onto a silica surface, the final polymer with a siloxane group was functionalized. These groups are known to couple onto silica surfaces under mild conditions.[54] The commercially available triethoxy(3-isocyanatopropyl)-silane was used for functionalization as isocyanates are known to smoothly react with hydroxyl groups under basic conditions. After precipitation the product was obtained and characterized with ^{1}H and ^{1}H DOSY NMR spectroscopy as well as with MALD-TOF MS.

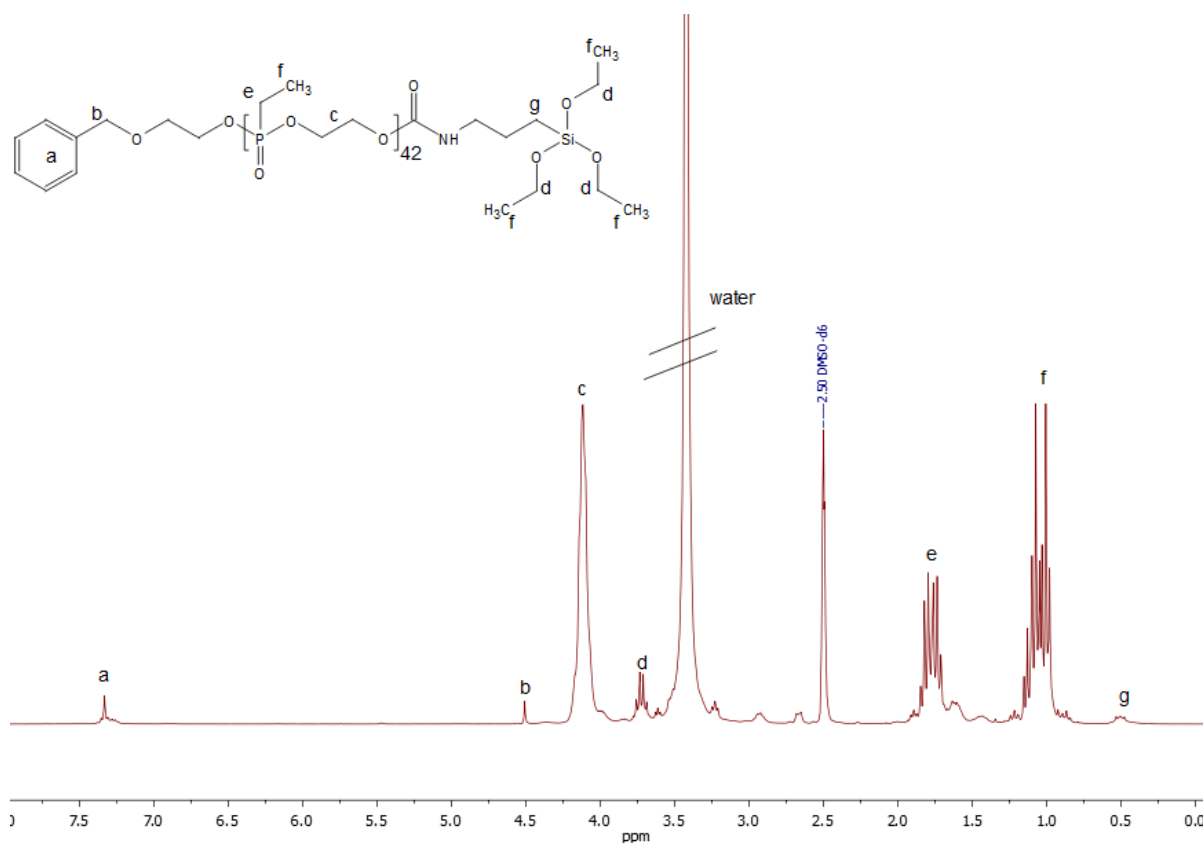**Figure 4-1:** ^{1}H NMR (500 MHz) of Poly((ethylene ethyl phosphonate)-ω-)(3-(triethoxysilyl)propyl)carbamate in DMSO-d_6 at 298 K.

Figure 4-1 shows the ^{1}H NMR spectrum of the ω-functionalized P(EtPPn). The proton signals of the siloxane group (peak d at 3.68 ppm and peak g at 0.51 ppm) are well separated from the rest of the peaks. Therefore the degree of functionalization could be determined via

^{1}H NMR (Table 4-1). The peak of the terminal CH_3 group of the siloxane superimposed the peak of the CH_3 side chain. Over ^{31}P NMR the peak at 34.52ppm (backbone) and 34.47 ppm (terminal) could assign to the polymer (Figure 4-2).[6]

Table 4-1: Calculated molar mass of poly(ethylene ethyl phosphonate)-ω-)(3-(triethoxysilyl)propyl)carbamate via ^{1}H NMR.

$M_{Initiator}$/g mol^{-1}	$M_{Isocyanate}$/ g mol^{-1}	$M_{Monomer}$ /g mol^{-1}	Sequence$_{calc.}$ by NMR	$M_{Polymer}$/ g mol^{-1}
152.19	247.37	135.97	42	6110.3

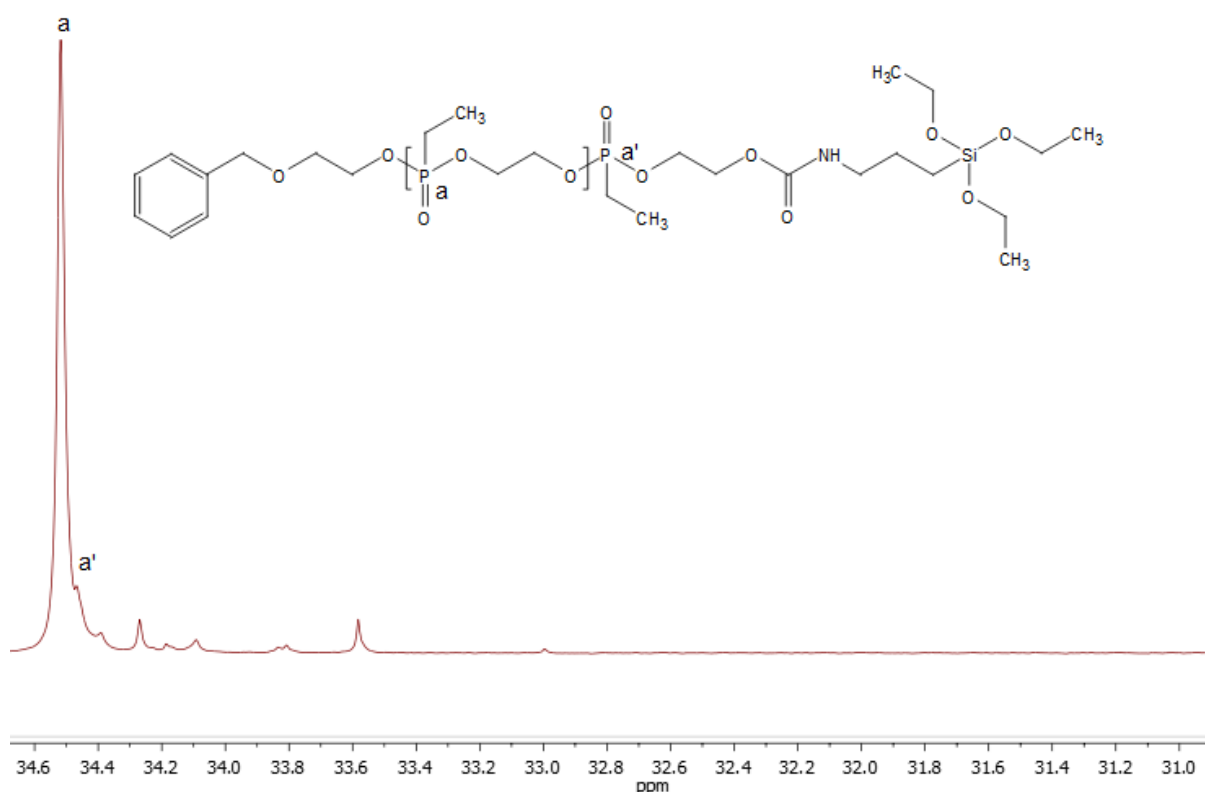**Figure 4-2: ^{31}P{H} NMR (201 MHz) of Poly((ethylene ethyl phosphonate)-ω-)(3-(triethoxysilyl)propyl)carbamate in DMSO-d_6 at 298 K.**

To guarantee the attachment of the functional group to the polymer backbone, a ^{1}H DOSY NMR measurement was performed. In this kind of measurement, the diffusion coefficient of each compound is measured and plotted against the ^{1}H proton signal it creates. Hence, it was important to see the -CH_2 methoxy group showing the same diffusion as the polymer backbone. The [1]H-DOSY measurement (Figure 4-3) shows that the peak of the methoxy group is on the same level as the backbone (4.12 ppm), indicating a successful functionalization.

Over ^{31}P NMR the peak at 34.52ppm (backbone) and 34.47 ppm (terminal) could assign to the polymer (Figure 4-2).[6]

Further prove the attachment of one functional group onto the polymer a MALDI TOF MS (Matrix-assisted Laser Desorption/Ionization- Time Of Flight) was measured. Figure 4-4 shows the MALDI TOF spectrum of the siloxane terminated P(EtPPn).

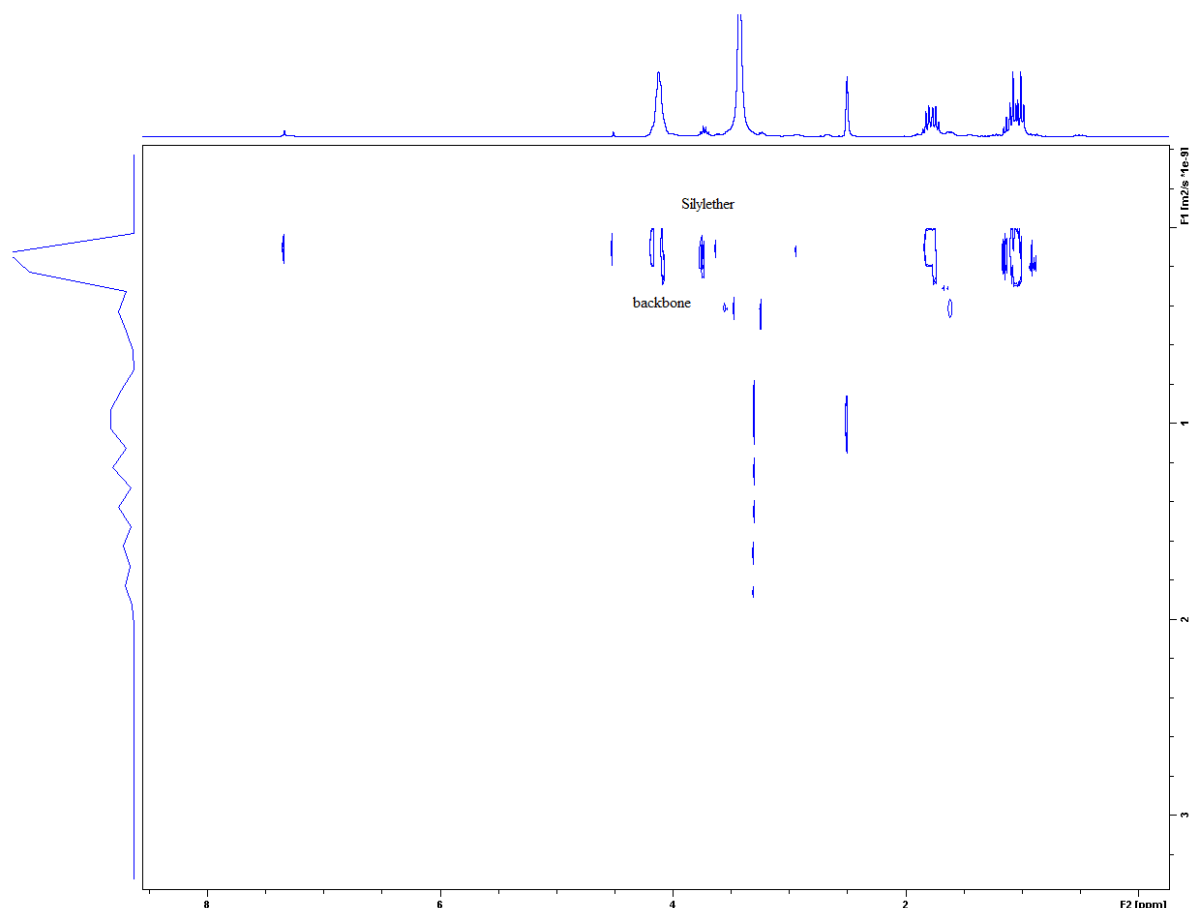**Figure 4-3: [1]H DOSY (500 MHz) of poly((ethylene ethyl phosphonate)-ω-)(3-(triethoxysilyl)propyl)carbamate in DMSO-d_6.**

In the spectrum several polymer peaks with their calculated molar mass/charge ratio are shown. To calculate how successful the functionalization was, following calculation was done.
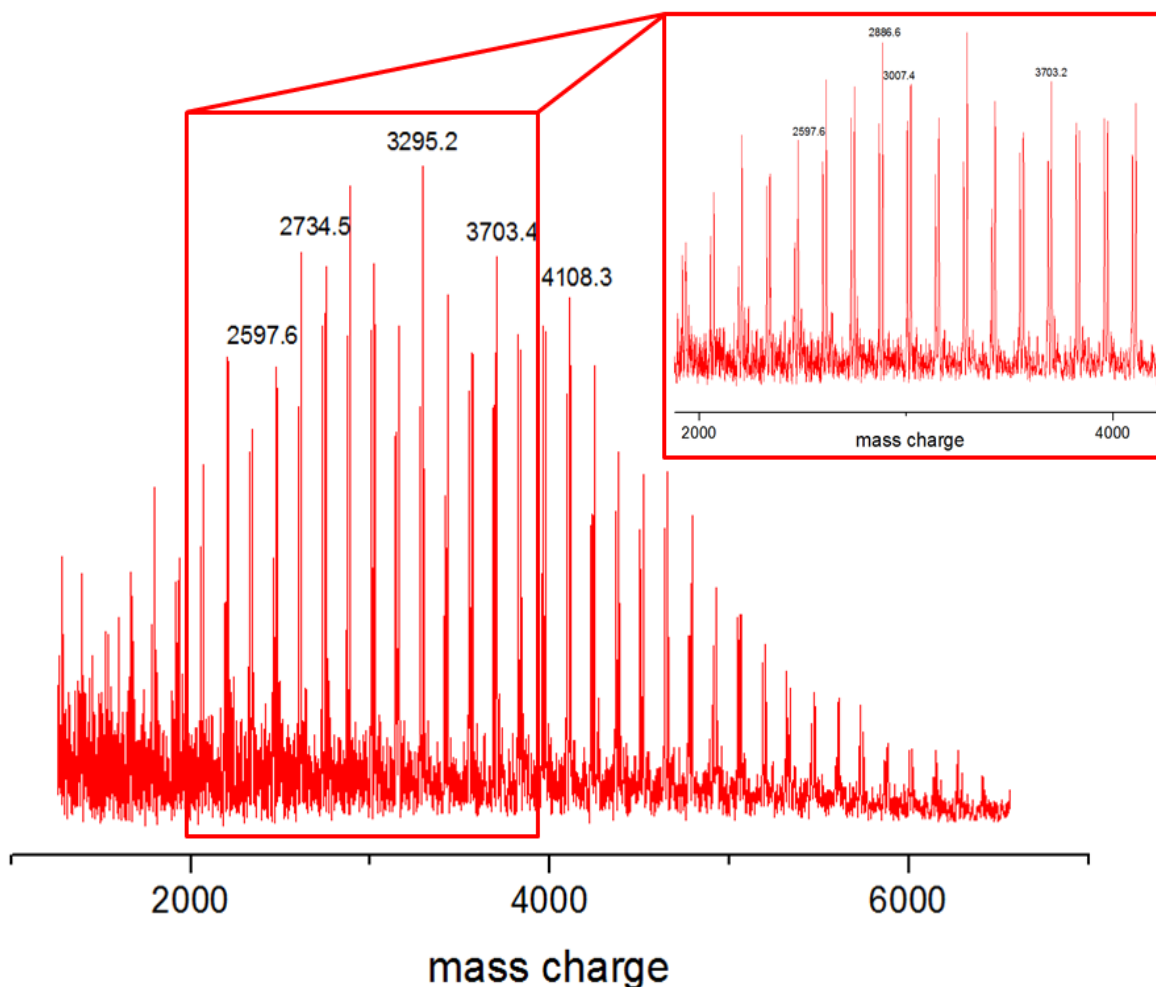
Figure 4-4: MALDI TOF mass spectrum of Poly((ethylene ethyl phosphonate)-ω-)(3-(triethoxysilyl)propyl)carbamate.

At 2597.6 g mol^{-1} there is a signal for polymer. The used monomer EtPPn has a molar mass of 135.97 g mol^{-1}.

The mass difference between two adjacent peaks is 135, which is fitting to our monomer sequence. To calculate how many groups were functionalized, first the molar mass of the initiator (151 g mol^{-1}) was subtracted from the polymer sequence ([1]).

$$2597.6 \ \tfrac{g}{mol} - 151 \ \tfrac{g}{mol} = \ 2446.6 \ \tfrac{g}{mol} \quad [1]$$

After subtraction the monomer sequence was subtracted. The sequence was calculated till the value is fitting to the molar mass of the isocyanate ([2] and [3]).

$$135 \tfrac{g}{mol} \times 16 \ Sequence = \ 2160 \ \tfrac{g}{mol} \ [2]$$

$$2446.6 \ \tfrac{g}{mol} - 2160 \ \tfrac{g}{mol} = 286.6 \ \tfrac{g}{mol} \ [3]$$

The polymer is charged negatively, so we have a counter ion which is either Sodium (21 g mol^{-1}) or Potassium (38 g mol^{-1}). But in this polymer there is an small amount of DBU (151 g mol^{-1}), which can act as counter ion, too. For this example potassium is the counter ion.

$$286.6 \frac{g}{mol} - 38 \frac{g}{mol} = 248.6 \frac{g}{mol} \quad [4]$$

After subtraction of the mass of potassium 248.6 g mol^{-1} remains ([4]). If we compare this mass with the theoretical mass of our terminal group of 247.37 g mol^{-1}, the conclusion is, the functionalization of our polymer was successful.

Gel permeation chromatography (GPC) (Figure 4-5) the polydispersity index ($Đ=M_n/M_w$) of poly((ethylene ethyl phosphonate)-ω-)(3(triethoxysilyl)propyl)carbamate was measured. The dispersity of 1.19 indicates a well-defined polymer.

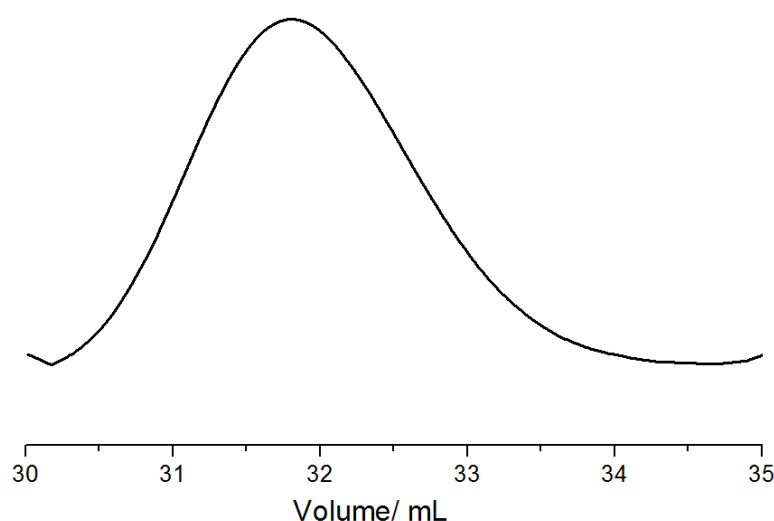
Figure 4-5: GPC of poly((ethylene ethyl phosphonate)-ω-)(3-(triethoxysilyl)propyl)carbamate.
The successfully synthesized a well-defined and ω-functionalized P(EtPPn) was proven by GPC, ^{1}H NMR, [1]HDOSY NMR and MALDI TOF MS.

4.1.2 Synthesis of N-(2,6-diisopropylphenyl)-N'-(4-hydroxyphenyl)-1,6,7,12-tetra-tert-octyl-phenoxy-perylene-3,4,9,10-tetracarboxydiimide initiated poly(ethylene ethyl phosphonate)-ω-)(3-(triethoxysilyl)propyl)carbamate

The synthesis of P(EtPPn), initiated by the dye N-(2,6-diisopropylphenyl)-N'-(4-hydroxyphenyl)-1,6,7,12-tetra-tert-octyl-phenoxy-perylene-3,4,9,10-tetracarboxydiimide (phenoxylated/N/-4-OH-ph-/N'/-DIPP-PDI) from Daniel Jänsch (AK Müllen), was synthesized at the condition, which are described in chapter 5-2. The ^{1}H NMR is shown in Figure 4-6. And over ^{1}H NMR the molar mass can be determined (Table 4-2).

Table 4-2: Calculated molar mass of poly(ethylene ethyl phosphonate)-ω-)(3-(triethoxysilyl)propyl)carbamate via ^{1}H NMR.

$M_{Initiator}$/ g mol^{-1}	$M_{Isocyanate}$/ g mol^{-1}	$M_{Monomer}$/ g mol^{-1}	Sequence$_{calc.}$ by NMR	$M_{Polymer}$/ g mol^{-1}
1459.96	247.37	135.97	18	4154,79

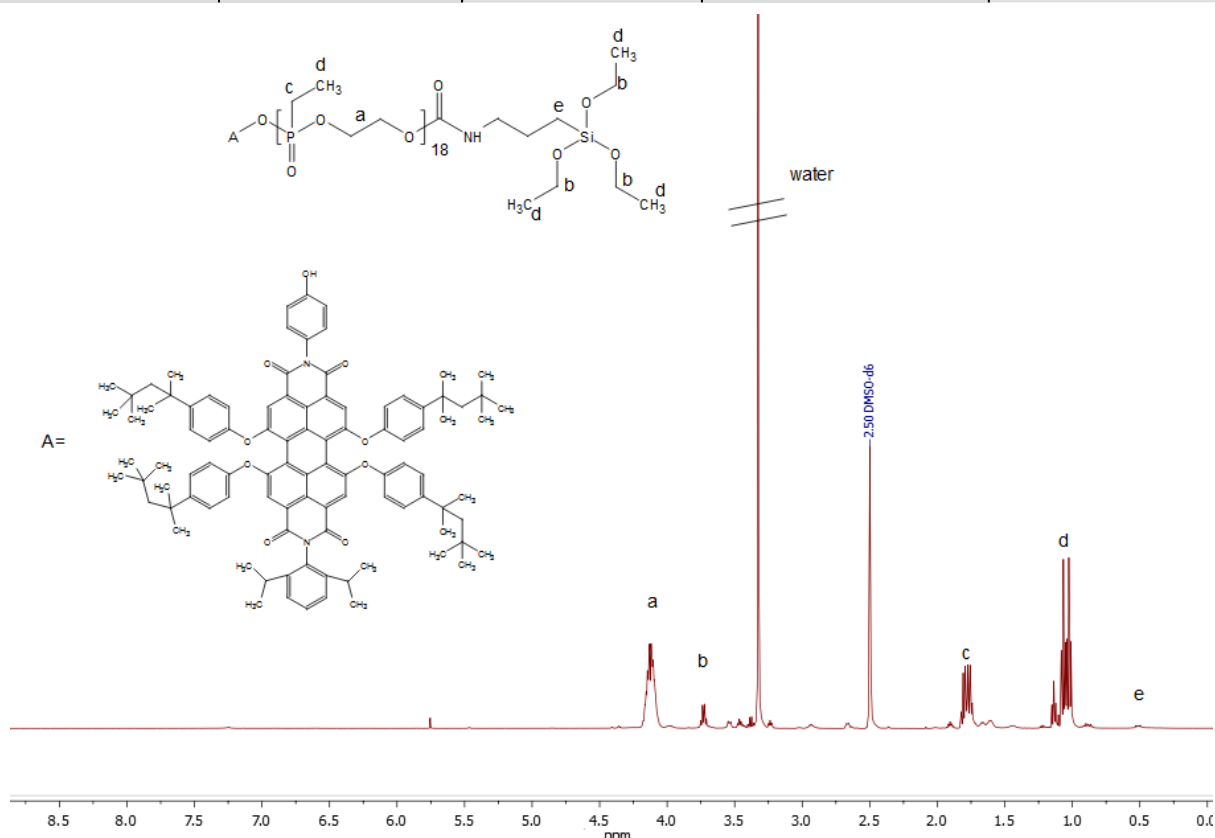**Figure 4-6: ^{1}H NMR (500 MHz) of poly((ethylene ethyl phosphonate)-ω-)(3-(triethoxysilyl)propyl)carbamate in DMSO-d_6 at 298 K.**

It is getting clear that the proton signals of the siloxane group (peak b at 3.73 ppm and peak e at 0.51 ppm) are well separated from the rest of the peaks, too. In this spectrum the proton peaks of the dye can not calculate because they are not visible. But it can be said that the

polymerization of the polymer was successful because the peak of the backbone at 4.13 ppm is visible.

Over ^{31}P NMR the peak of the backbone (34.51 ppm).and terminal (34.38 ppm) phosphorus can calculate. The ^{31}P NMR is shown in Figure 4-7.
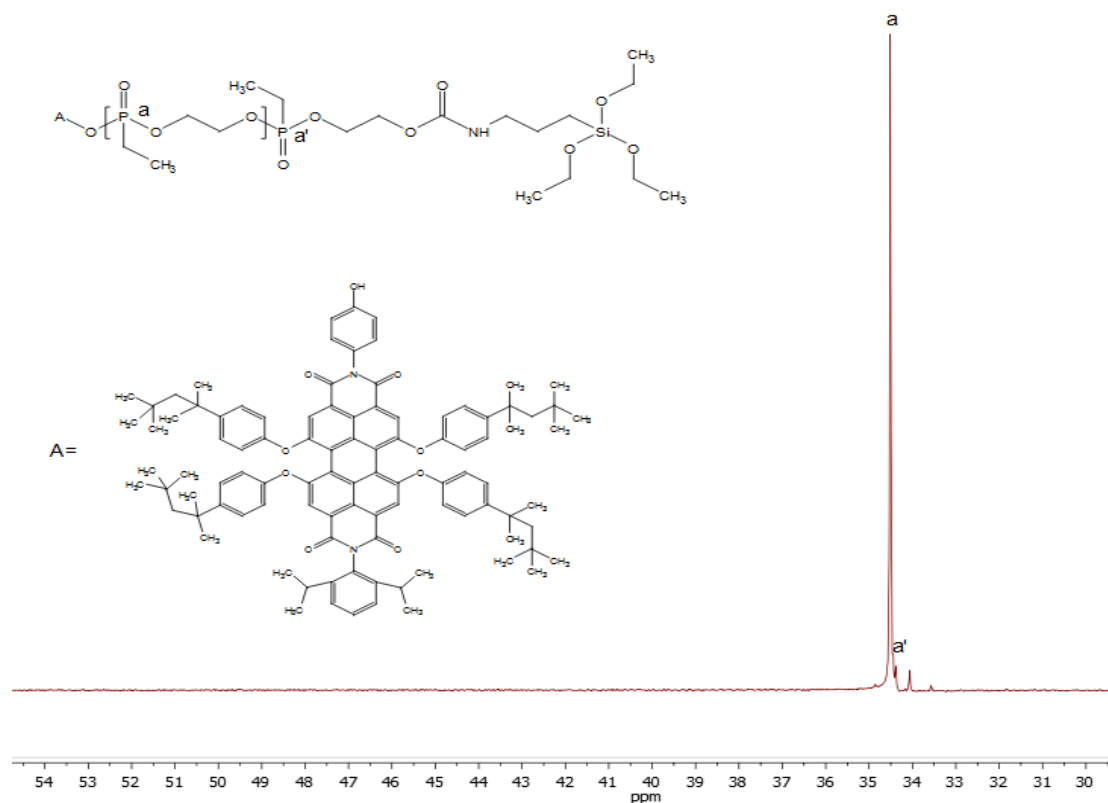
Figure 4-7: ^{31}P{H} NMR (201 MHz) of Poly((ethylene ethyl phosphonate)-ω-)(3-(triethoxysilyl)propyl)carbamate in DMSO-d_6 at 298 K.

Over ^{1}H-DOSY measurement (Figure 4-8) the peak of the methoxy group (3.73 ppm) is on the same level as the backbone (4.13 ppm), which assign a successful functionalization.

Gel permeation chromatography (GPC) (Figure 4-9) shows a polydispersity index (Đ=M_n/M_w) of 1.26, which indicates a well-defined polymer.
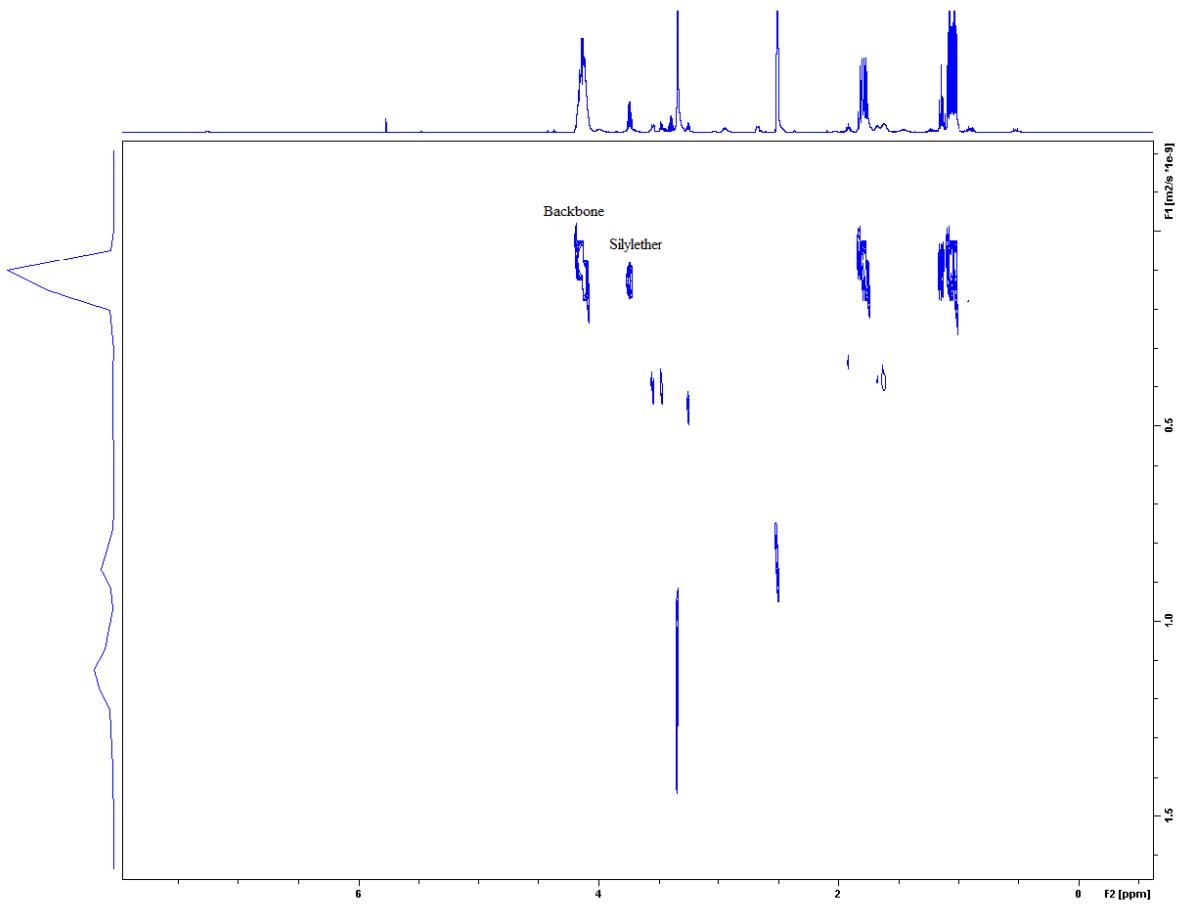
Figure 4-8: ^{1}H DOSY (500 MHz) of poly((ethylene ethyl phosphonate)-ω-)(3-(triethoxysilyl)propyl)carbamate in DMSO-d_6.
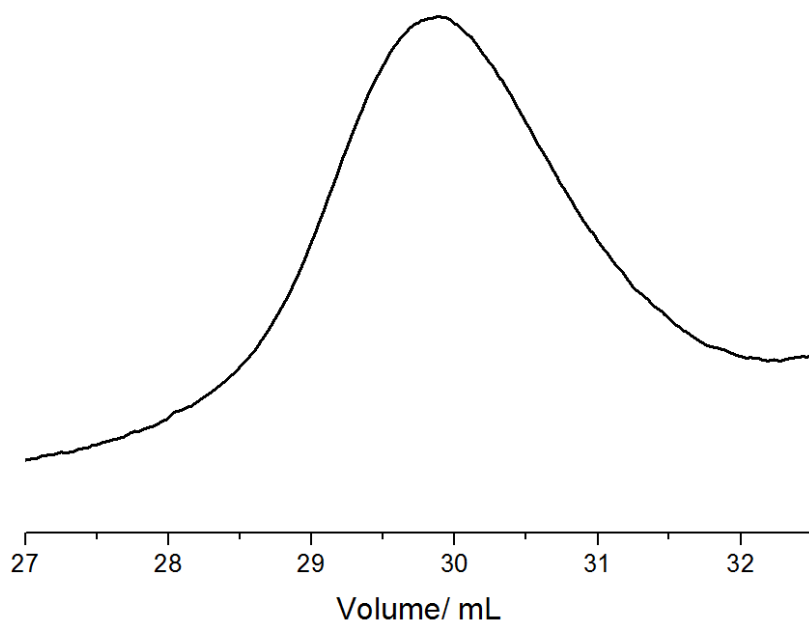
Figure 4-9: GPC of poly((ethylene ethyl phosphonate)-ω-)(3-(triethoxysilyl)propyl)carbamate.

The dye initiated polymer is very interesting for surface functionalization and for surface measurements. The cooperation with Dr. Encinas (AK Butt) shows that functionalization of Janus Pillars (SiO_2) by the dye initiated polymer was successful. In Figure 4-10 is a 3D laser scanning images of polymer functionalized Janus Pillars, which was measured by Dr. Encinas.
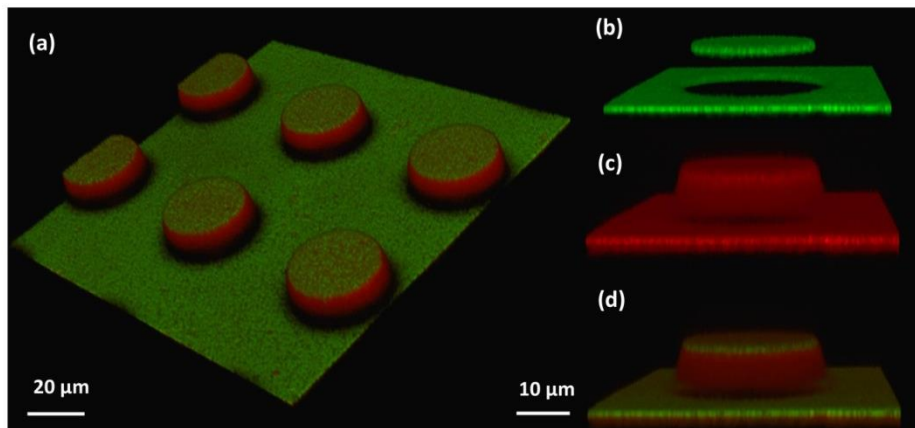
Figure 4-10: 3D laser scanning images of the polymer chemically attached to Janus pillars (a) showing the different channels of fluorescence and reflection arising from the labelled polymer (green, a), the pillars (red, b) and the overlay of every interface.

So it can be said that the synthesis of dye initiated polymer and functionalization was successful which can be used for further surface experiments.

4.1.3 α-METHOXY POLY(ETHYLENE GLYCOL)-ω-(3-(TRIETHOXYSILYL)PROPYL)CARBAMATE

The procedure of the synthesis is shown in chapter 5.2. As already shown in chapter 4.1.2 ¹H NMR and a ¹H DOSY NMR spectroscopy were used for characterization. The ¹H NMR is shown in Figure 4-11. Again ¹H DOSY NMR (Figure 4-12) shows that the crucial signals of the backbone (3.55 ppm) and the siloxane group (3.81 ppm) show the same diffusion coefficient. It was important like in the previous chapter that the siloxane group and the backbone peak are at the same level. To conclude the results of these two NMR measurements, the functionalization takes place and it can be used for following experiments.

Figure 4-11:¹H NMR of α-methoxy poly(ethylene glycol)-ω- (3-(*tri*ethoxysilyl)propyl)carbamate.

Figure 4-12: ¹H-DOSY measurement of α-methoxypoly(ethylene glycol)-ω- (3-(triethoxysilyl)propyl)carbamate.

4.2 FUNCTIONALIZATION OF SILICA
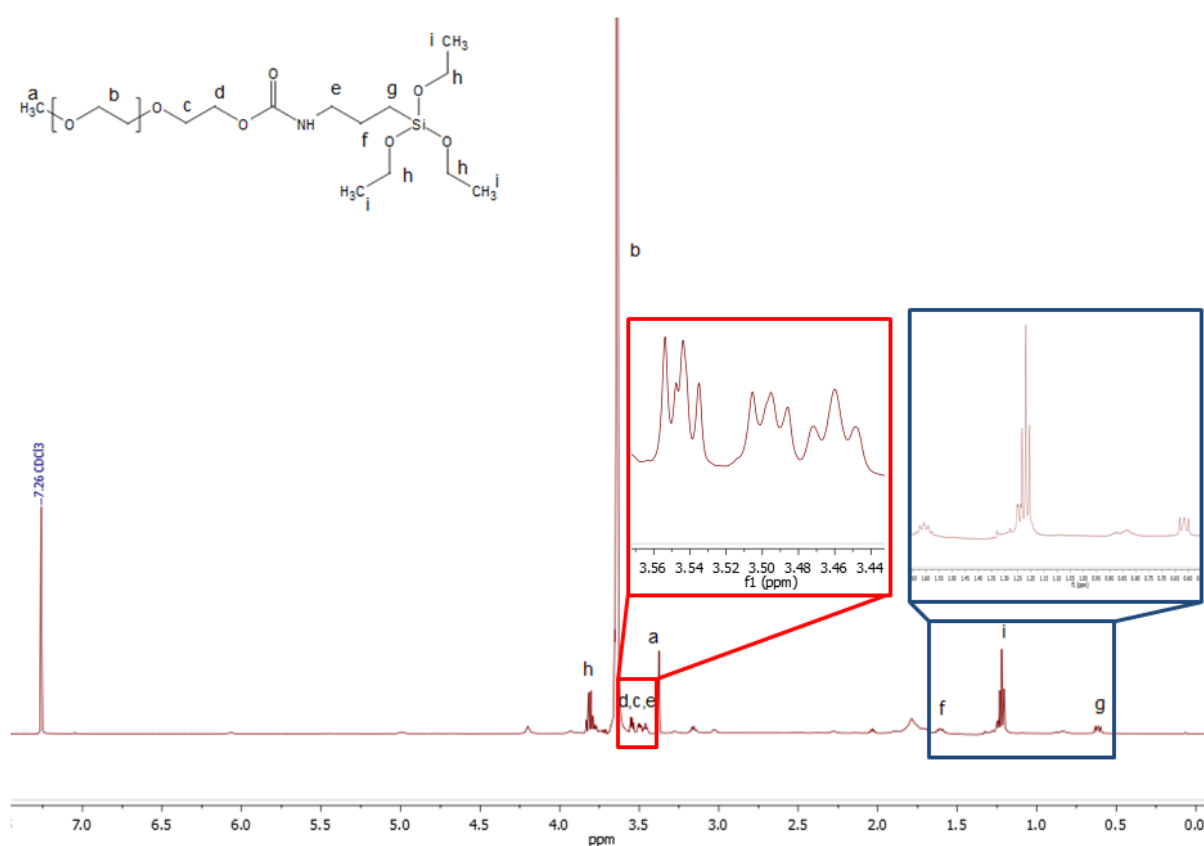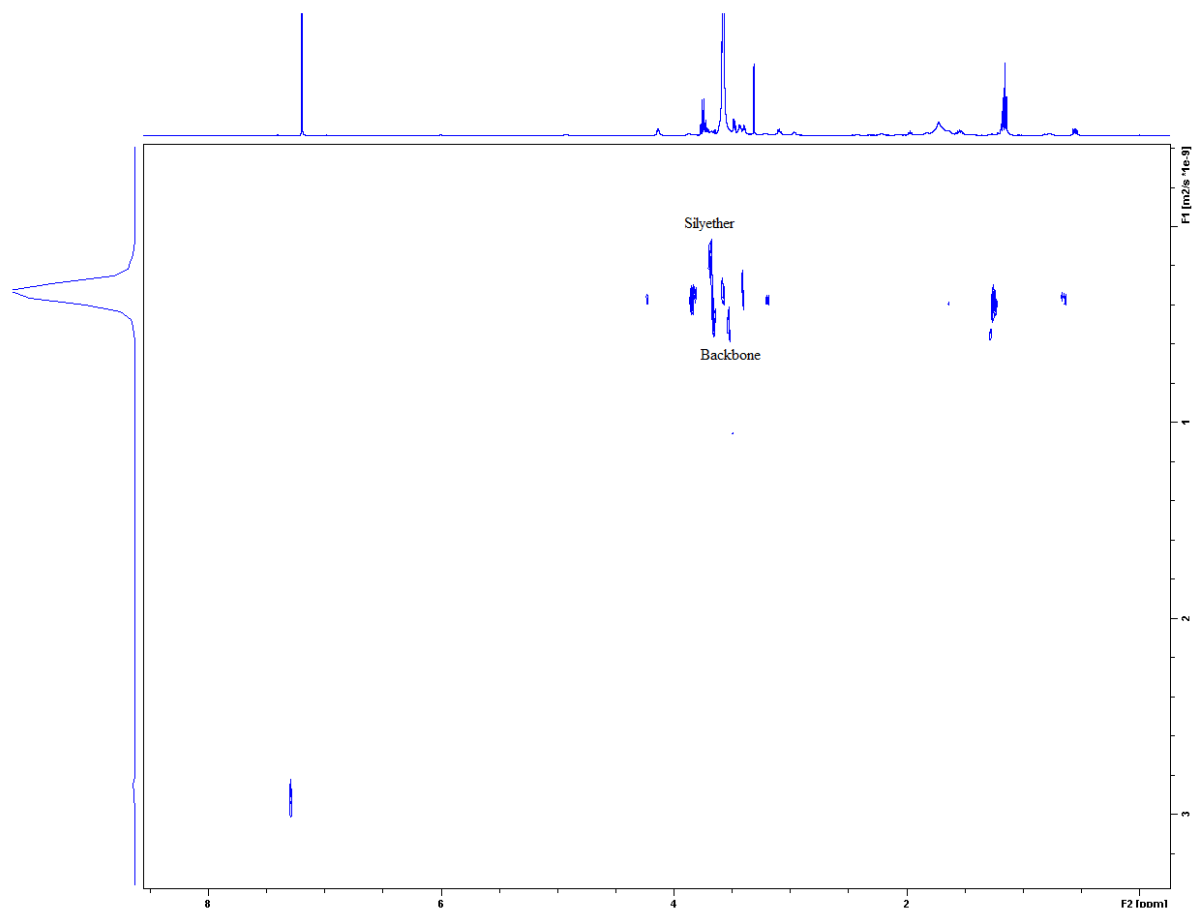
Silica 60 (0.063 - 0.2 mm) from Macherey-Nagel GmbH& Co. KG (Germany) was used for the functionalization.[55] The execution of the functionalization is described in chapter 5.3.1, 5.3.2.

For characterization of the functionalized particles, SS-NMR spectroscopy was used. We measured for every sample ^{29}Si MAS spectra and other nuclei, depending on the decoration of the specific particles. The spectra were analyzed via the software TopSpin 3.0. (Bruker) and are shown in Figure 4-13 till 4-16.
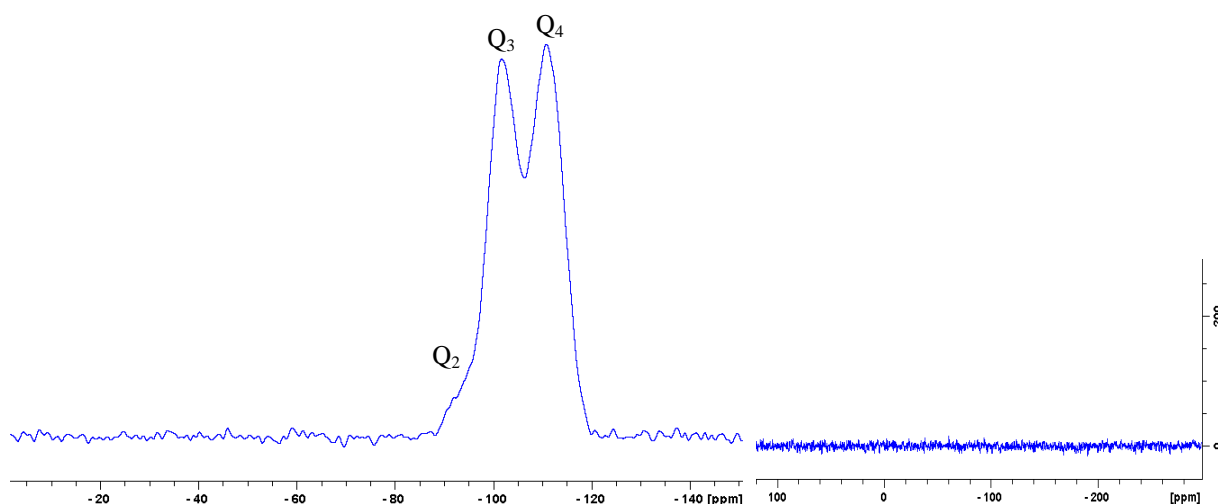
Figure 4-13: ^{29}Si CP MAS-NMR (left) and ^{31}P MAS-NMR (right) of SiO$_2$.

Figure 4-13 shows the ^{29}Si NMR spectrum (10 kHz) of pure silica particle. Only the quaternary (Q$_4$), tertiary (Q$_3$) and secondary (Q$_2$) siloxane peaks (-94.9 ~ - 110.9 ppm) are visible.[56] In ^{31}P NMR spectra no signals are detected as expected because we do not any phosphorus compounds.

For the ω-siloxane functionalized poly(2-ethyl-2-oxo-1,3,2-dioxaphospholane) (P(EtPPn)) grafted onto Silica a peak at 34.4 ppm in the ^{31}P-MAS NMR spectrum is detected which shows that our phosphor containing polymer is grafted onto the silica surface (Figure 4-14). That means the functionalization of the silica particles was successful.[57] In the ^{29}Si CP MAS spectrum the quaternary, tertiary and secondary siloxane peaks (-94.9 ~ - 110.9 ppm) can detected. The peak at -91.3 ppm, which can be assigned to secondary siloxane, is much more pronounced.[56]
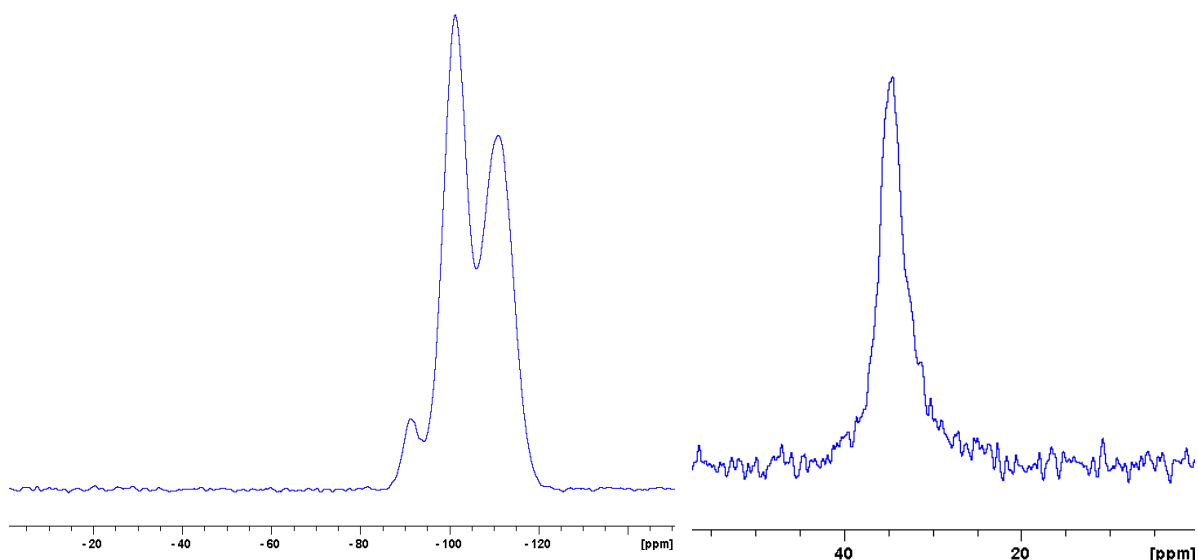
Figure 4-14: ^{29}Si CP MAS-NMR (left) and ^{31}P CP-NMR (right) of P(EtPPn) SiO$_2$.

For PEG functionalized silica particle (Figure 4-15) the ^{29}Si CP MAS-NMR spectrum looks similar to Figure 4-14. In ^{13}C NMR the peaks 59.4 ppm results from the carboxylic ester and the backbone peak can be found at 70.9 ppm for the PEG functionalized SiO$_2$. At 15.65 ppm the peak could the alkyl peak of the Si-(CH$_2$)$_3$ chain.
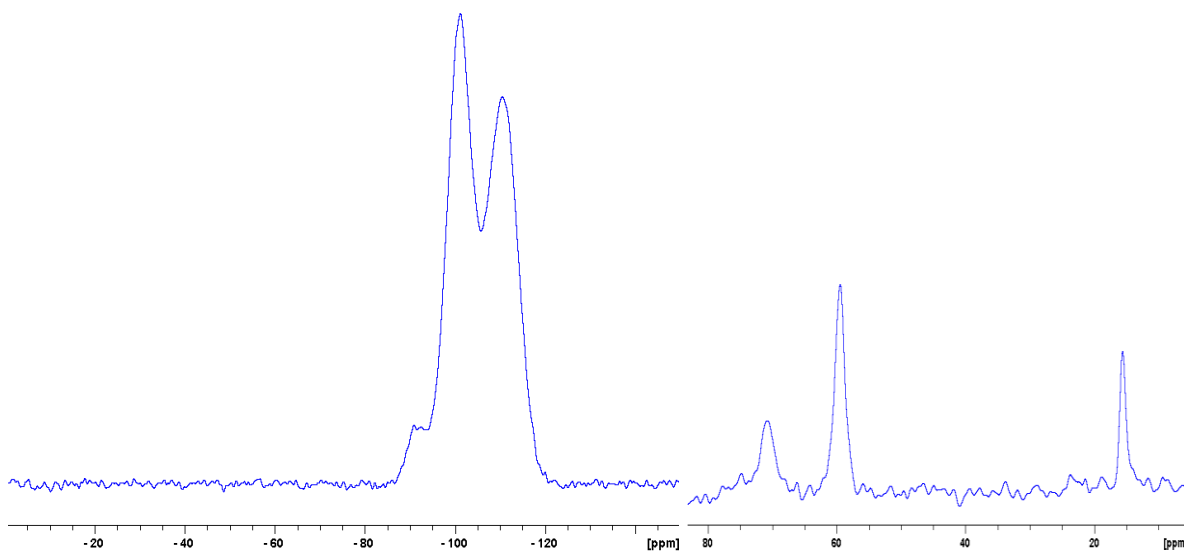
Figure 4-15: ^{29}Si CP MAS-NMR (left) and ^{13}C CP MAS-NMR (right) of PEG functionalized SiO$_2$.

Characterization of the grafting from (g.f.) approach was conducted in a similar way. The ^{29}Si CP MAS and ^{31}P CP MAS-NMR spectra are shown in Figure 4-16. The characteristic siloxane peaks are recognizable. In addition, two peaks at - 57.1 ppm and - 65.5 ppm are visible. These are the peaks of the Si-C Bonds. The peak at - 57.1 ppm is the secondary silylether and the peak at - 65.5 ppm is the tertiary silylether.[58,59] This shows that the density of the silylether is higher than the other samples as these signals were otherwise non

distinguishable from the background. That proves that the grafting from methods results in a higher density of silylether groups compared to the grafting onto method. In ^{31}P spectrum peaks at 27.1 ppm and 34.6 ppm are detectable. The peak at 34.6 ppm can be assigned to the characteristic signal for the P(EtPPn), but it is hard to conclude whether or not the polymerization was successful since in this area signals for ring opened phosphodiester are observe.[6] The peak at 27.1 ppm can assign a signal for the ring-opened phosphoester.[60] To conclude the monomer reacts with the particle. At the moment it is not possible to say, whether the polymerization occurred or if the surface is functionalized with oligomers.
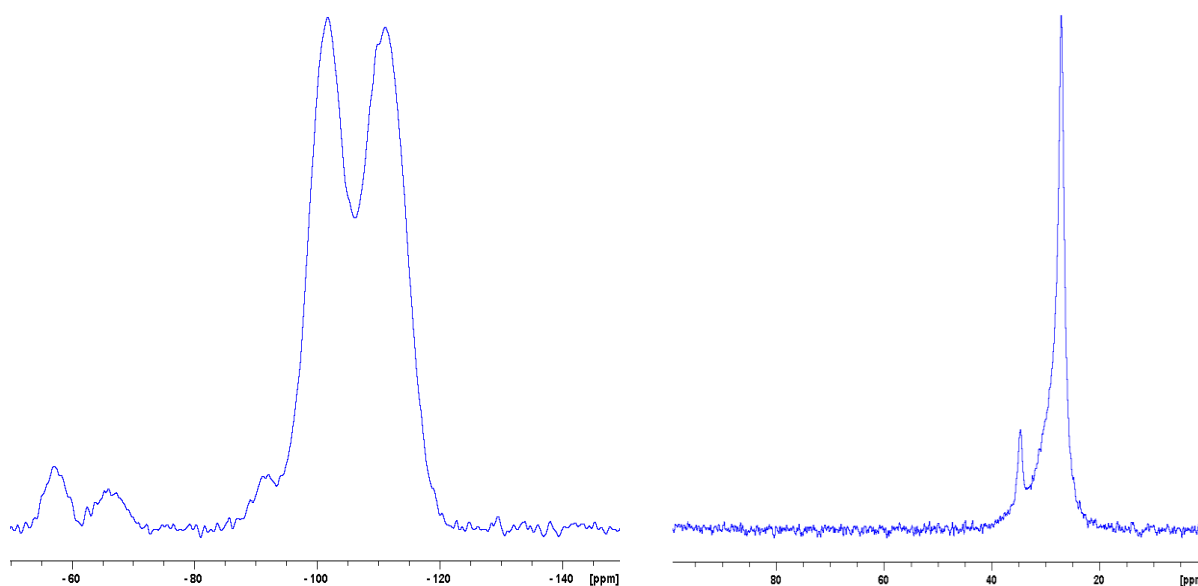
Figure 4-16: ^{29}Si CP MAS-NMR (left) and ^{31}P CP MAS-NMR (right) of grafting from functionalized SiO$_2$.

To conclude, we were able to prove the functionalization of our silica particles was achieved successfully. The solid state NMR shows that a characterization of the silica particle is possible for the respective nuclei. All "grafting onto" functionalized silica do not show the Si-C signal at around − 60 ppm due to low degree of functionalization. Only for the grafting from method the characteristic Si-C peaks were observed. In grafting from silica particles ^{31}P NMR shows that ring opened phosphodiester was formed, but no information regarding the degree of polymerization could be obtained.

4.3 SDS PAGE AND PROTEIN CONCENTRATION

In this chapter the results of SDS PAGE and the calculation of the protein concentration by pierce assay will be discussed.

First SDS PAGE of pure silica (SiO$_2$) is shown in Figure 4-17. From left to right the molecular weight marker, the removed plasma (Pl) from the particle, the washed water

fractions 1-3 (each 0.5 ml wash water) (w1, etc.), elution process 1-3 (each 0.5 ml 7M urea/ 3M thiourea mixture) (e1, etc.) are seen. For every measurement the same volume of the fraction was loaded (25 µL).
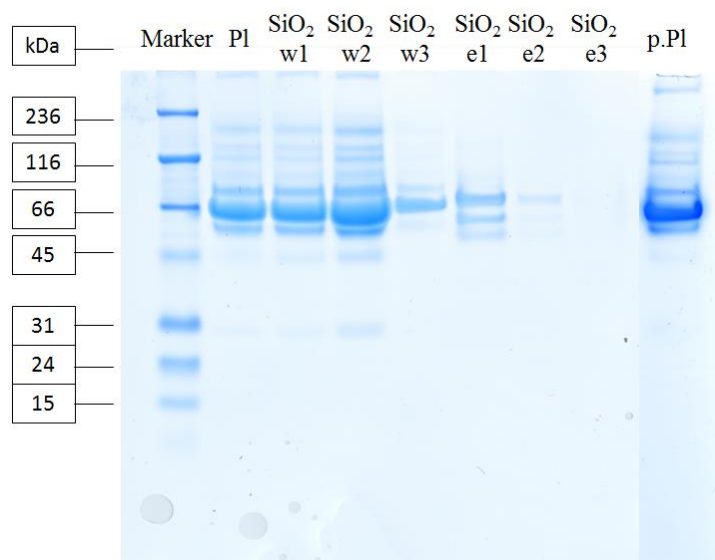
Figure 4-17: SDS PAGE of SiO$_2$ with human heparin plasma.

In the first three fractions of SiO$_2$ we have a strong band at around 66 kDa, which can be attributed to serum albumin (Figure 4-17), the most abundant protein in human serum. After the 3rd wash of SiO$_2$ the intensity of the band gets weaker. This shows that the concentration of the proteins is very low. After the 1st elution the concentration of protein bands gets stronger, but after the 2nd elution the concentration decreases. This shows that most proteins are removed from the silica particle after the 1st elution.

The same process was performed with the grafting onto (g.o.) functionalized Polyphosphoester SiO$_2$ (Figure 4-18). Compared to the pure silica SiO$_2$, the protein concentration in the elution fractions of the g.o. functionalized polyphosphoesters SiO$_2$ is much higher. The difference is particularly obvious for the third elution fraction, where almost no proteins were detected for the pure SiO$_2$. The strong bands in the elution fractions of the g.o. functionalized PPEs SiO$_2$ indicate a much better adsorption of proteins to the modified SiO$_2$.
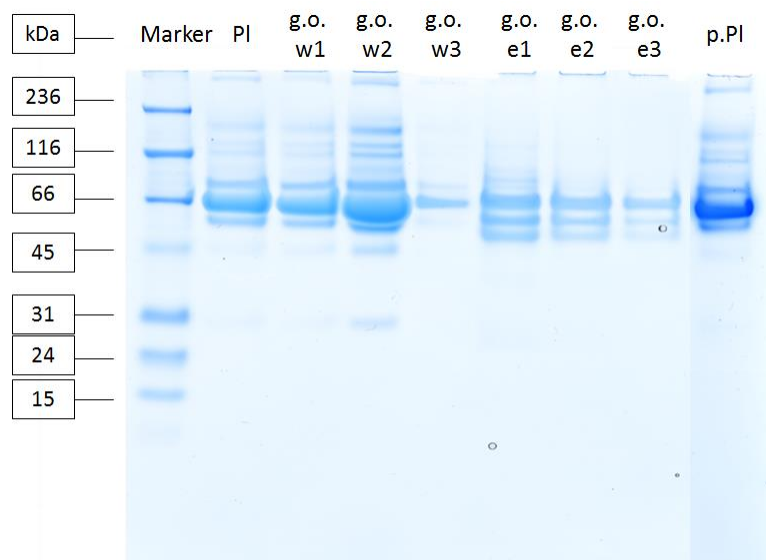
Figure 4-18: SDS PAGE of grafting onto functionalized PPEs SiO$_2$ with human heparin plasma.

To have a reference we used the grafting onto functionalized PEG silica (Figure 5-19). In polymer chemistry PEG is a standard used for example for polymer based drug delivery. We see that the intensity of the bands from the 1st wash till the 2nd elution is very similar. After the 3rd elution the bands do not change on intensity, which means after the 3rd elution it include a lot of proteins. To confirm a strong interaction of the proteins with the PEG surface, more wash processes would be needed. After the 1st and 2nd elution we see a very thin band around 25 kDa (Figure 5-19 red). This could be the light chains of Immunglobulin G, an antibody, which can be found in human blood, indicating an enrichment of this protein on the modified silica.

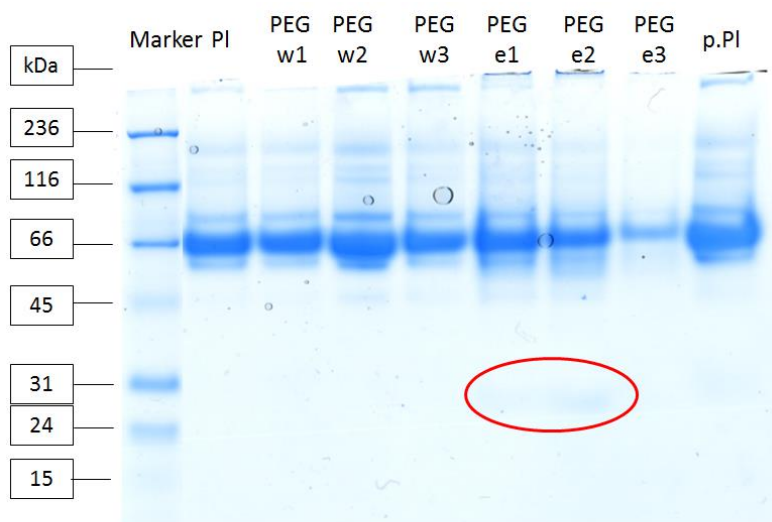**Figure 4-19: SDS PAGE of grafting onto functionalized PEG SiO$_2$ with human heparin plasma.**

Solid state NMR of the grafting onto indicates a very low the density of functionalization is very low (chap. 4.5). Therefore we used a grafting from method which showed a higher degree of functionalization and compare it with the grafting onto functionalized silica (Figure 4-20). After incubation, wash and elution process we see on the SDS PAGE a huge difference compared to the grafting onto functionalized Polyphosphoester SiO_2.
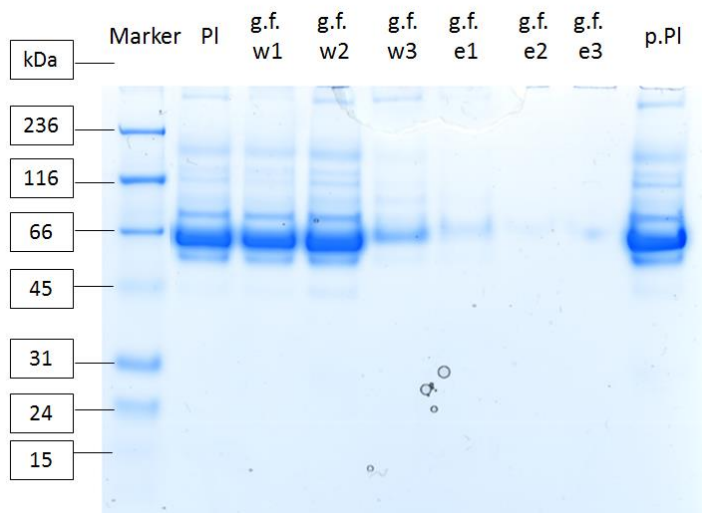
Figure 4-20: SDS PAGE of grafting from "functionalized" Phosphoester SiO_2 with human heparin plasma.

After the 3rd wash and elution process the bands of proteins are very low. Comparing this process with the grafting onto, it indicates that the interaction between proteins and particle in the grafting from is lower. To have a confirmation we calculated the protein concentration with protein pierce assay. We used for the incubation 27.7 mg of protein, calculated via Pierce Assay and ~50 mg SiO_2 ($25m^2$ of surface).

For calculating of the protein concentration a calibration curve was needed. Over the absorption of the BSA standards the protein concentration of the samples can calculate. The precision of the protein concentration depends on the range of the absorption measurement. So if the value of the absorption is out of the range the value of the protein concentration is not precise.

We see in the graph (Figure 8-3, Table 8-1~8-4) that the amount of proteins in the removed plasma from the particle is around 60 % for silica and PEG, 80 % for polyphosphoester grafting onto functionalized silica particle and 100 % for grafting from. This indicates that the interaction of the plasma with the surface is in the case of SiO_2 and PEG functionalized silica looks very similar because the mass ratio of the proteins is similar, too. After elution

the total calculated mass ratio of the protein in these two samples are around 75 %. The calculation shows that 25 % of the proteins should on the relative silica surface.

In the case of g.o. functionalized Polyphosphoester silica the mass ratio shows that the interaction of the protein is lower compared to the two samples mentioned before. First the amount of the removed plasma (80 %) shows that more proteins were gained after incubation. That means less proteins are on the surface of the particle.

For the g.f. functionalized Polymer this effect is even more distinctive. The bar graph shows the effect very well. That indicates that the proteins do not interact very well with the surface compared to the g.o. functionalized Polyphosphoester.

After having discussed the protein amount in the removed plasma, now the focus goes to the wash and elution fractions. In all cases the calculated values of proteins were nearly around 10 %. After the 1st wash nearly 7~8 % of proteins for all samples were calculated. In the 2nd wash process the concentration of proteins in the sample of PEG and g.f. were around 0.7 % compared to the other two samples (SiO_2, g.f.) where they were around 1.2~1.4 %.

Figure 8-2 shows that the protein concentration of PEG, g.o. functionalized Polyphosphoester after the 1st elution process is higher compared to the other two samples (Figure 8-3, green). After the 1st elution there is no huge difference of these two samples. After the 2nd wash process the concentration of the proteins for the g.f. functionalized Phosphoester getting smaller, which can see in Figure 8-2 and Table 8.4. That indicates that after every step there are less proteins on the particles compared to the other samples.

4.3.1 CONCLUSION OF SDS PAGE AND PROTEIN ASSAY

To conclude these experiments, it was shown that the interaction of the proteins between g.f. and g.o. SiO_2 are less compared to the other sample, which was shown by the protein concentration of the removed plasma. But PEG SiO_2 shows a better interaction with the proteins, which is identified over the protein bands by the 3rd wash process.

In this experiment it was important to see the differences of the protein concentration between the samples of the grafting onto functionalized particles and the differences of the grafting onto and grafting from functionalized particle.

4.4 SYNTHESIS OF 3-((*TERT*-BUTYLDIMETHYLSILYL)OXY)PROPANE-1,2-DIOL

The synthesis of this product is shown in chapter 5.1. For characterization ^{1}H NMR and IR measurements was conducted. The product was purified over silica chromatography.
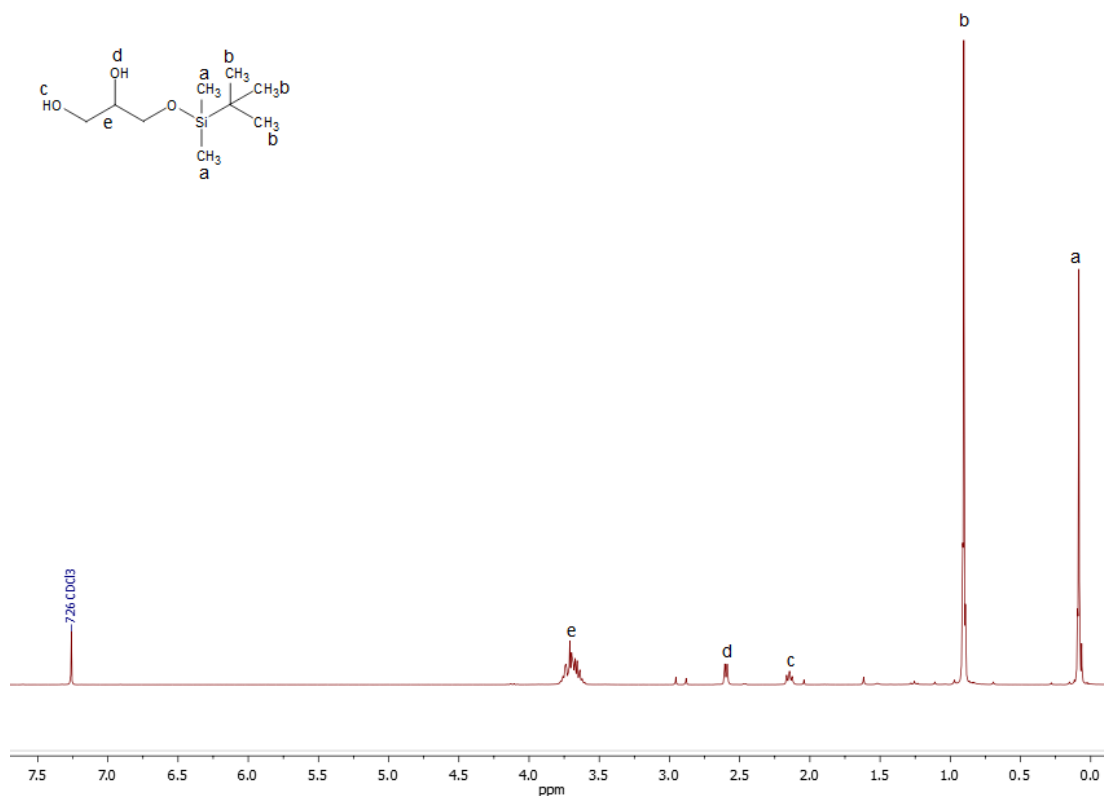
Figure 4-21: ^{1}H NMR (300MHz) of 3-((*tert*-butyldimethylsilyl)oxy)propane-1,2-diol in CDCl₃ at 298 K.

The ^{1}H NMR is shown in Figure 4-21. At 0.06 and 0.90 ppm the typical TBDMS group is seen. Around 2.0 ppm the primary hydroxyl group was calculated because we see a triplet where the proton is coupling with 2 close protons. The secondary hydroxy group proton shows a doublet which means it couples only with 1 close proton.

In the ^{13}C NMR the secondary carbon is detected at 71.50 ppm. The primary carbons are detected at 64.78 ppm and 64.08 ppm. The *tert*-butyl group of the TBDMS group can recognize at 25.84 ppm and -5.48 ppm. And the dimethyl group was calculated at 18.25 ppm. The spectrum is shown in Figure 4-22.

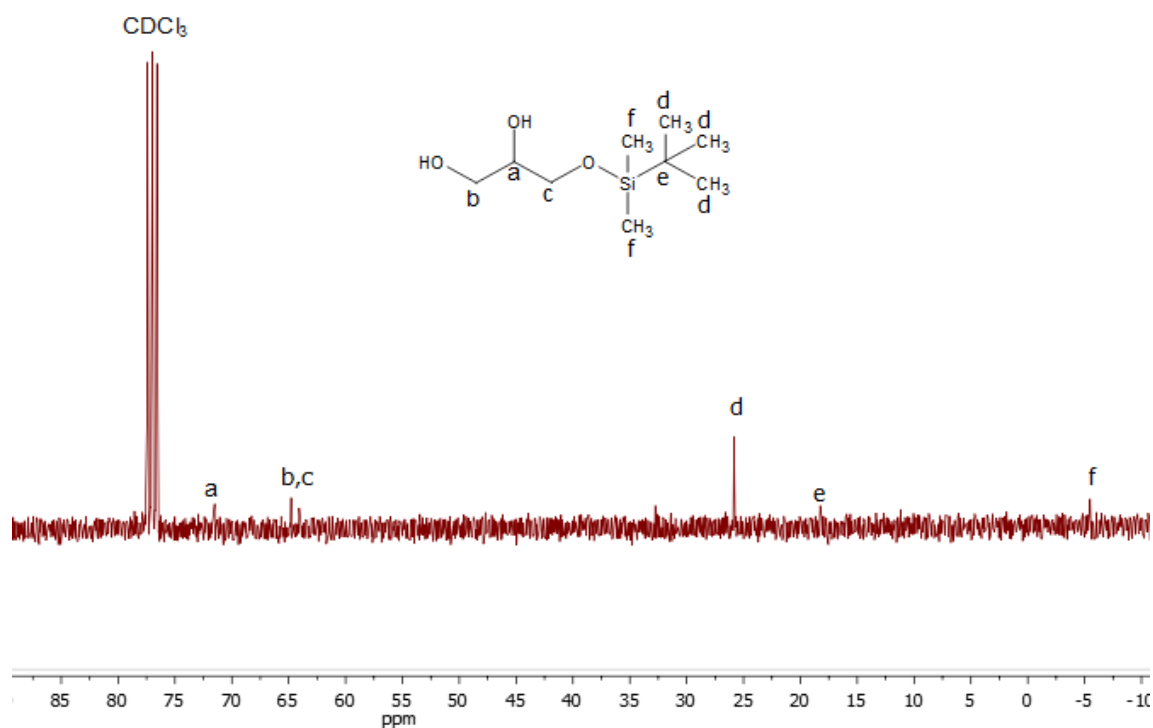**Figure 4-22:** $^{13}C\{H\}$ **NMR (125 MHz) of 3-((*tert*-butyldimethylsilyl)oxy)propane-1,2-diol in CDCl₃ at 298 K.**

From IR measurements the band of the hydroxyl group at 3397 cm^{-1}, the C-H bands at 2929, 2857 cm^{-1}, the Si-O-C bands at 1108 cm^{-1} can be assigned (Figure 4-23).[61]
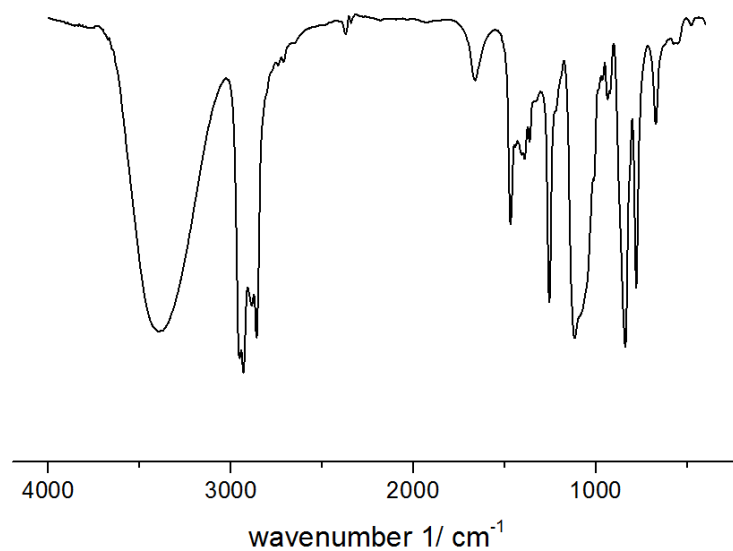
Figure 4-23: FTIR of 3-((*tert*-butyldimethylsilyl)oxy)propane-1,2-diol.

4.5 RESULTS OF 4-(((*TERT*-BUTYLDIMETHYLSILYL)OXY)METHYL)-2-ETHTYL-2-OXO-1,3,2-DIOXAPHOSPHOLANE

As explained in chapter 4.1 4-(((*tert*-butyldimethylsilyl)oxy)methyl)-2-ethtyl-2-oxo-1,3,2-dioxaphospholane **(1)** was synthesized via ring closing reaction of TBDMS glycerol and EtPCl$_2$.
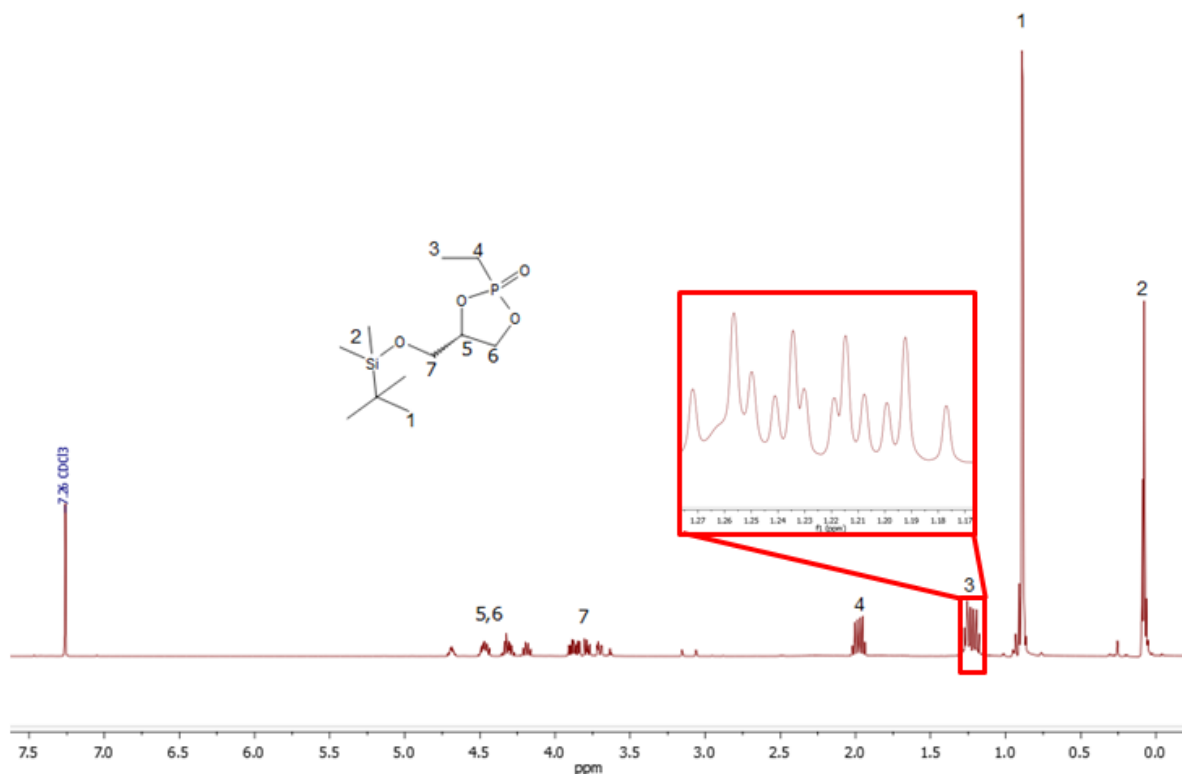
Figure 4-24: ^{1}H NMR (500 MHz) of (1) in CDCl$_3$ at 298 K.

^{1}H, ^{31}P, ^{13}C, HMBC-NMR, HSQC-NMR and FTIR spectra were measured to thoroughly characterize the structure of the final product. The ^{1}H NMR is shown in Figure 4-24.[6]

In Figure 4-24 the signal 3 (1.22 ppm) shows the complex splitting pattern of a doublet of doublets of triplets (ddt). The splitting arises from the coupling to the ethylene protons and the phosphorous atom. As the product is not planar, but has an envelope conformation the position of the alkyl group (cis, trans) results in different coupling between the proton of the CH$_3$ group and the phosphorus, which conclude the peak of ddt (Figure 4-24).[26,62]

Penczek:

$^1J_{PH}$=727.5 (^{1}H: 6.06 ppm), 730.3 Hz (^{1}H: 6.08 ppm)
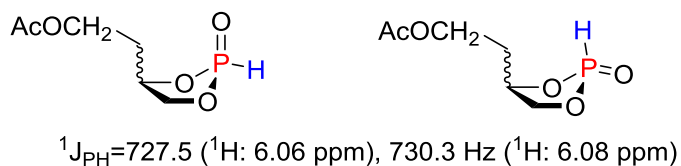
This Work:
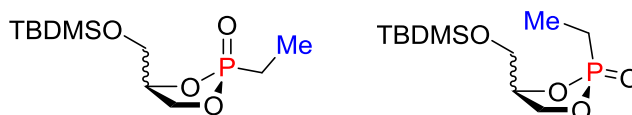
Figure 4-25: Trans/ cis conformation of substituted pholspholanes.

A similar observation was already described by Penczek in the five ring system shown in Figure 4-25. Two different signals were found in the ^{31}P NMR spectrum for the phosphonic acid proton. Penczek et al. assigned these peaks to the two different conformer of the ring.[26,62] Due to the high homology to our system we expected a similar result in our ^{31}P NMR spectrum. The spectrum is shown in Figure4-26.[6]
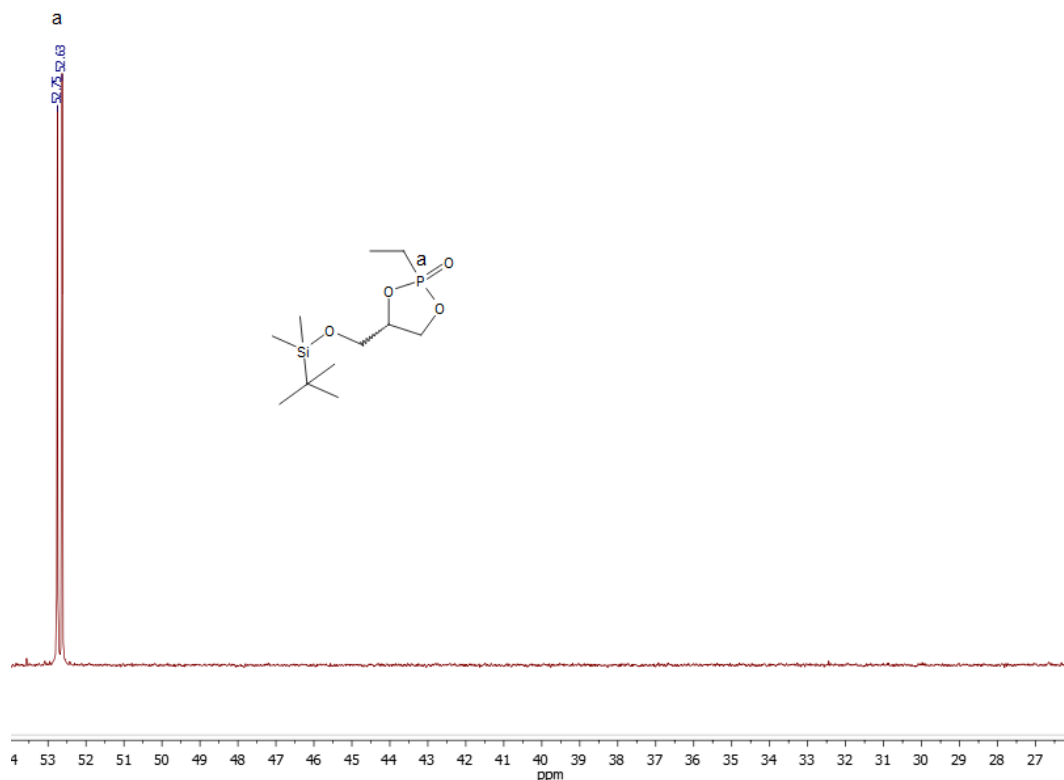
Figure 4-26: ^{31}P{H} NMR (201 MHz) of (1) in CDCl$_3$ at 298 K.

As expected, two distinct ^{31}P signals at 52.76 and 52.62 ppm were found in the ^{31}P NMR. We see two peaks because we have at C-4 a functional group, which shows each peak an isomer dependent on the position of the ethyl group on the phosphorus nucleus. This effect was observed in the molecule system of Penczek (Figure 4-27), too. It was found out that the peak was 16.8 ppm for trans and 16.5 ppm cis enantiomer.

^{31}P{^{1}H}:   δ= 16.8 ppm (trans)   δ= 16.5 ppm (cis)
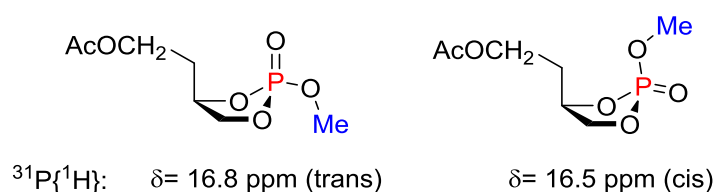
Figure 4-27: Effect of trans/cis isomers on chemical shift (^{31}P NMR measurements).

^{31}P^{1}H Heteronuclear Multiple Bond Correlation (HMBC) experiments were used to further visualize the coupling between the protons and the phosphorus nuclei.
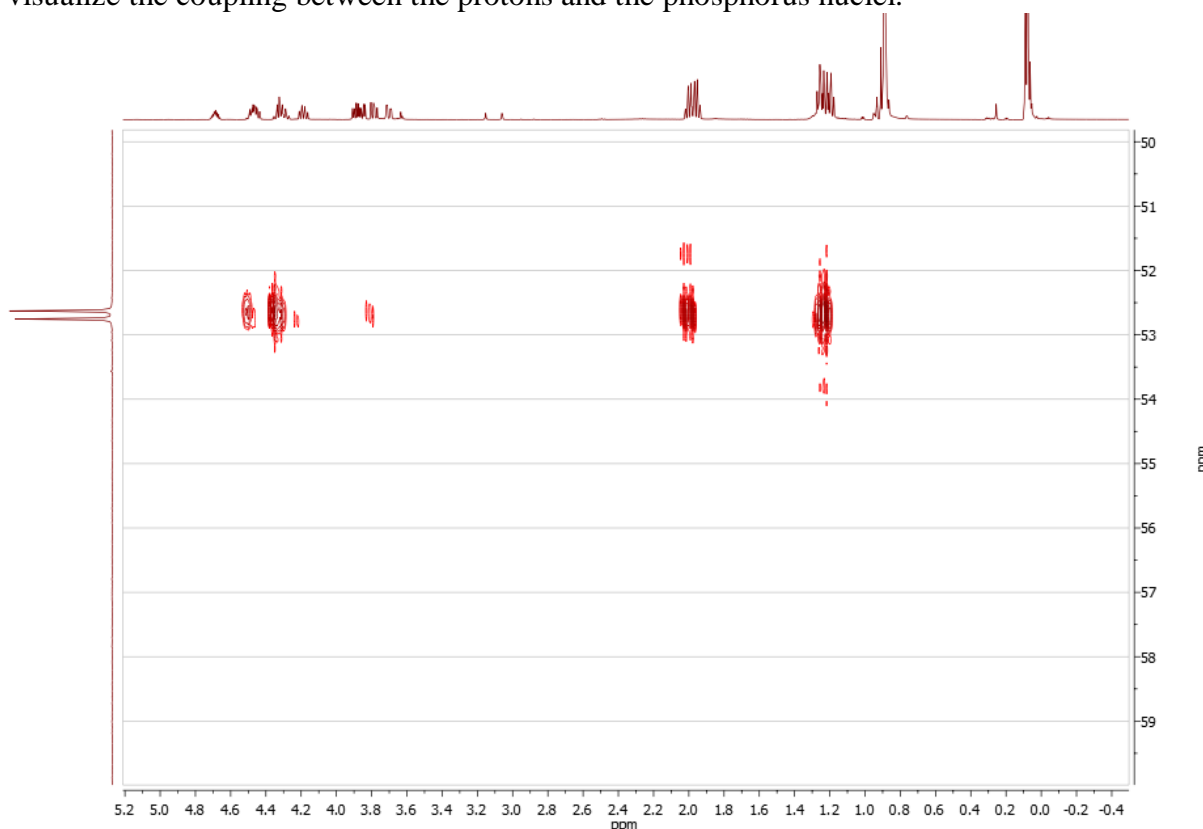
Figure 4-28: ^{1}H^{31}P HMBC NMR (500 MHz) of (1) in CDCl$_3$ at 298 K.

In Figure 4-28 every proton of the side chain at 1.22, 1.98 ppm (^{2}J, ^{3}J coupling), 4.72 - 4.16 ppm ring (^{3}J) and the methoxy group 3.94 - 3.61 ppm (^{4}J) couple with the phosphorus are able to assign. The proton signals originating from the TBDMS group (0.06, 0.90 ppm) do

not show coupling with phosphorus as they are too far away from the phosphorus (^{7}J -CH$_3$, ^{8}J –CH$_2$).

The ^{13}C NMR shows more peaks compared to the no functionalized monomer.[6]

To assign the peaks of the ^{13}C NMR a 2D NMR measurement were used to clarify the different signals. In Figure 4-29 we see a Heteronuclear Single Quantum Coherence (HSQC) experiment of ^{1}H^{13}C nuclei. In this experiment coupling between two neighboring nuclei is observed and long range is suppressed.

As the peaks of the ^{1}H peaks of the monomer are known, we can assign the peaks of ^{13}C-NMR (Figure 4-24).
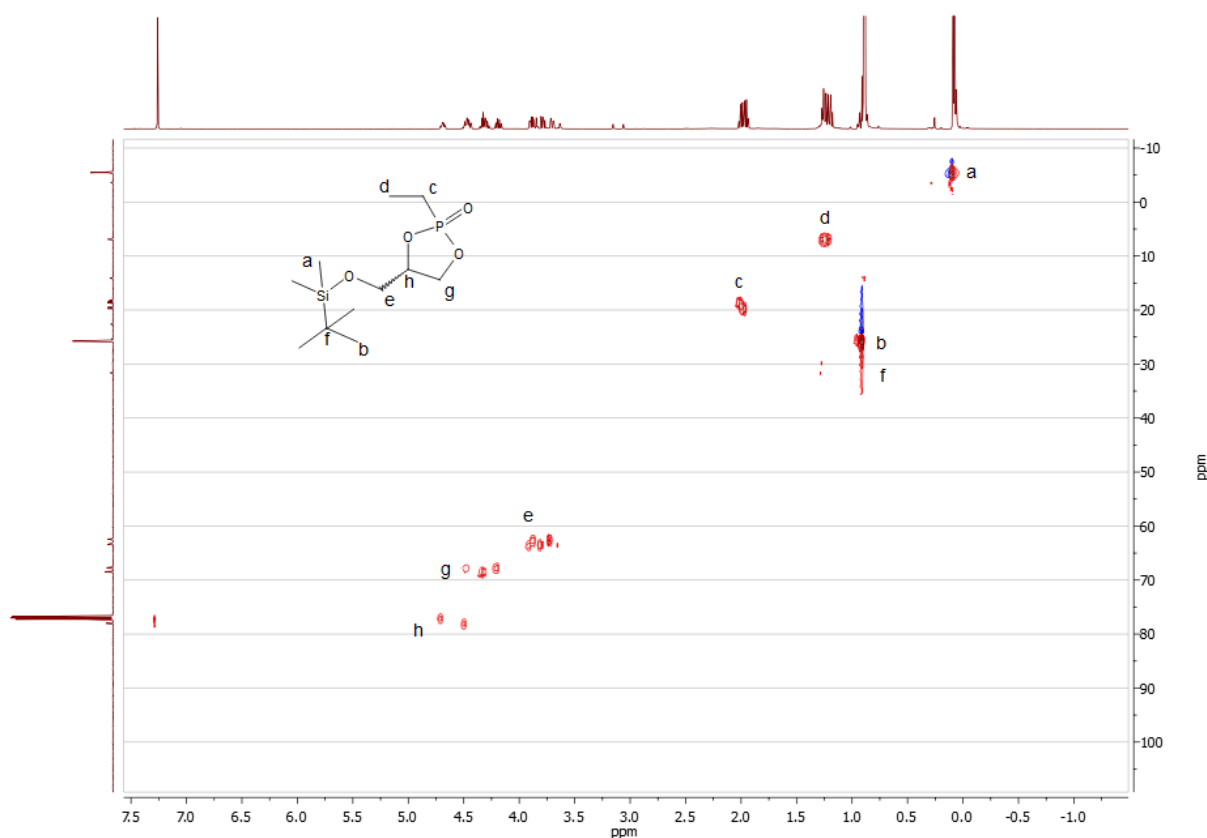
Figure 4-29: ^{1}H^{13}C HSBC NMR (500 MHz) of (1) in CDCl$_3$ at 298 K.

With this method we can assign the peaks of the ^{13}C NMR. The assignment is shown in Figure 4-30. We see in peak g (68.76 – 67.31 ppm) a multiplet, which are the carbon in the ring. The multiplet of 63.90 – 62.15 ppm is the carbon of the methoxy group (peak e). Peak f (31.59 ppm) and b (25.79 ppm) are the carbon from the *tert*-butyl group. At 19.63 ppm (peak c), 18.57 ppm (peak d) and 18.26 ppm (peak a) we see duplets. These are the peaks of

the carbon coupling to the phosphorus (CH$_2$ side chain), cis trans isomerization and enantiomer.[63,64] At 6.87 ppm the CH$_3$ side chain shows a duplet of duplet, which are caused by the carbon-phosphorus coupling. The peak at -5.49 ppm is the peak of the dimethyl group.
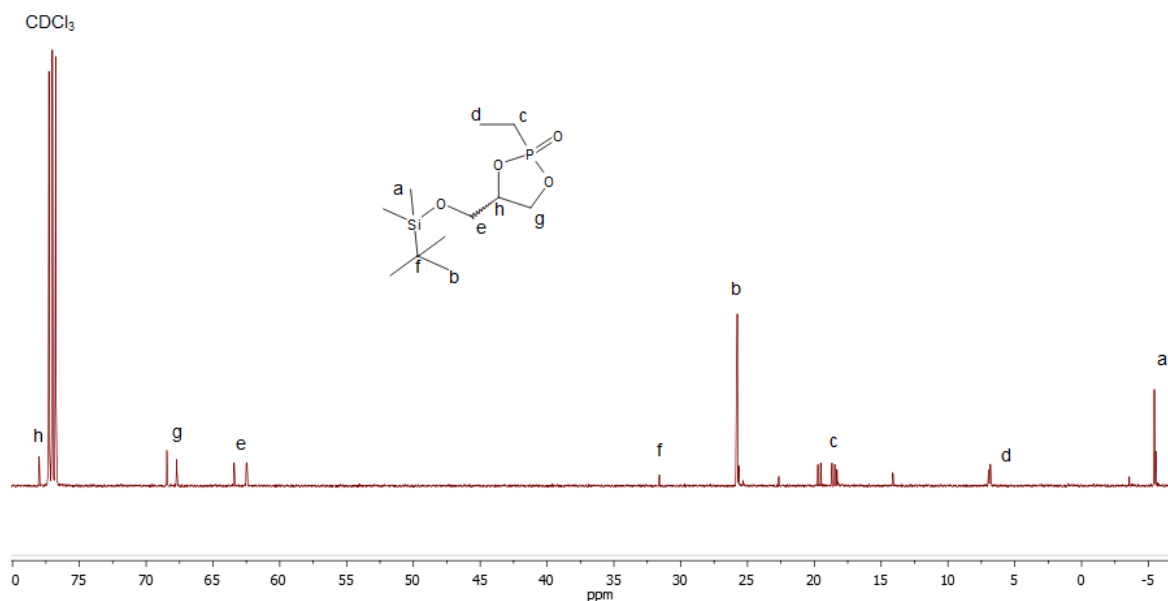
Figure 4-30: ^{13}C{H} NMR (125 MHz) of (1) in CDCl$_3$ at 298 K.
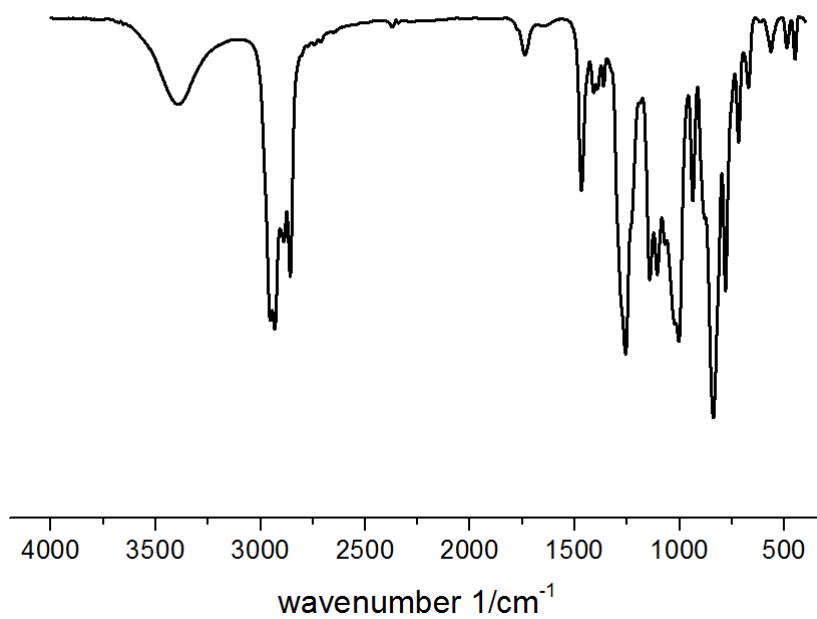
Figure 4-31: FTIR of (1).

In Figure 4-31 the signal of the hydroxyl group at 3390 cm^{-1} could observe. At 2883, 2856 cm^{-1} the P-C bands, 1463, 1262 cm^{-1} the P=O bands and at 1137, 998 cm^{-1} the Si-O-C bands can be observed.[61]

To conclude, the desired product was obtained in moderate yield (62 %), high purity and thoroughly characterized through several spectroscopic means.

4.6 REACTION OF 4-(((*TERT*-BUTYLDIMETHYLSILYL)OXY)METHYL)-2-ETHTYL-2- OXO-1,3,2- DIOXAPHOSPHOLANE

In this chapter the first attempts to polymerize the new monomer are elucidated. First the polymerization was tested under the several conditions (Figure 4-32).
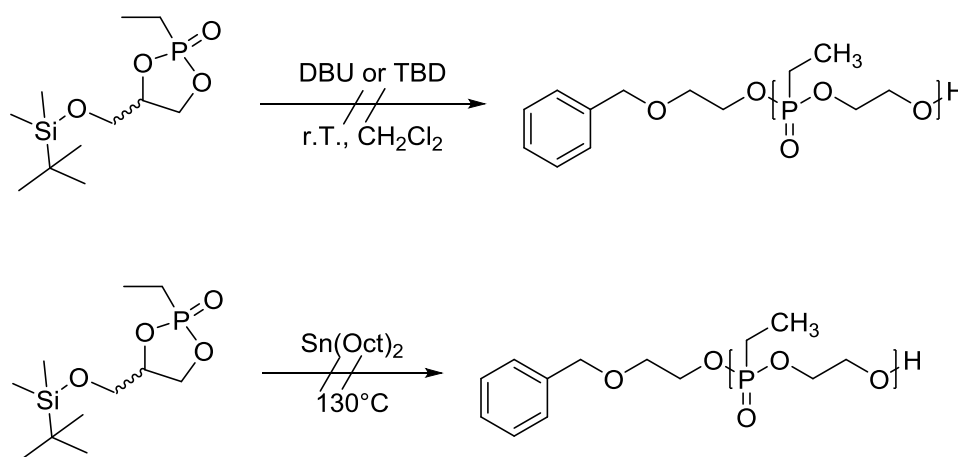
Figure 4-32: Ring-opening reaction in several conditions.

After the unsuccessful polymerization attempts, harder reaction conditions were tested. Therefore, ring-opening was attempted under strongly basic conditions with NaOH and under strongly acid with trifluroacetic acid in D$_2$O for 18 h directly in a NMR tube (Figure 4-33).
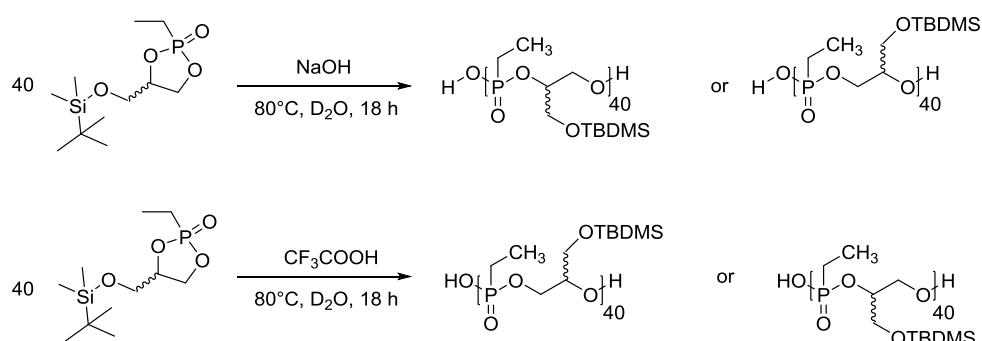
Figure 4-33: Proposed products of the reaction of monomer in basic and acidic conditions.

In both cases a colorless solid was separated from the reaction mixture. After 18 h the solid was removed and a ^{31}P NMR spectrum of the solution was measured, see Figure 4-34.
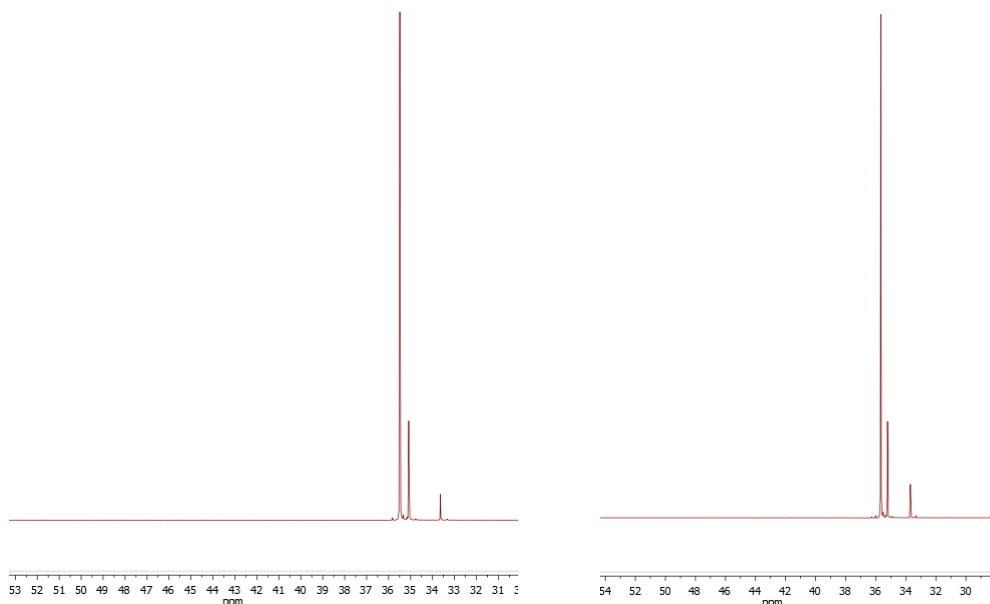
Figure 4-34: $^{31}P\{H\}$ NMR (201 MHz) of the reaction mixture in basic (left) and acidic (right) conditions in D$_2$O after 18 h at 298 K.

The vanishing monomer peak at 52.76 and 52.62 ppm confirmed the ring opening of the monomer. The new signal at 35.51, 35.15 and 33.69 ppm furthermore suggest the presence of linear phosphonic acid derivatives. These different peaks could be the results of the two different possible isomers forming during the ring opening, see Figure 4-33.

Figure 4-35: ^{1}H NMR (500 MHz) of the ring opened product in basic condition in D$_2$O at 298 K.
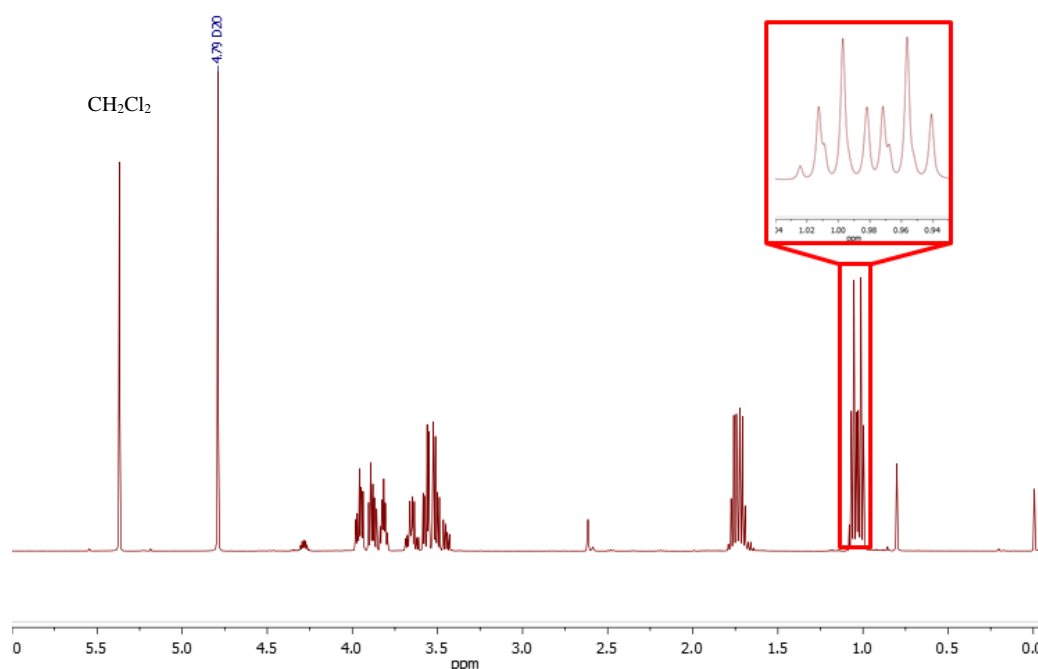
Figure 4-36: ^{1}H NMR (500 MHz) of the ring opened product in acidic condition in D$_2$O at 298 K.

The ^{1}H NMR spectra of the mixture show little difference from the cyclic monomer. No typically broad backbone peak around 4.1 ppm (Figure 5-35/36) is visible. The peak of the CH$_3$ side chain (1.01 ppm) however shows a duplet of triplet which does not belongs to the reactant as explained in chapter 4.5. This splitting pattern is known from ethylphosphonic Acid Dichloride as well as from 2-ethyl-2oxo-1,3,2-dioxophospholane (Figure 5-35/36).[6] We therefore conclude, that ring opening of the monomer took place, however, no actual polymerization occurred. The possible structures of the ring opened are shown in Figure 4-37.
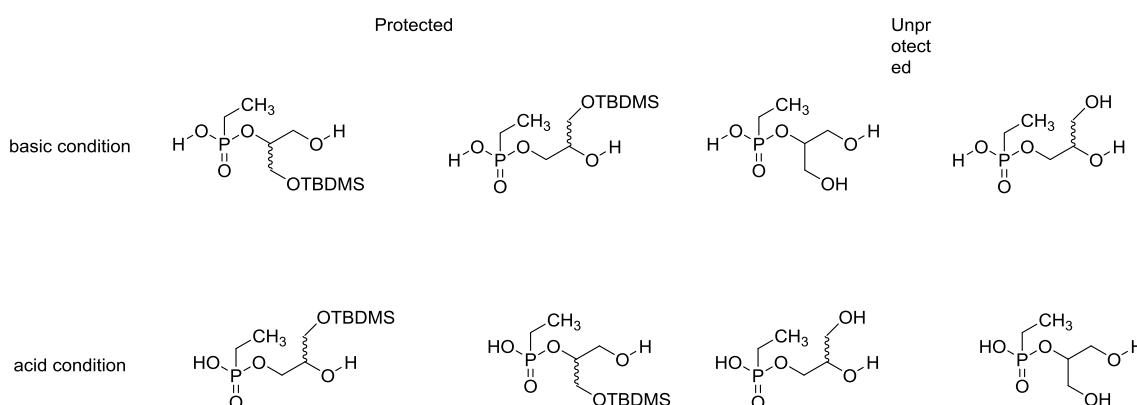
Figure 4-37: Proposed products of the ring opening reaction.

It is further more recognizable that the protecting group was cleaved from the monomer. The peak of the TBDMS group around 0.06 and 0.1 ppm vanished nearly completely. The above

mentioned solid which is precipitated during the reaction was found to contain the cleaved protecting group. Figure 4-38 shows the ^{1}H NMR spectra in CDCl$_3$.
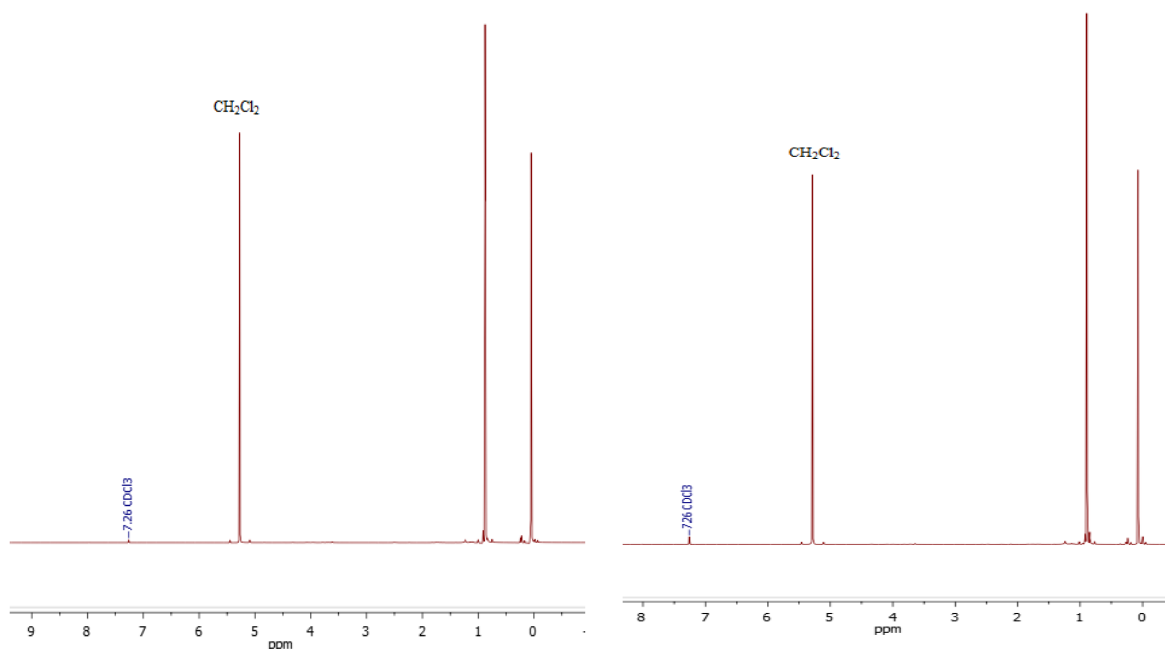
Figure 4-38: ^{1}**H NMR (500 MHz) of the residue [acidic (left) and basic (right) condition] in CDCl$_3$ at 298 K.**

In both spectra the typical peaks of the TBDMS group at 0.09 ppm and 0.90 ppm are recognizable. This concludes that under these harsh conditions in both conditions the ring can open but at the same time the protecting group is cleaved.

With this two NMR measurements we can say that the ring opening was successful but the polymerization do not occur and the protecting group was separated at the same time. So in Figure 5-37 following structure can be proposed.

Now we can calculate the peak to the nuclei. The CH$_2$ and CH$_3$ side chain at 1.71 and 1.01 ppm can calculate in the ^{1}H NMR. The multiplet at 3.71 ppm can be calculated the protons of the glycerol chain. Over ^{13}C^{1}H HSQC NMR the carbon peaks can assign. The spectra of ^{13}C NMR is shown in Figure 4-39/40.
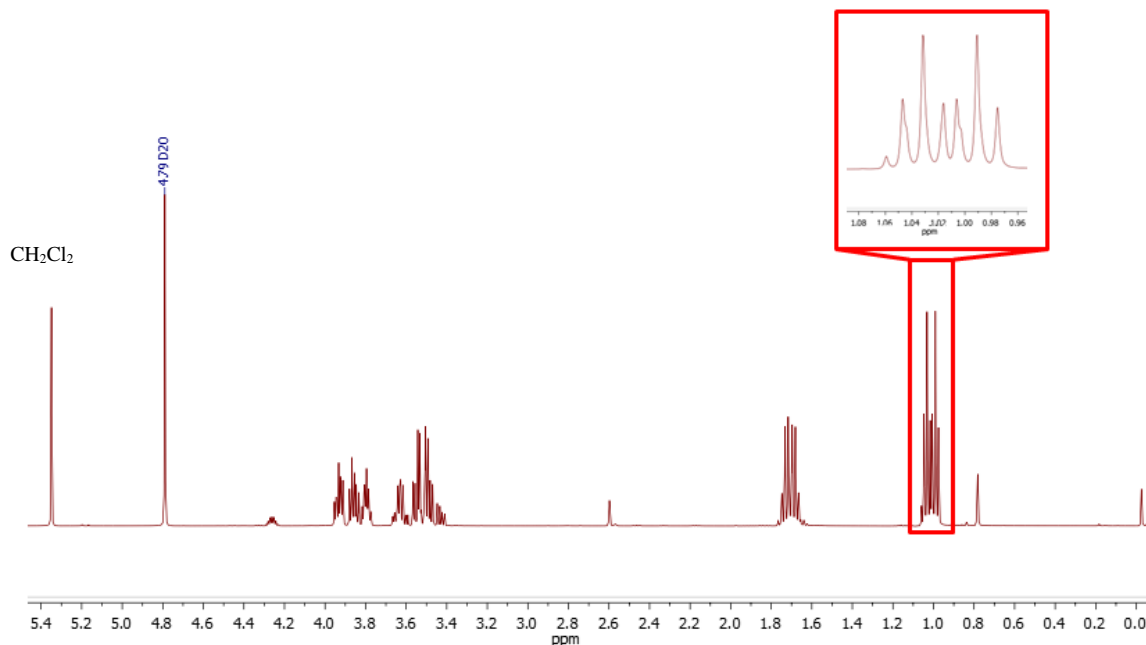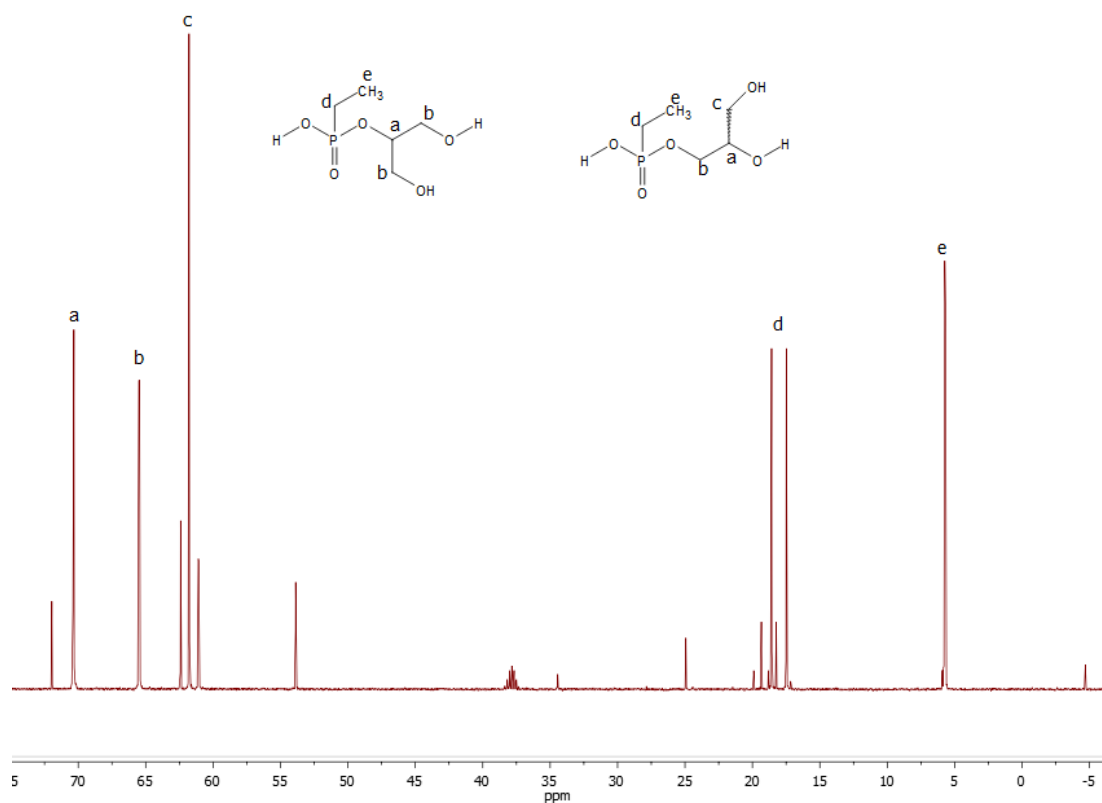
Figure 4-39: ^{13}C{H} NMR (125 MHz) of the ring opened product in basic condition in D_2O at 298 K.
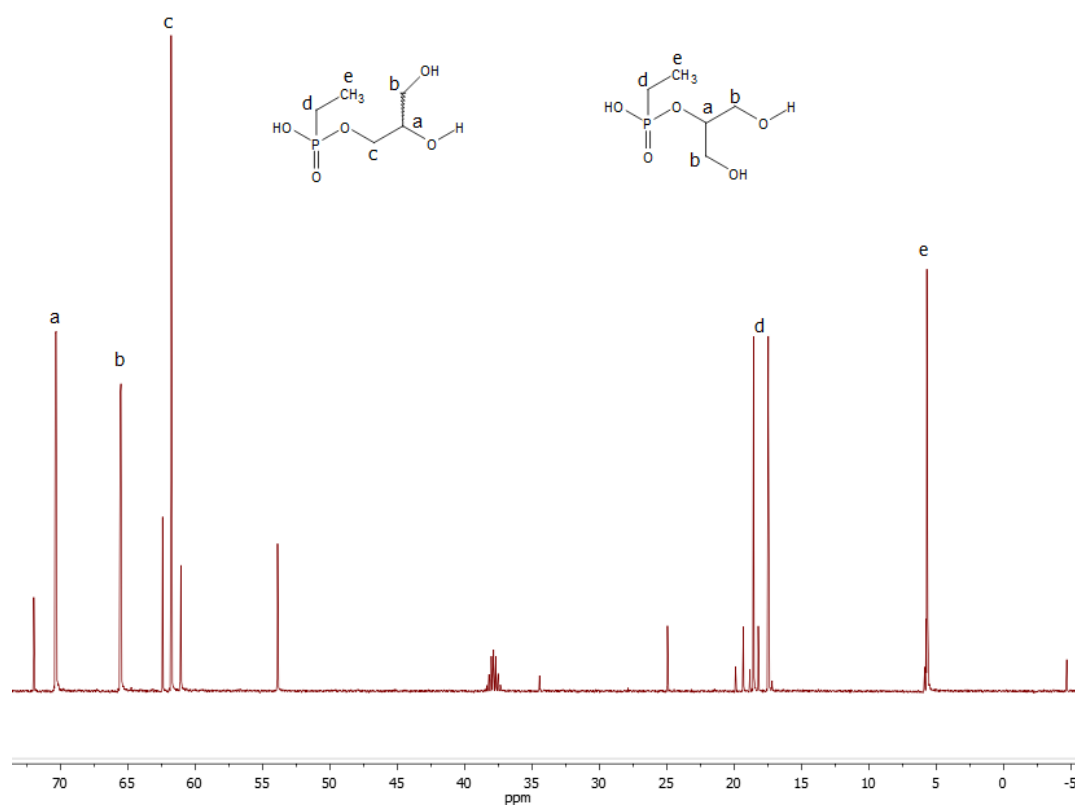
Figure 4-40: ^{13}C{H} NMR (125 MHz) of the ring opened product in acidic condition in D_2O at 298 K.

We can assign the peaks at 18.00 ppm to the CH_2 side chain and the peak at 5.70 ppm to CH_3 side chain. The peak at 70 ppm belongs to the secondary carbon. The peaks at 65 and 60 ppm belong to the primary carbons (65, 60 ppm). If the proposed product has a stereo center we get two primary carbon peaks. The proposed product without stereo center has only one primary carbon peak (65 ppm). It is possible to assign the ^{13}C NMR for both unprotected products. This gives the conclusion that there is a mixture of both products.

In the $^{13}C^1H$ HSQC measurement of both conditions are shown in Figure 8-4 and 8-5.

To conclude, ring-opening polymerization was not yet successfully achieved. Preliminary experiments showed, however, that ring-opening of the monomer is feasible, however under both basic and acidic conditions the protective group is lost. Further investigations to find optimal conditions for polymerization and preservation of the protecting group are still needed.

5 EXPERIMENTAL

Instrumentation and characterization techniques

For size exclusion chromatography (SEC) measurements following equipment were used. The samples were solved in DMF with lithium bromide 1.00 g·L^{-1} as an additive) at 60 °C and a flow rate of 1 mL min^{-1}, including a PSS Gram column (100/1000/1000 g·mol-1), a SECcurity VWD (270nm) and a SECcurity refractive index (RI) detector. Calibration was carried out using poly(ethylene glycol) standards provided by Polymer Standards Service.

The ^{1}H-NMR experiments were measured on a 300 MHz Bruker Avance III system. The ^{13}C{H} and ^{31}P{H} NMR spectra were measured at 500 MHz Bruker Avance III system. Every sample was referenced on solvent signals. The ^{31}P{H} NMR spectra were referenced externally to phosphoric acid.

2D NMR experiments (^{1}H^{1}H COSY, ^{1}H^{31}P{H} HMBC and ^{1}H^{13}C{H} HSQC) were measured on a Bruker 500 MHz Avance III NMR spectrometer under the same conditions as mentioned above. The samples were referenced to the residual proton signals of the deuterated solvent (CDCl$_3$ (^{1}H) = 7.26 ppm; DMSO-d_6 (^{1}H) = 2.50 ppm). All 1D spectra were processed with the MestReNova-10.0.2-15465 software. ^{1}H DOSY (Diffusion ordered spectroscopy) was analyzed with the Top Spin 3.0 software.

The SS NMR was measured on a 500 MHz Bruker Avance III NMR or 300 MHz Avance II system. All measurements of solid state NMR were analyzed with the Top Spin 3.0 software.

5.1 MONOMER SYNTHESIS

Synthesis of 3-((*tert*-butyldimethylsilyl)oxy)propane-1,2-diol[65]

Figure 5-1: Reaction scheme of 3-((*tert*-butyldimethylsilyl)oxy)propane-1,2-diol.

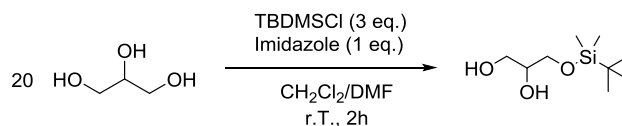Imidazole (5.41 g, 79.50 mmol) and glycerol (48.81 g, 530 mmol) were disolved in dichloromethane / dimethylformamide (DMF) (80 mL/32 mL). *Tert*-buthyldimethylsilyl chloride (TBDMSCl) was dissolved in 10 mL dichloromethane and added dropwise at room temperature (r.T.). After 3 mL DMF was added for full conversion. The reaction was stirred

for 2 h and quenched with the addition of 200 mL H_2O. The mixture was concentrated under reduced pressure and extracted with Et_2O (4x 100 mL), The organic phase was washed three times with water (100 mL) to remove residual DMF and dried with $MgSO_4$. The organic phase was concentrated *in vacuo*. Purification by silica gel chromatography with ethylacetate (EtOAc) yielded the desired product as yellow oil (3.29 g, yield 65 %, R_f= 0.74)

^{1}H NMR (CDCl$_3$-*d*, ppm): δ 3.81 - 3.60 (m, 5H), 2.60 (d, ^3J = 5.0 Hz, 1H), 2.11 (t, ^3J = 9 Hz, 1H), 0.90 (s, 9H), 0.06 (s, 6H). ^{13}C{H} NMR (CDCl$_3$-*d*, ppm): δ 71.50 (s), 64.78 (s), 64.08 (s), 25.84 (s), 18.25 (s), -5.48 (s). FTIR (cm^{-1}): 3397 (-OH), 2929, 2857 (C-H), 1463, 1250, 1108, 836, 775, 665.

Synthesis of 4-((((*tert*-butyldimethylsilyl)oxy)methyl)-2-ethtyl-2-oxo-1,3,2-dioxaphospholane (1)
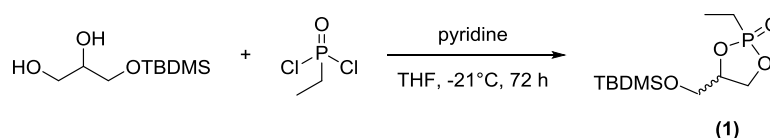
Figure 5-2: Reaction scheme of 4-((((*tert*-butyldimethylsilyl)oxy)methyl)-2-ethtyl-2-oxo-1,3,2-dioxaphospholane (1).

The synthesis based on the publication of Thomas Wolf.[6] In a dried 3-necked-round bottom flask equipped with two dropping funnels 60 mL THF were added in the flask and cooled to -21 °C. Ethylphosphonic acid dichloride (7.35 g, 50.02 mmol) was filled up with dry THF to 70 mL and transferred into one dropping funnel. In the other dropping funnel 3-((*tert*-butyldimethylsilyl)oxy)propane-1,2-diol (10.26 g, 49.72 mmol) and dry pyridine (8.01 g, 100.0 mmol) were filled up with dry THF to 70 mL. Both mixtures were added into the flask at the same dropping speed.

After 72 h the precipitated pyridinium hydrochloride was filtered. The solvent was removed under reduced pressure and 150 mL hexane was added to precipitate the rest the pyridinium hydrochloride. After 3 h the mixture was filtered with through flash silica gel and the hexane was evaporated. A viscous light yellow liquid was obtained (11.67g, yield 62 %, R_f= 0.13).

^{1}H NMR (CDCl$_3$-*d*, ppm): δ 4.72 - 4.16 (m, 3H), 3.94 - 3.61 (m, 2H), 1.98 (dq, J = 18.2, 7.7 Hz, 2H), 1.22 (ddt, J = 21.2, 11.2, 7.7 Hz, 3H), 0.90 (s, 9H), 0.06 (s, 6H). ^{31}P NMR (CDCl$_3$-*d*, ppm): δ 52.76, 52.62. ^{13}C{H} NMR (CDCl$_3$-*d*, ppm): δ 78.01(s), 68.76 − 67.31 (m), 63.90 − 62.15 (m), 31.59 (s), 25.79 (s), 19.63 (d, J= 25.8 Hz), 18.57 (d, J = 25.9 Hz),

18.26 (d, J = 9.7 Hz), 6.87 (dd, J = 9.8, 6.8 Hz), -5.49 (d, J = 13.0 Hz). FTIR (cm^{-1}): 3390 (-OH), 2883, 2856 (P-C), 1463, 1262 (-P=O), 1137, 998 (-Si-O-C), 843.

5.2 SYNTHESIS OF SILYLETHER FUNCTIONALIZED POLYMER

Synthesis of Poly(ethylene ethyl phosphonate)-ω -)(3-(triethoxysilyl)propyl)carbamate
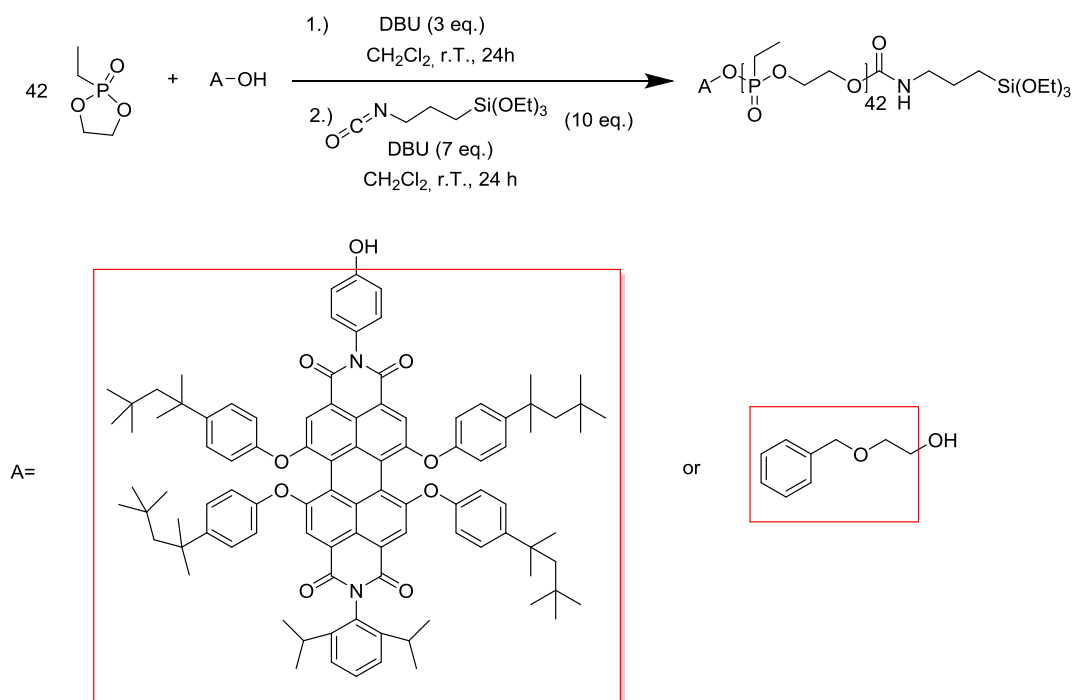
Figure 5-3: Reaction scheme of poly(ethylene ethyl phosphonate)-ω-)(3-(triethoxysilyl)propyl)carbamate.

In the dried Schlenk tube 2-ethyl-2-oxo-1,3,2-dioxaphospholane was dissolved in 1 mL benzene for lyophilization. Afterwards dry dichloromethane was added to a concentration of 4.0 mol L^{-1}. A stock solution of the initiator 2-(benzyloxy)-ethanol or N-(2,6-diisopropylphenyl)-N'-(4-hydroxyphenyl)-1,6,7,12-tetra-tert-octyl-phenoxy-perylene-3,4,9,10-tetracarboxydiimide (phenoxylated/N/-4-OH-ph-/N'/-DIPP-PDI) (0.2 mol L^{-1}) and the organo base 1,8-diazabicyclo[5.4.0]undec-7-en (DBU) (0.2 mol L^{-1}) was prepared in dry dichloromethane. 1 equivalent of the initiator and afterwards 3 equivalent of DBU were added to the monomer solution. The reaction was stirred at room temperature for 24 h. Then DBU (7eq.) and triethoxy (3-isocyanatopropyl)-silane (10 eq.) were added to the polymer solution. The mixture was stirred at room temperature for 24 h. The polymer was precipitated three times in 30 mL cold diethylether. The yield for this polymerization is between 70 % and 95 %.

2-(benzyloxy)-ethanol initiated P(EtPPn):

^{1}H NMR (DMSO-d_6, ppm): δ 7.37 - 7.29 (m, aromatic protons, 5H), 4.22 - 4.01 (m, backbone -CH$_2$-CH$_2$-), 3.76 - 3.68 (q, Si-O-C**H$_2$**, 6H), 1.89 - 1.66 (m, side-chain –CH$_2$), 1.18 - 0.94 (m, -P-CH$_2$-C**H$_3$**, -Si-O-CH$_2$-C**H$_3$**), 0.51 (m, -Si-C**H$_2$**, 2H). ^{31}P NMR (DMSO-d_6, ppm): δ 34.52 (backbone), 34.47 (terminal).

Phenoxylated/N/-4-OH-ph-/N'/-DIPP-PDI initiated P(EtPPn):

^{1}H NMR (DMSO-d_6, ppm): δ 4.30 - 4.06 (m, backbone -CH$_2$-CH$_2$-), 3.78 - 3.67 (q, Si-O-C**H$_2$**, 6H), 1.83 - 1.72 (m, side-chain –CH$_2$), 1.16 - 0.95 (m, -P-CH$_2$-C**H$_3$**, -Si-O-CH$_2$-C**H$_3$**), 0.51 (m, -Si-C**H$_2$**, 2H). ^{31}P NMR (DMSO-d_6, ppm): δ 34.51 (backbone), 34.38 (terminal).

Synthesis of *α-methoxy* poly(ethylene glycol) -ω- (3-(triethoxysilyl)propyl)carbamate
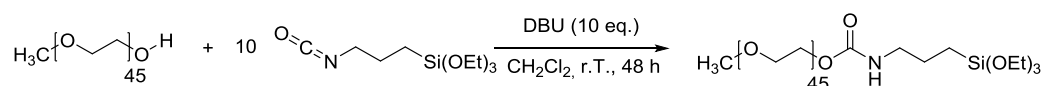
Figure 5-4: Reaction scheme of *α-methoxy* poly(ethylene glycol) -ω- (3-(*tri*ethoxysilyl)propyl)carbamate.

In a 50 mL flask methoxy polyethylene glycol (2000 g mol^{-1}) (0.460 g, 0.23 mmol) was dissolved in 2.6 mL dichloromethane. DBU (0.18 g, 1.15 mmol) and triethoxy(3-isocyanatopropyl)-silane (0.28 g, 1.15 mmol) were added and the mixture was stirred at room temperature. After 48 h the product was precipitated three times in 30 mL cold diethylether. (308 mg, 0.14 mmol, yield 61 %).

^{1}H NMR (CDCl$_3$-d, ppm): δ 3.81 (q, ^3J = 7.0 Hz, 6H), 3.68 - 3.60 (m, backbone -CH$_2$-CH$_2$-), 3.56-3.53 (m, -O-CH$_2$-C**H$_2$**-OCO, 2H) 3.50 (t, ^3J = 5 Hz, -O-C**H$_2$**-CH$_2$-OCO, 2H), 3.46 (t, ^3J = 5 Hz, -NH-C**H$_2$**-, 2H), 3.38 (s, terminal, -C**H$_3$**, 3H), 1.61 (p, ^3J = 7.3 Hz, -CH$_2$-C**H$_2$**-CH$_2$-, 1H), 1.22 (t, ^3J = 7.0 Hz, -Si-O-CH$_2$-C**H$_3$**, 9H), 0.62-0.58 (m, -Si-C**H$_2$**, 2H).

5.3 FUNCTIONALIZATION OF SILICA GEL PARTICLES[66]

5.3.1 GRAFTING ONTO FUNCTIONALIZATION
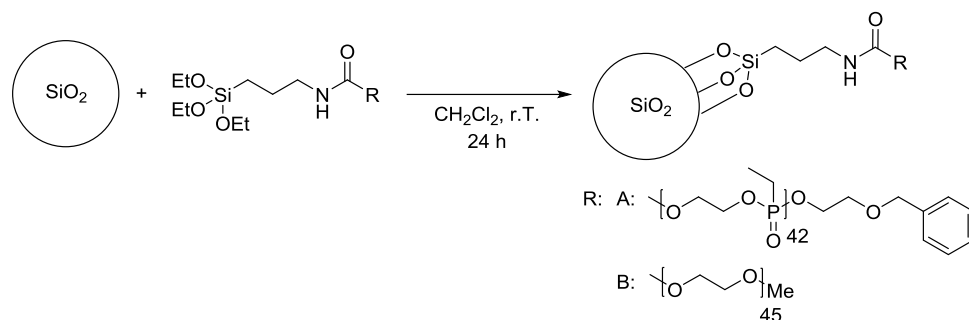
Figure 5-5: Reaction scheme of grafting onto functionalized silica gel particles.

Before functionalization the silica gel was purified in a flask with 35 % H_2O_2 (8 mL g^{-1}) at room temperature for 4h. Then the silica gel was filtrated, washed with ethanol (3x 30 mL) and dried at room temperature *in vacuo* for 1 h to remove remaining solvents.

25 mg of siloxane functional polymer and 1.5 g of silica gel were suspended in 5 mL dry dichloromethane and stirred at r.T. for 24 h. Afterwards the suspension was filtered and washed thoroughly with dichloromethane (3x 30 mL) and collected as a white solid. Characterization is shown in chapter 4.2.

5.3.2 GRAFTING FROM FUNCTIONALIZATION[57]
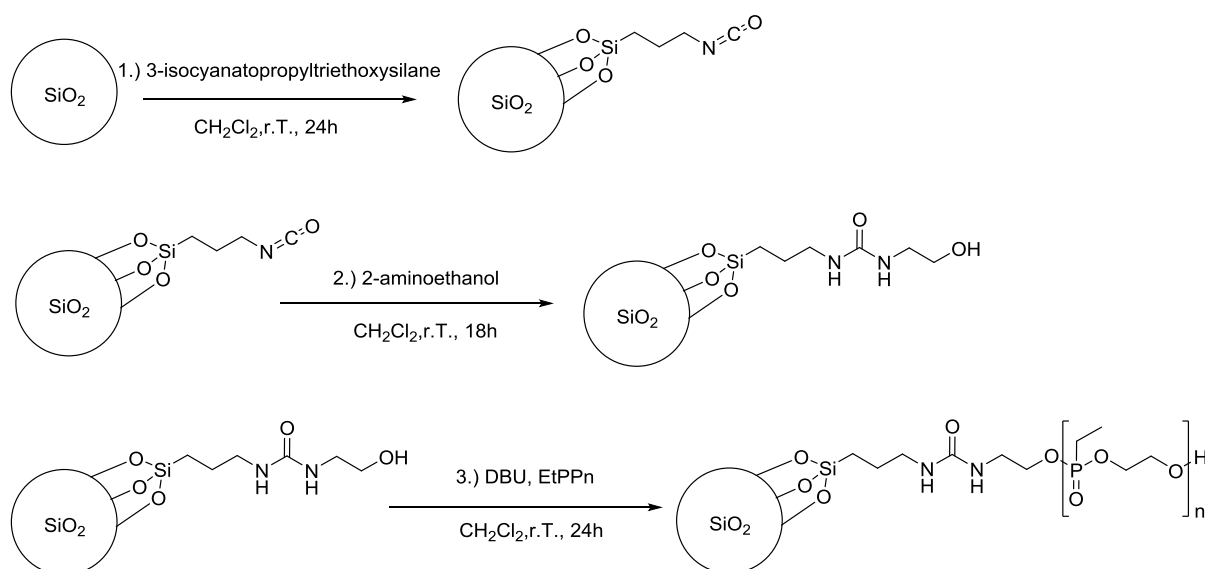
Figure 5-6: Reaction scheme of grafting from functionalized silica gel particles.

As previously described purified silica gel was suspended in 10 mL dichloromethane and 1 mL triethoxy (3-isocyanatopropyl)-silane (1 g, 4.03 mmol) was added. The solution was shaken 300 min^{-1} for 24 h. Then 2-aminoethanol (5 g, 81.86 mmol) was added to the solution, which was shaken for another 18 h. The product was filtered and washed with dichloromethane (3x 50 mL). A slightly light yellow solid was obtained.

The light yellow solid, EtPPn were solved in dichloromethane and DBU was added. It was stirred for 24 h and the solution was filtered. 137.9 mg of a white solid was obtained.

Characterization is shown in chapter 4.2.

5.4 Synthesis of Ring-opened Monomer (1)
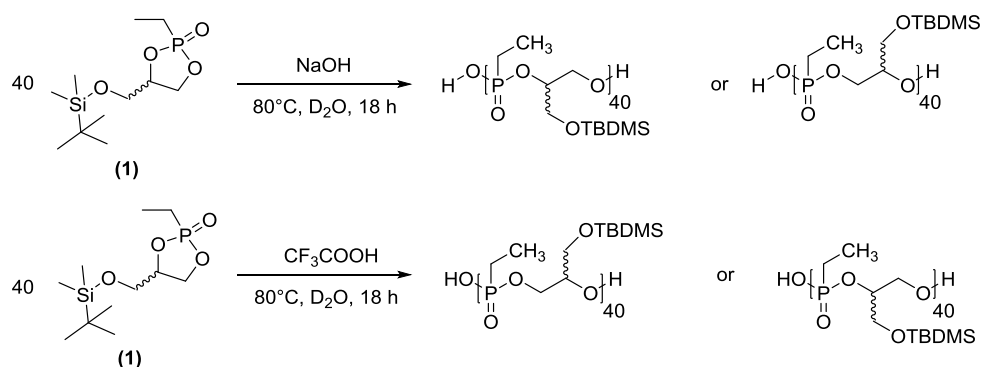
Figure 5-7: Reaction scheme of ring-opened Monomer (1).

In a NMR tube the monomer (1) (40 eq.) was dissolved in D_2O. A solution of sodium hydroxide (NaOH) in D_2O was prepared. To the monomer solution 1 eq. of NaOH solution or trifluoroacetic acid was added. After 18 h the solution was separated from the precipitate, a colorless liquid was obtained and ^{31}P NMR was measured.

5.5 Protein Assay and SDS PAGE

5.5.1 Pierce Protein Assay[46]

To determine the protein concentration the commercially available 660 nm Pierce Assay by Thermo Scientific (USA)[41] was used. Bovine serum albumin (BSA) was used a standard.

The assay was performed according to the provided protocol. Typically 10 μL of sample and 150 μL of Pierce™ 660nm Protein Assay Reagent were added to a Greiner 96 Flat Bottom Transparent Polystyrene plate. This was incubated for 5 minutes.

After 5 min of incubation the absorption at 660 nm was measured with a plate reader (infinite M1000) with the program Tecan i-control, 1.10.4.0. The protein concentration was calculated with Microsoft Excel 2010 via external calibration with the BSA standards. Each sample was measured in triplicate.

5.5.2 SDS PAGE (Sodium Dodecyl Sulfate Polyacrylamide Gel Electrophoresis)

The functionalized silica particles (~50 mg) were incubated with 500 µL human blood plasma at room temperature for 1 h under constant agitation. After incubation the particles were separated from the plasma by centrifugation at 10 000 g for 2 minutes (min). The particles were washed with 0.5 mL water (MilliQ water with a conductivity <18.2 MΩ cm) for 5 min under constant agitation. Then the particles were centrifuged at 10 000g for 2 min. The procedure was repeated three times. To elute the adsorbed proteins 0.5 mL 7M urea/ 3M thiourea mixture was used. After elution under constant agitation for 5 min, the samples were centrifuged at 10 000 g for 2 min. The procedure was repeated three times.[46]

For the SDS PAGE 16.25 µL of the sample, 2.5 µL of 10X Bolt® Sample Reducing Agent and 6.25 µL of the 4X Bolt® LDS Sample Buffer were mixed in Eppendorftubes. The sample was incubated for 10 minutes at 70°C.

After incubation the samples were added to the Gel (NuPAGE™ Novex™ 10% Bis-Tris Protein Gels, 1.0 mm, 10-well) and the separation was performed for 2 h at 100 V. The NuPAGE® MES SDS Running Buffer (20X) and Roti®-Mark PRESTAINED (T852.1) were used as running buffer and marker, respectively. The sort of proteins and their molecular weight are shown in table 8.5 (chapter 8).

The gel was stained with Simply Blue™ Safe Stain from Thermo Scientific overnight. On the next day the stain was removed and decolorized with purified water. After 1 h the water was exchanged. This process was repeated 3 times.

6 CONCLUSION

Furthermore, the successful functionalization of both PEG and P(EtPPn) with the triethoxy (3-isocyanatopropyl)-silane was shown. Characterization was done with ^{1}H, ^{1}H DOSY NMR and MALDI-MS measurments. Functionalization of silica gel particles under ambient conditions was successful. Characterization of these particles was done via SS NMR After incubation of the differently functionalized particles with human blood plasma we could show qualitatively with SDS PAGE and quantitatively with a protein concentration assay that the interaction of the phosphoester functionalized particle is much more less compared to the PEG functionalized particle. And the interaction between the proteins and g.f. SiO_2 is less than the g.o. SiO_2 which were concluded over Protein Assay.

For the variation of the hydrophilicity of the polymers, that can be attached to silica, a new TBDMS-protected monomer 4-(((*tert*-butyldimethylsilyl)oxy)methyl)-2-ethtyl-2-oxo-1,3,2-dioxaphospholane in high yield (62 %) (chapt. 5.1.) was synthesized. This should, after successful polymerization and deprotection of the TBDMS groups allow the attachment of PPEs with a higher hydrophilicity and thus probably the adsorption of different protein patterns. First attempts towards the ring-opening polymerization of the new monomer were performed. The ring was found to be more resilient towards ring-opening than related compounds. Traditional reaction conditions like DBU and TBD at different temperatures showed no results. Ring-opening was successfully achieved under both under harsh acidic and basic conditions as shown by ^{1}H and ^{31}P NMR spectroscopy. No polymer was obtained, rather, the right polymerization conditions remain to be found.

7 OUTLOOK

The functionalization of the silica gel particle, their incubation with human plasma and the measurements show that there are differences in each type of the functionalized silica gel particle (chapt. 4.2/ 4.3).The characterization over SS-NMR, however, does not yield quantitative information concerning neither the degree of functionalization nor the degree of polymerization in the case of the grafting from attempt.

For better characterization and future investigations, other analytic methods need to be found.

SDS PAGE and protein assay shows that the phosphoester functionalized silica gel particle has a lower interaction with proteins. This leads to the conclusion that a selective protein adsorption can be induced by phosphoesters surface modification. For further research it would be interesting to use several different polyphosphoesters with different side chain to change the property of the polymer. However it is important to increase and quantitatively determine the density of the polyphosphoesters on the silica surface.

In this work the synthesis of 4-(((*tert*-butyldimethylsilyl)oxy)methyl)-2-ethtyl-2-oxo-1,3,2-dioxaphospholane and characterization over NMR with several techniques was successful. The effort to polymerize under several conditions, however, was not yet successful. Ring-opening under harsher conditions was observed but no polymerization occurred.. Suitable reaction conditions for successful polymerization need to be found. It would then be possible to characterize and finally deprotect the functional groups inside the polymer to change the hydrophilicity or to modify it with different functional group. Furthermore, deprotection prior to polymerization would result in the formation of an inimer possible to produce the first hyperbranched poly(phosphoester)s.

8 ATTACHMENT

Table 8-1: Pierce Assay of SiO₂ with heparin plasma: Absorption average and calculated values with standard deviation.

SiO$_2$	Removed Plasma	w1	w2	w3	e1	e2	e3	Total
Absoption(Average)	0.323	0.4024	0.6264	0.1403	0.1871	0.0989	0.0834	
σ	0.0094	0.0469	0.0301	0.0071	0.0011	0.0022	0.0048	
C$_{real}$ mg/mL	34.3398	4.2787	0.666	0.1491	0.1989	0.1051	0.0886	
σ	0.9377	0.4686	0.0301	0.0071	0.0011	0.0022	0.0048	
m$_{protein}$ mg	17.1699	2.1393	0.333	0.0746	0.0994	0.0526	0.0443	
σ	0.4689	0.2343	0.0151	0.0036	0.0006	0.0011	0.0024	
Mass ratio	0.6199	0.0772	0.012	0.0027	0.0036	0.0019	0.0016	0.7189
σ	0.0169	0.0085	0.0005	0.0001	0	0	0.0001	
%	61.9852	7.7232	1.2021	0.2692	0.359	0.1897	0.16	71.8883
σ	1.6927	0.8458	0.0544	0.0129	0.002	0.004	0.0086	

Table 8-2: Pierce Assay of PEG functionalized SiO₂with heparin plasma: Absorption average and calculated values with standard deviation.

PEG	Removed Plasma	w1	w2	w3	e1	e2	e3	Total
Absoption(Average)	0.3382	0.3748	0.369	0.2898	0.5284	0.4928	0.1831	
σ	0.0143	0.0512	0.0656	0.026	0.0158	0.0169	0.0047	
C$_{real}$ mg/mL	35.9558	3.9847	0.3922	0.3082	0.5617	0.5239	0.1947	
σ	1.4337	0.5118	0.0656	0.026	0.0158	0.0169	0.0047	
m$_{protein}$ mg	17.9779	1.9923	0.1961	0.1541	0.2809	0.262	0.0973	
σ	0.7169	0.2559	0.0328	0.013	0.0079	0.0084	0.0024	
Mass ratio	0.649	0.0719	0.0071	0.0056	0.0101	0.0095	0.0035	0.7567
σ	0.0259	0.0092	0.0012	0.0005	0.0003	0.0003	0.0001	
%	64.9021	7.1926	0.708	0.5562	1.014	0.9457	0.3514	75.6701
σ	2.588	0.9238	0.1183	0.047	0.0284	0.0305	0.0085	

Table 8-3: Pierce Assay of g.o. functionalized SiO₂with heparin plasma: Absorption average and calculated values with standard deviation.

Grafting onto	Removed Plasma	w1	w2	w3	e1	e2	e3	Total
Absoption(Average)	0.429	0.375	0.7691	0.135	0.4026	0.247	0.1645	
σ	0.0501	0.0123	0.1163	0.0018	0.0248	0.0141	0.0082	
C$_{real}$ mg/mL	45.6092	3.9868	0.8177	0.1435	0.428	0.2626	0.1749	
σ	5.0087	0.1229	0.1163	0.0018	0.0248	0.0141	0.0082	
m$_{protein}$ mg	22.8046	1.9934	0.4088	0.0717	0.214	0.1313	0.0874	
σ	2.5043	0.0615	0.0581	0.0009	0.0124	0.0071	0.0041	
Mass ratio	0.8233	0.072	0.0148	0.0026	0.0077	0.0047	0.0032	0.9282
σ	0.0904	0.0022	0.0021	0	0.0004	0.0003	0.0001	
%	82.327	7.1964	1.4759	0.259	0.7726	0.474	0.3157	92.8207
σ	9.0409	0.2219	0.2099	0.0032	0.0448	0.0255	0.0149	

Table 8-4: Pierce Assay of g.f. functionalized SiO$_2$ with heparin plasma: Absorption average and calculated values with standard deviation.

Grafting from	Removed Plasma	w1	w2	w3	e1	e2	e3	Total
Absoption(Average)	0.5331	0.4017	0.3873	0.1627	0.1058	0.0849	0.0811	
σ	0.0286	0.0476	0.0362	0.0113	0.0021	0.0022	0.0023	
C$_{real}$ mg/mL	56.6766	4.2712	0.4117	0.173	0.1125	0.0903	0.0862	
σ	2.8589	0.4757	0.0362	0.0113	0.0021	0.0022	0.0023	
m$_{protein}$ mg	28.3383	2.1356	0.2059	0.0865	0.0563	0.0451	0.0431	
σ	1.4295	0.2378	0.0181	0.0057	0.0011	0.0011	0.0012	
Mass ratio	1.023	0.0771	0.0074	0.0031	0.002	0.0016	0.0016	1.1159
σ	0.0516	0.0086	0.0007	0.0002	0	0	0	
%	102.3043	7.7098	0.7432	0.3122	0.2031	0.1629	0.1556	111.5911
σ	5.1605	0.8648	0.0659	0.0206	0.0038	0.0039	0.0042	

Table 8-5: Molecular Weight of the proteins of the Roti®-Mark PRESTAINED.

Protein	Molecular Weight (kDa)
Myosin, beef[67]	236
β-Galactosidase, E.coli[68]	116
Serum albumin, beef[69]	66
Ovalbumin, chicken[70]	45
Carbonic anhydrase[71]	31
Trypsin inhibitor, soy[72]	24
Lysozyme, chicken[73]	15
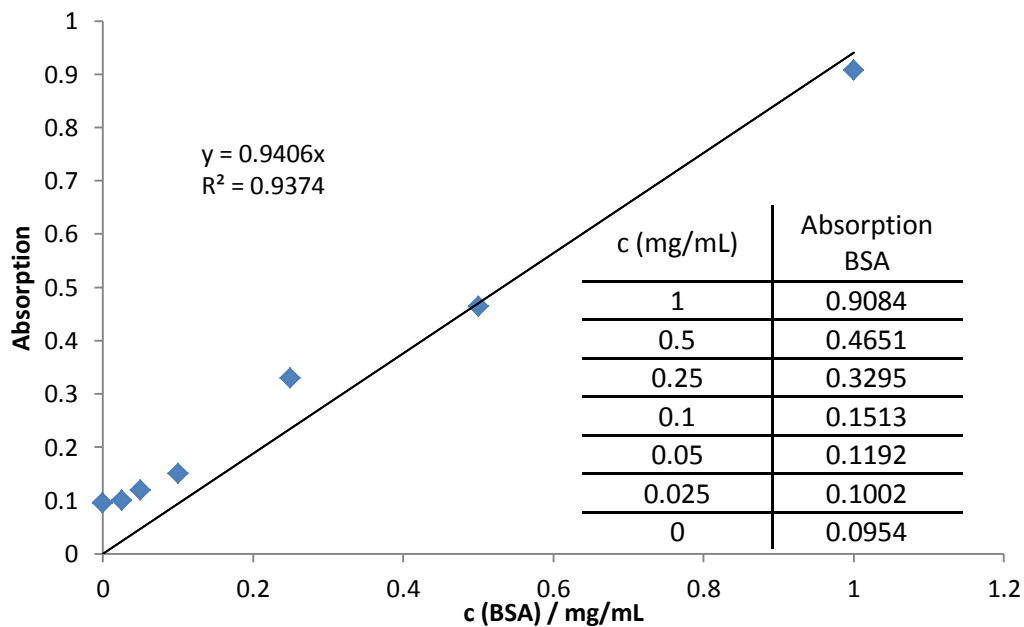
Figure 8-1: Calibration Curve and absorption of BSA in several concentrations.

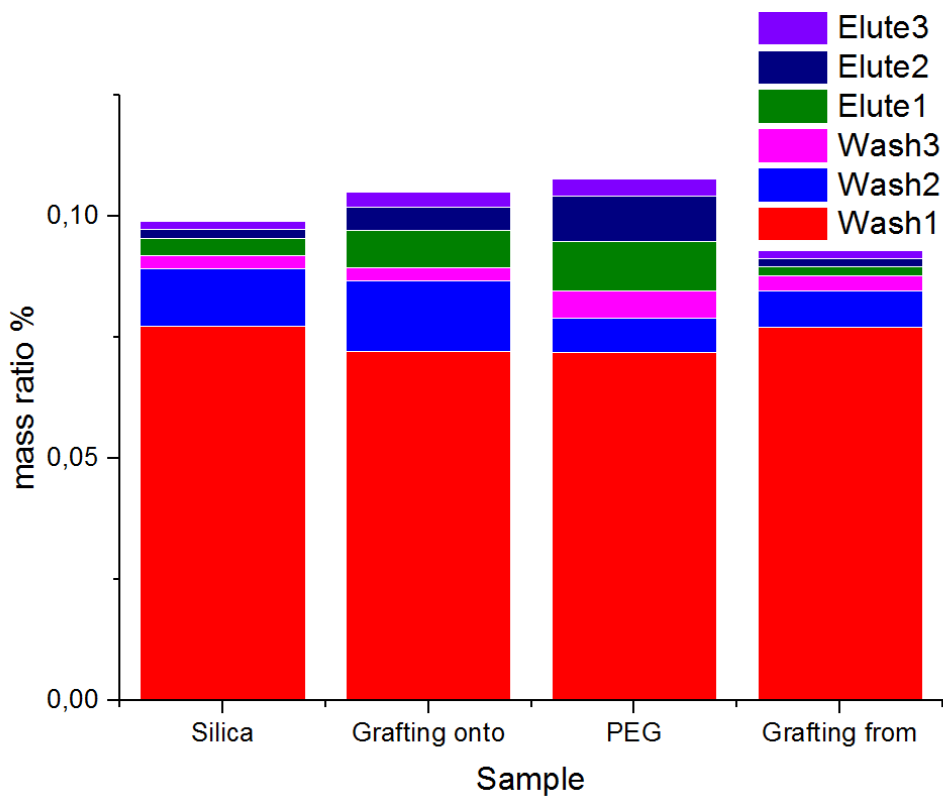| c (mg/mL)	Absorption BSA
1	0.9084
0.5	0.4651
0.25	0.3295
0.1	0.1513
0.05	0.1192
0.025	0.1002
0	0.0954

y = 0.9406x
R^2 = 0.9374

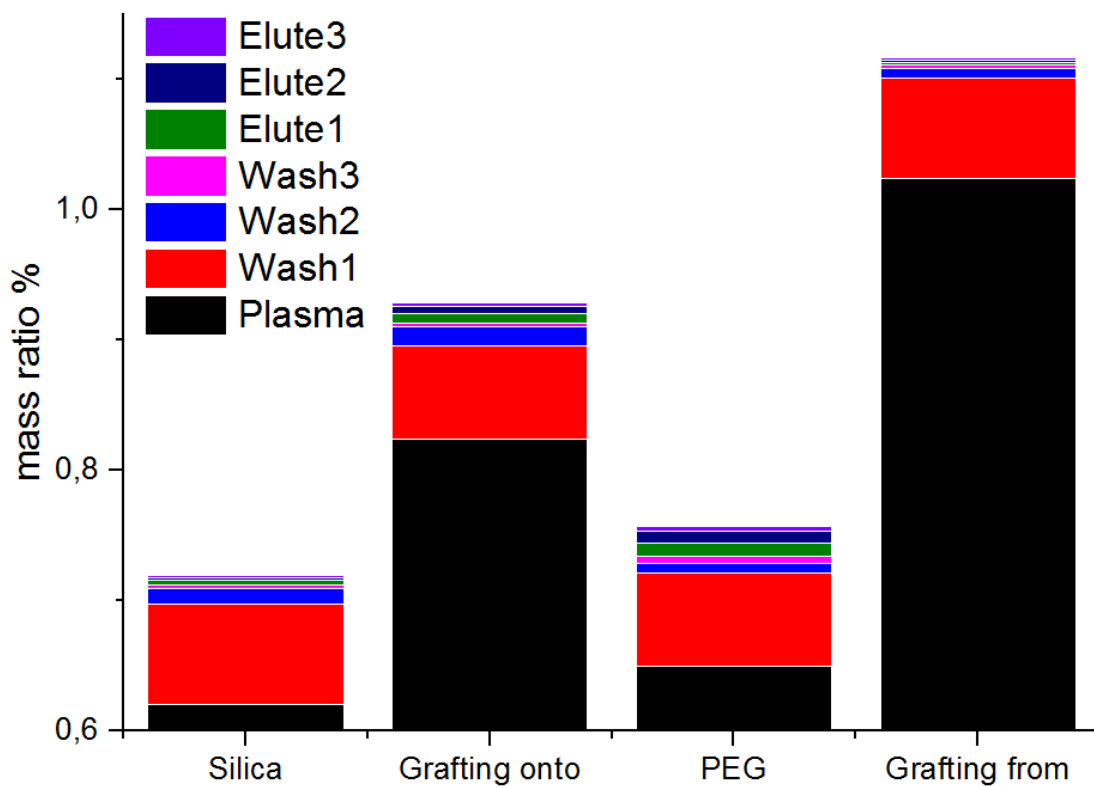**Figure 8-2: Mass ratio of wash and elute fraction against sample.**

Figure 8-3: Mass ratio of plasma, wash and elute fraction against sample.
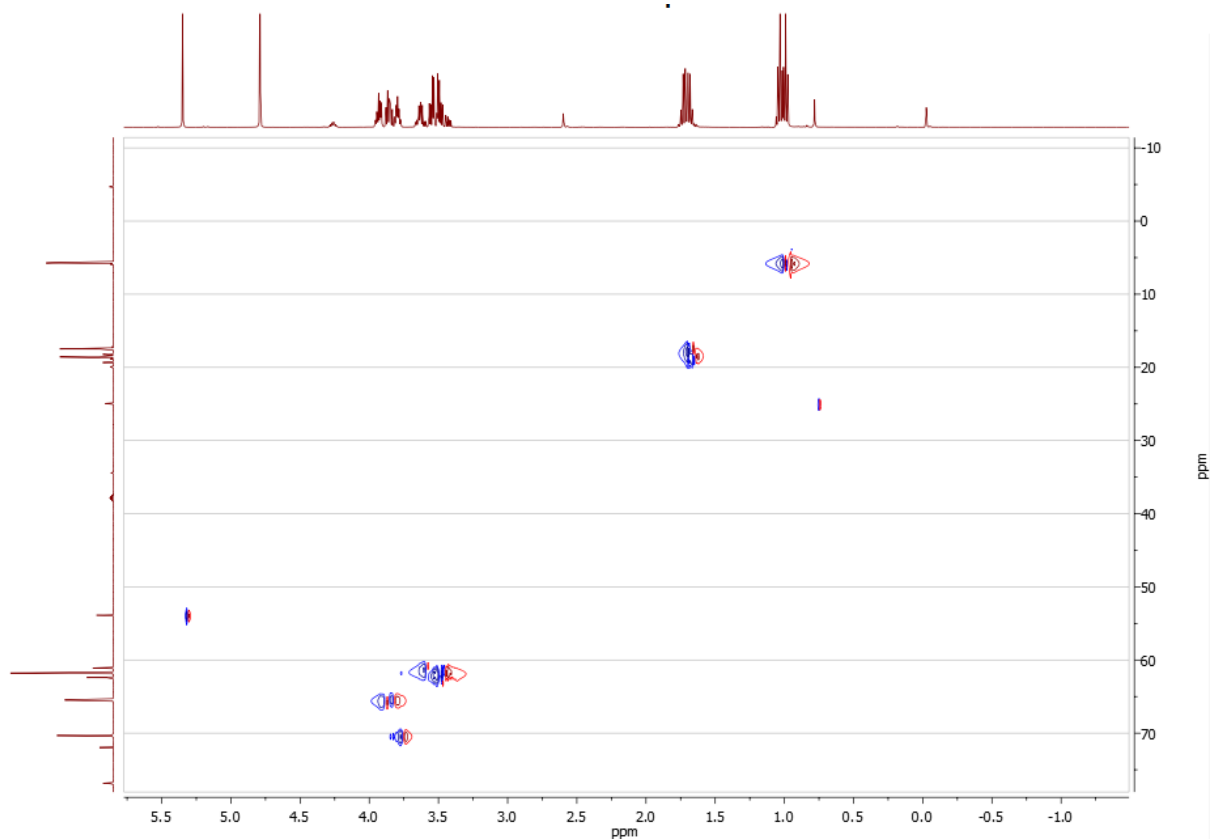

Figure 8-4: $^{13}C^{1}H$ HSQC of the ring-opened product under basic condition in D$_2$O at 298 K.
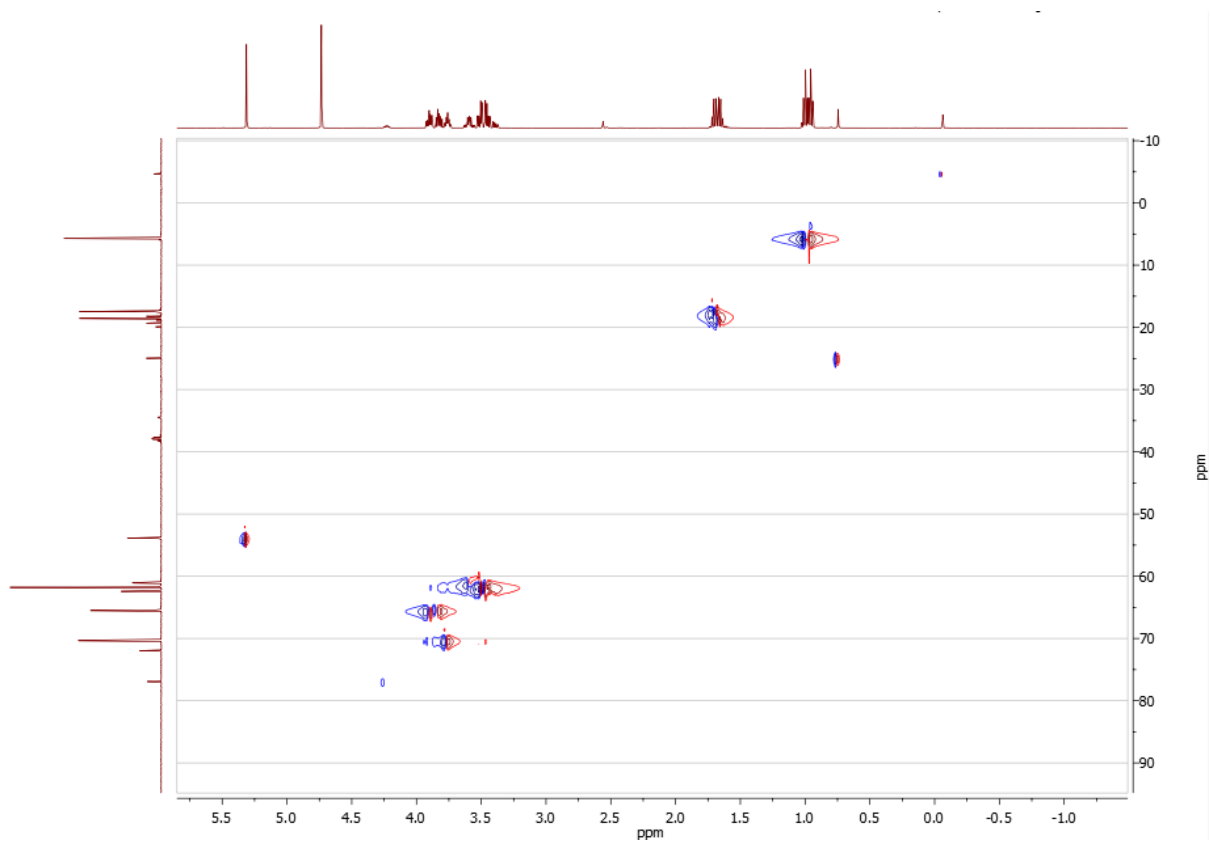
Figure 8-5: $^{13}C^1H$ HSQC of the ring-opened product under acidic condition in D_2O at 298 K.

9 REFERENCES

[1]   Gref, R.; Luck, M.; Quellec, P.et al., 'Stealth' corona-core nanoparticles surface modified by polyethylene glycol (PEG): influences of the corona (PEG chain length and surface density) and of the core composition on phagocytic uptake and plasma protein adsorption, *Colloid Surface B*, **2000**, *18*, 301-313.

[2]   Caracciolo, G.; Palchetti, S.; Colapicchioni, V.et al., Stealth Effect of Biomolecular Corona on Nanoparticle Uptake by Immune Cells, *Langmuir*, **2015**, *31*, 10764-10773.

[3]   Fleischer, C. C.; Payne, C. K., Nanoparticle-cell interactions: molecular structure of the protein corona and cellular outcomes, *Acc. Chem. Res.*, **2014**, *47*, 2651-2659.

[4]   Doorley, G. W.; Payne, C. K., Cellular binding of nanoparticles in the presence of serum proteins, *Chem. Commun. (Camb)*, **2011**, *47*, 466-468.

[5]   Casals, E.; Pfaller, T.; Duschl, A.et al., Time evolution of the nanoparticle protein corona, *ACS Nano*, **2010**, *4*, 3623-3632.

[6]   Wolf, T.; Steinbach, T.; Wurm, F. R., A Library of Well-Defined and Water-Soluble Poly(alkyl phosphonate)s with Adjustable Hydrolysis, *Macromolecules*, **2015**, *48*, 3853-3863.

[7]   Knop, K.; Hoogenboom, R.; Fischer, D.et al., Poly(ethylene glycol) in drug delivery: pros and cons as well as potential alternatives, *Angew. Chem. Int. Ed. Engl.*, **2010**, *49*, 6288-6308.

[8]   Torchilin, V. P., Drug targeting, *Eur. J. Pharm. Sci.*, **2000**, *11 Suppl 2*, S81-91.

[9]   Yamaoka, T.; Tabata, Y.; Ikada, Y., Distribution and tissue uptake of poly(ethylene glycol) with different molecular weights after intravenous administration to mice, *J. Pharm. Sci.*, **1994**, *83*, 601-606.

[10]   Pasut, G.; Veronese, F. M., Polymer-drug conjugation, recent achievements and general strategies, *Progress in Polymer Science*, **2007**, *32*, 933-961.

[11]   Greco, F.; Vicent, M. J.; Gee, S.et al., Investigating the mechanism of enhanced cytotoxicity of HPMA copolymer-Dox-AGM in breast cancer cells, *J. Control. Release*, **2007**, *117*, 28-39.

[12]   Ulbricht, J.; Jordan, R.; Luxenhofer, R., On the biodegradability of polyethylene glycol, polypeptoids and poly(2-oxazoline)s, *Biomaterials*, **2014**, *35*, 4848-4861.

[13]   Santerre, J. P.; Labow, R. S.; Duguay, D. G.et al., Biodegradation evaluation of polyether and polyester-urethanes with oxidative and hydrolytic enzymes, *J. Biomed. Mater. Res.*, **1994**, *28*, 1187-1199.

[14]   Herold, D. A.; Keil, K.; Bruns, D. E., Oxidation of polyethylene glycols by alcohol dehydrogenase, *Biochem. Pharmacol.*, **1989**, *38*, 73-76.

[15]   Bruns, D. E.; Herold, D. A.; Rodeheaver, G. T.et al., Polyethylene glycol intoxication in burn patients, *Burns. Incl. Therm. Inj.*, **1982**, *9*, 49-52.

[16]   Herold, D. A.; Rodeheaver, G. T.; Bellamy, W. T.et al., Toxicity of topical polyethylene glycol, *Toxicol. Appl. Pharmacol.*, **1982**, *65*, 329-335.

[17]   Romberg, B.; Metselaar, J. M.; Baranyi, L.et al., Poly(amino acid)s: promising enzymatically degradable stealth coatings for liposomes, *Int. J. Pharm.*, **2007**, *331*, 186-189.

[18]   Li, C.; Wallace, S., Polymer-drug conjugates: recent development in clinical oncology, *Adv. Drug Deliv. Rev.*, **2008**, *60*, 886-898.

[19]   Hoogenboom, R., Poly(2-oxazoline)s: a polymer class with numerous potential applications, *Angew. Chem. Int. Ed. Engl.*, **2009**, *48*, 7978-7994.

[20]   Lapienis, G.; Penczek, S., Cationic Polymerization of 2-Alkoxy-2-Oxo-1,3,2-Dioxaphosphorinanes (1,3-Propylene Alkyl Phosphates), *Macromolecules*, **1977**, *10*, 1301-1306.

[21]   Penczek, S.; Pretula, J., High-molecular-weight poly(alkylene phosphates) and preparation of amphiphilic polymers thereof, *Macromolecules*, **1993**, *26*, 2228-2233.

[22]   Penczek, S.; Pretula, J. B.; Kaluzynski, K.et al., Polymers with Esters of Phosphoric Acid Units: From Synthesis, Models of Biopolymers to Polymer-Inorganic Hybrids, *Israel Journal of Chemistry*, **2012**, *52*, 306-319.

[23]   Baran, J.; Klosinski, P.; Penczek, S., Poly(Alkylene Phosphate)S by Polycondensation of Phosphonic Diamides with Diols, *Makromol. Chem.*, **1989**, *190*, 1903-1917.

[24]   Pretula, J.; Penczek, S., High-Molecular-Weight Poly(Alkylene Phosphonate)S by Condensation of Dialkylphosphonates with Diols, *Makromol. Chem.*, **1990**, *191*, 671-680.

[25]   Penczek, S.; Duda, A.; Kaluzynski, K.et al., Thermodynamics and Kinetics of Ring-Opening Polymerization of Cyclic Alkylene Phosphates, *Makromol. Chem.-M. Symp.*, **1993**, *73*, 91-101.

[26]   Klosinski, P.; Penczek, S., Synthesis of Models of Teichoic-Acids by Ring-Opening Polymerization, *Macromolecules*, **1983**, *16*, 316-320.

[27] Iwasaki, Y.; Yamaguchi, E., Synthesis of Well-Defined Thermoresponsive Polyphosphoester Macroinitiators Using Organocatalysts, *Macromolecules*, **2010**, *43*, 2664-2666.

[28] Wang, J.; Mao, H. Q.; Leong, K. W., A novel biodegradable gene carrier based on polyphosphoester, *J. Am. Chem. Soc.*, **2001**, *123*, 9480-9481.

[29] Zhang, S.; Wang, H.; Shen, Y.et al., A Simple and Efficient Synthesis of an Acid-labile Polyphosphoramidate by Organobase-catalyzed Ring-Opening Polymerization and Transformation to Polyphosphoester Ionomers by Acid Treatment, *Macromolecules*, **2013**, *46*, 5141-5149.

[30] Elsabahy, M.; Zhang, S.; Zhang, F.et al., Surface charges and shell crosslinks each play significant roles in mediating degradation, biofouling, cytotoxicity and immunotoxicity for polyphosphoester-based nanoparticles, *Sci. Rep.*, **2013**, *3*, 3313.

[31] Steinbach, T.; Wurm, F. R., Poly(phosphoester)s: A New Platform for Degradable Polymers, *Angew. Chem. Int. Ed. Engl.*, **2015**, *54*, 6098-6108.

[32] Steinbach, T.; Alexandrino, E. M.; Wahlen, C.et al., Poly(phosphonate)s via Olefin Metathesis: Adjusting Hydrophobicity and Morphology, *Macromolecules*, **2014**, *47*, 4884-4893.

[33] Steinmann, M.; Marsico, F.; Wurm, F. R., Reactive poly(phosphoester)-telechelics, *Journal of Polymer Research*, **2015**, *22*.

[34] Nuyken, O.; Pask, S., Ring-Opening Polymerization—An Introductory Review, *Polymers*, **2013**, *5*, 361-403.

[35] Koltzenburg, S.; Maskos, M.; Nuyken, O. In *Polymere: Synthese, Eigenschaften und Anwendungen*; Springer Berlin Heidelberg: 2014, p 341-366.

[36] Odian, G. In *Principles of Polymerization*; John Wiley & Sons, Inc.: 2004, p 544-618.

[37] Steinbach, T.; Ritz, S.; Wurm, F. R., Water-Soluble Poly(phosphonate)s via Living Ring-Opening Polymerization, *Acs Macro Letters*, **2014**, *3*, 244-248.

[38] Allcock, H. R., Ring-Chain Equilibria, *J. Macromol. Sci.-Rev. M.*, **1970**, *C 4*, 149-&.

[39] Koltzenburg, S.; Maskos, M.; Nuyken, O. In *Polymere: Synthese, Eigenschaften und Anwendungen*; Springer Berlin Heidelberg: 2014, p 217-258.

[40] Hostalka, H.; Figini, R. V.; Schulz, G. V., Zur Anionischen Polymerisation Des Styrols in Tetrahydrofuran, *Makromolekul. Chem.*, **1964**, *71*, 198-203.

[41] Ritz, S.; Schottler, S.; Kotman, N.et al., Protein corona of nanoparticles: distinct proteins regulate the cellular uptake, *Biomacromolecules*, **2015**, *16*, 1311-1321.

[42]   Kim, J. A.; Salvati, A.; Aberg, C.et al., Suppression of nanoparticle cytotoxicity approaching in vivo serum concentrations: limitations of in vitro testing for nanosafety, *Nanoscale*, **2014**, *6*, 14180-14184.

[43]   Walkey, C. D.; Chan, W. C., Understanding and controlling the interaction of nanomaterials with proteins in a physiological environment, *Chem. Soc. Rev.*, **2012**, *41*, 2780-2799.

[44]   Walczyk, D.; Bombelli, F. B.; Monopoli, M. P.et al., What the cell "sees" in bionanoscience, *J. Am. Chem. Soc.*, **2010**, *132*, 5761-5768.

[45]   Anderson, N. L.; Anderson, N. G., The human plasma proteome: history, character, and diagnostic prospects, *Mol. Cell. Proteomics*, **2002**, *1*, 845-867.

[46]   Winzen, S.; Schoettler, S.; Baier, G.et al., Complementary analysis of the hard and soft protein corona: sample preparation critically effects corona composition, *Nanoscale*, **2015**, *7*, 2992-3001.

[47]   Pozzi, D.; Colapicchioni, V.; Caracciolo, G.et al., Effect of polyethyleneglycol (PEG) chain length on the bio-nano-interactions between PEGylated lipid nanoparticles and biological fluids: from nanostructure to uptake in cancer cells, *Nanoscale*, **2014**, *6*, 2782-2792.

[48]   Laws, D. D.; Bitter, H. M.; Jerschow, A., Solid-state NMR spectroscopic methods in chemistry, *Angew. Chem. Int. Ed. Engl.*, **2002**, *41*, 3096-3129.

[49]   Pines, A., Proton-Enhanced Nuclear Induction Spectroscopy. A Method for High Resolution NMR of Dilute Spins in Solids, *The Journal of Chemical Physics*, **1972**, *56*, 1776.

[50]   Hennel, J.; Klinowski, J. In *New Techniques in Solid-State NMR*; Klinowski, J., Ed.; Springer Berlin Heidelberg: 2005; Vol. 246, p 1-14.

[51]   Kolodziejski, W.; Corma, A.; Wozniak, K.et al., 13C →1H Cross-Polarization NMR in Solids at Natural13C Abundance, *The Journal of Physical Chemistry*, **1996**, *100*, 7345-7351.

[52]   Schaefer, J.; Stejskal, E. O., Carbon-13 nuclear magnetic resonance of polymers spinning at the magic angle, *Journal of the American Chemical Society*, **1976**, *98*, 1031-1032.

[53]   Kurien, B.; Scofield, R. H. In *Protein Electrophoresis*; Kurien, B. T., Scofield, R. H., Eds.; Humana Press: 2012; Vol. 869, p 403-405.

[54] Qu, R. J.; Wang, M. G.; Sun, C. M.et al., Chemical modification of silica-gel with hydroxyl- or amino-terminated polyamine for adsorption of Au(III), *Applied Surface Science*, **2008**, *255*, 3361-3370.

[55] http://www.mn-net.com/LCadsorbents/Irregularsilica/StandardsilicaforLC/tabid/6009/language/de-DE/Default.aspx, 28.10.2015 12:35

[56] Leonardelli, S.; Facchini, L.; Fretigny, C.et al., Silicon-29 NMR study of silica, *Journal of the American Chemical Society*, **1992**, *114*, 6412-6418.

[57] McDonald, A. R.; Dijkstra, H. P.; Suijkerbuijk, B. M. J. M.et al., "Click" Immobilization of Organometallic Pincer Catalysts for C−C Coupling Reactions, *Organometallics*, **2009**, *28*, 4689-4699.

[58] Blinka, T. A.; Helmer, B. J.; West, R. In *Advances in Organometallic Chemistry*; Stone, F. G. A., Robert, W., Eds.; Academic Press: 1984; Vol. Volume 23, p 193-218.

[59] www.pascal-man.com/periodic-table/29Si.pdf, 29.10.2015 10:48

[60] Hirschmann, R.; Yager, K. M.; Taylor, C. M.et al., Phosphonate Diester and Phosphonamide Synthesis. Reaction Coordinate Analysis by31P NMR Spectroscopy: Identification of Pyrophosphonate Anhydrides and Highly Reactive Phosphonylammonium Salts1, *Journal of the American Chemical Society*, **1997**, *119*, 8177-8190.

[61] Li, Y. N.; Kawakami, Y., Efficient synthesis of poly(silyl ether)s by Pd/C and RhCl(PPh3)(3)-catalyzed cross-dehydrocoupling polymerization of bis(hydrosilane)s with diols, *Macromolecules*, **1999**, *32*, 6871-6873.

[62] Stec, W. J., Heteronuclear Spin-Spin Coupling Constants Between Directly Bonded Atoms as a Probe of Configuration at Phosphorus Atom Involved in Diastereoisomeric 4-Methyl-1,3,2-dioxaphosphorinans, *Zeitschrift für Naturforschung B*, **1974**, *29*, 109.

[63] Poznanski, J.; Ejchart, A.; Wierzchowski, K. L.et al., 1H- and 13C-NMR investigations on cis-trans isomerization of proline peptide bonds and conformation of aromatic side chains in H-Trp-(Pro)n-Tyr-OH peptides, *Biopolymers*, **1993**, *33*, 781-795.

[64] Perez-Trujillo, M.; Monteagudo, E.; Parella, T., 13C NMR spectroscopy for the differentiation of enantiomers using chiral solvating agents, *Anal. Chem.*, **2013**, *85*, 10887-10894.

[65]   Syed, M. K.; Murray, C.; Casey, M., Stereoselective Synthesis of Lignans of Three Structural Types from a Common Intermediate, Enantioselective Synthesis of (+)-Yangambin, *European Journal of Organic Chemistry*, **2014**, *2014*, 5549-5556.

[66]   Park, S. W.; Kim, Y. I.; Chung, K. H.et al., Covalent immobilization of GL-7-ACA acylase on silica gel through silanization, *React. Funct. Polym.*, **2002**, *51*, 79-92.

[67]   Oliver, T. N.; Berg, J. S.; Cheney, R. E., Tails of unconventional myosins, *Cell. Mol. Life Sci.*, **1999**, *56*, 243-257.

[68]   Jacobson, R. H.; Zhang, X. J.; DuBose, R. F.et al., Three-dimensional structure of beta-galactosidase from E. coli, *Nature*, **1994**, *369*, 761-766.

[69]   Reed, R. G.; Putnam, F. W.; Peters, T., Sequence of Residues 400-403 of Bovine Serum-Albumin, *Biochemical Journal*, **1980**, *191*, 867-868.

[70]   Yamasaki, M.; Takahashi, N.; Hirose, M., Crystal structure of S-ovalbumin as a non-loop-inserted thermostabilized serpin form, *J. Biol. Chem.*, **2003**, *278*, 35524-35530.

[71]   Badger, M. R.; Price, G. D., The Role of Carbonic-Anhydrase in Photosynthesis, *Annu. Rev. Plant. Phys.*, **1994**, *45*, 369-392.

[72]   Kunitz, M., Crystalline Soybean Trypsin Inhibitor, *J. Gen. Physiol.*, **1946**, *29*, 149-154.

[73]   Blake, C. C.; Mair, G. A.; North, A. C.et al., On the conformation of the hen egg-white lysozyme molecule, *Proc. R. Soc. Lond. B Biol. Sci.*, **1967**, *167*, 365-377.